

EFFECT OF HIGH CURING TEMPERATURES ON THE STRENGTH,
DURABILITY AND POTENTIAL OF DELAYED ETTRINGITE FORMATION IN
MASS CONCRETE STRUCTURES

By

LUCY ACQUAYE

A DISSERTATION PRESENTED TO THE GRADUATE SCHOOL
OF THE UNIVERSITY OF FLORIDA IN PARTIAL FULFILLMENT
OF THE REQUIREMENTS FOR THE DEGREE OF
DOCTOR OF PHILOSOPHY

UNIVERSITY OF FLORIDA

2006

Copyright 2006

by

LUCY ACQUAYE

This document is dedicated to David and Anna.

ACKNOWLEDGMENTS

My sincere gratitude goes to Dr. Abdol Chini whose constant advice, encouragement, patience and dedication to my graduate studies has resulted in this dissertation. Dr. Chini admitted me into this distinguished university and program where all my academic and professional goals were met and exceeded. He was the committee chair for both my master's thesis and doctoral dissertation, and his kindness and inspiration have sustained me throughout my studies. Dr. Chini provided outstanding academic and professional guidance during my doctoral studies and gave me wonderful opportunities to excel academically and professionally.

The research reported here was sponsored by the Florida Department of Transportation (FDOT). Sincere appreciation is due to the FDOT State Materials Office Concrete Lab employees in Gainesville and Richard DeLorenzo for his guidance and help in sampling and testing concrete specimens. My sincere thanks go to Barbara Beatty of the FDOT chemical lab for her support

My sincere thanks go to Dr. Jo Hassel for her constant encouragement and financial assistance during my doctoral studies. My thanks also go to members of my doctoral committee for their help in completing this dissertation. I am grateful to the faculty and staff at the Rinker School of Building Construction for providing a stimulating environment for my graduate studies. My thanks go to the faculty of the Department of Building Technology, Kwame Nkrumah University of Science and Technology, Ghana, for their support throughout my studies.

I am utterly grateful to God for all the wonderful blessings in my life. I am very grateful to my parents for all the sacrifices they made to see me to such great heights and for their constant support. I am grateful to my siblings who supported and expanded my dreams. I am grateful to my husband, Mark for his support and encouragement. I wish to thank my children David and Anna, whose interest in “mama’s homework” spurred me on to complete this dissertation.

TABLE OF CONTENTS

	<u>page</u>
ACKNOWLEDGMENTS	iv
LIST OF TABLES	ix
LIST OF FIGURES	xi
ABSTRACT.....	xiv
CHAPTER	
1 INTRODUCTION	1
Background.....	1
Objectives and Scope of Research.....	5
Research Methodology	6
Importance of Research	7
2 LITERATURE REVIEW	8
Introduction.....	8
Cement Hydration.....	9
Effect of Curing Temperature on the Microstructure of Hydrated Cement Paste	12
Dense Shell of Hydration Products.....	14
Effect of Curing Temperature on Concrete Strength Development	15
Effect of Temperature on the Durability of Concrete.....	17
Fly ash and Slag in Concrete	19
Delayed Ettringite Formation (DEF) in Concrete	22
3 RESEARCH METHODOLOGY	27
Introduction.....	27
Degree of Hydration	28
Introduction	28
Methodology.....	29
Calculations to Determine the Degree of Hydration	35
Problems Encountered in the Experimental Process	35
Mass Concrete Experiments	42
Compressive Strength.....	44

Resistance to Chloride Penetration.....	44
Time to Corrosion.....	45
Density and Percentage of Voids in Hardened Concrete	45
Microstructure analysis – Scanning Electron Microscope (SEM)	46
Introduction	46
Signals of Interest.....	46
SEM Use in Concrete	48
Experimental Work	48
Sample Preparation for SEM Examination	49
4 TEST RESULTS AND DISCUSSION	51
Introduction.....	51
Phase 1 – Determination of Degree of Hydration	51
Phase 2 – Tests of Mass Concrete	57
Degree of Hydration Results	63
Compressive Strength Results.....	65
Resistance to Chloride Ion Penetration	68
Density and Percentage of Voids Results.....	69
Time to Corrosion Results.....	72
Phase 3 – Microstructural Analysis	74
SEM Observations of Plain Cement Mixes.....	74
Effect of Curing Temperature on the Presence of Ettringite Crystals.....	74
Effect of Curing Duration on the Amount of Ettringite Crystals formed	75
SEM Observations of Fly Ash Mixes.....	78
Introduction	78
Effect of Curing Temperature on the Presence of Ettringite Crystals.....	79
Effect of Curing Duration on the Amount of Ettringite Crystals formed in Voids.....	80
SEM Observations of Slag Mixes	82
Introduction	82
Effect of Curing Temperature on the Presence of Ettringite Crystals.....	83
Effect of Curing Duration on the Amount of Ettringite Crystals formed	83
5 CONCLUSIONS AND RECOMMENDATIONS	87
Introduction.....	87
Conclusions.....	87
Research Implications for Mass Concrete Structures.....	92
Recommendations.....	93
APPENDIX	
A CONCRETE MIX DESIGNS.....	96
Mix 1 – Plain Cement Mix	96
Mix 2 – 18% Fly Ash Mix	97

Mix 3 – Plain Cement Mix	98
Mix 4- 18% Fly Ash Mix.....	99
Mix 5 – Plain Cement Mix	100
Mix 6 – 50% Slag Mix.....	101
Mix 7 – Plain Cement Mix	102
B ADDITIONAL SEM IMAGES	103
Part 1 - Mix 1:Plain Cement Only Mix (0%FA)	103
Part 2 - Mix 2: 18% Fly Ash Mix	109
Part 3 - Mix 3: 50% Slag Mix.....	112
LIST OF REFERENCES	115
BIOGRAPHICAL SKETCH	119

LIST OF TABLES

<u>Table</u>	<u>page</u>
2.1 Major Compounds of Portland Cement	9
2.2 Measured Porosity	18
2.3 Results of compressive strength and AASHTO T-277 test.....	21
2.4 AASHTO T-277 tests for charge passed.....	22
2.5 Rate of chloride diffusion ppm/day (average of three replicates, Norwegian test)..	22
3.1 Properties of Cement and Fly ash	30
3.2 Properties of Blast furnace slag –ASTM C 989-97b, AASHTO M302.....	30
3.3 Mix proportions of paste mixes.....	31
3.4 Time to 70% hydration in plain cement mix	37
3.5 Concrete Mix 1 – 0% Fly Ash (Isothermal Curing).....	38
3.6 Binders used in mass concrete mixes by the FDOT	41
3.7 Mixture Proportions for FDOT Class IV mass concrete	43
4.1 Nonevaporabe water content for various Fly ash mixes Lam et al. (2000).....	54
4.2 Degree of hydration results for plain cement mixes	55
4.3 Degree of hydration for 18% fly ash mixes	56
4.4 Degree of hydration for 50% fly ash mixes	57
4.5 Degree of hydration for cement and blast furnace slag mixes	57
4.6 Summary of Plastic Properties of Fresh Concrete.	58
4.7 Results of concrete mixes M1 and M2	58
4.8 Results of concrete mixes M3 and M4.....	59

4.9	Results of concrete mixes M5 and M6.....	60
4.10	Results of concrete mixes M7 and M8.....	61
4.11	Summary of Results of concrete mixes M1 , M2, M3 and M4.....	62
4.12	Summary of Results of concrete mixes M5, M6, M7 and M8.....	63
4.13	Compressive strength as a ratio of 28-day samples cured at 73oF	66
4.14	Compressive strength as a ratio of the 28-day samples cured at 73oF	67
5.1	Compressive strength samples cured isothermally	89
5.2	RCP for samples cured isothermally	90
5.3	Compressive strength for adiabatically cured samples	90
5.4	RCP and Ettringite Formation for adiabatically cured samples	93

LIST OF FIGURES

<u>Figure</u>	<u>page</u>
2.1 External thermal cracking	10
2.2 Internal thermal cracking	11
2.3 Effect of curing temperature on concrete strength development	16
2.4 Pore size distribution with age for 30% Fly ash mix	20
3.1 Paste samples cast in one-ounce polypropylene screw cap jars.....	32
3.2 Oven used to cure samples at 200°F.....	32
3.3 Samples cured in four-ounce polypropylene jars after demolding	33
3.4 Samples crushed in mechanical crusher.....	33
3.5 Approximately 3 grams of samples weighed.	34
3.6 Samples removed after ignition at 1832°F.	34
3.7 Curing tanks used for samples at elevated temperatures.....	36
3.8 Degree of hydration (w _{nu} = 0.23).....	37
3.9 Compressive strength results.....	38
3.10 Rapid Chloride Permeability (RCP) results	39
3.11 Degree of hydration based on adiabatic curing (w _{nu} = 0.23)	42
3.12 Different interactions of an electron beam (PE) with the solid target. BSE = backscattered electrons, SE = secondary electrons, X = x-ray, AE = auger electrons	47
3.13 The EDAX analysis of “gel” showing calcium, sulfur, and aluminum peaks typical for ettringite	49
3.14 Mortar samples mounted on stubs for SEM examination	50

4.1	Degree of hydration for 0%FA and 18%FA mixes.....	64
4.2	Degree of hydration for 0%BFS and 50%BFS mixes.....	65
4.3	Compressive strengths for 0%FA and 18%FA mixes.....	66
4.4	Compressive strengths for 0%BFS and 50%BFS mixes.....	67
4.5	Chloride Ion Penetration results for 0%FA and 18%FA mixes	68
4.6	Chloride Ion Penetration results for 0%BFS and 50%BFS mixes	69
4.7	Density for 0%FA and 18%FA mixes.....	70
4.8	Density for 0%BFS and 50%BFS mixes.....	70
4.9	Percentage of voids for 0%FA and 18%FA mixes	71
4.10	Percentage of voids for 0%BFS and 50%BFS mixes	72
4.11	Time to Corrosion results for all mixes.....	73
4.12	The RCP at 91days expressed in terms of Time to Corrosion unit	73
4.13	Well-defined Monosulphate (M) crystals in a void.....	76
4.14	Void with clusters of Ettringite (E) crystals.....	76
4.15	Void containing both Monosulphate (M) and Ettringite (E) crystals.....	77
4.16	Voids containing Ettringite (E) some appear almost full of it.	77
4.17	Void completely filled with fibrous Ettringite (E)	78
4.18	Void containing hexagonal plates of Monosulphate (M).....	80
4.19	Void showing Monosulphate (M) transformed into Ettringite (E)	81
4.20	Clusters of Fibrous Ettringite (E) in void.....	81
4.21	Sample with empty air Voids (V)	84
4.22	Higher magnification of 4.32	84
4.23	Sample with empty air Void (V).....	85
4.24	Reacting Slag (S) particle with Ettringite (E) formed.....	85
4.25	Slag particle completely covered with Ettringite (E)	86

B.1	Void with monosulphate (M), no ettringite found	103
B.2	Close-up view of Figure B.1	104
B.3	Void with ettringite (E) and monosulphate (M).....	104
B.4	Void with ettringite (E) crystals	105
B.5	Void showing monosulphate and the early formation of ettringite (E) crystals	105
B.6	Void showing ball of ettringite (E) crystals	106
B.7	Void showing balls of ettringite (E) crystals.....	106
B.8	Voids showing ettringite (E) crystals some almost full	107
B.9	Voids showing ettringite (E) and monosulphate crystals.....	107
B.10	Ettringite (E) crystals in and around vicinity of void.....	108
B.11	Ettringite (E) crystals in void	108
B.12	Fly ash particle with reaction around rim.....	109
B.13	Fly ash particle with reaction around rim.....	109
B.14	Void containing monosulphate.....	110
B.15	Void containing ettringite crystals	110
B.16	Close up view of ettringite crystals in Figure B.15.....	111
B.17	Reacting fly ash particle	111
B.18	Slag particles showing some early reaction	112
B.19	Slag particles showing reaction on surface	112
B.20	Slag particle showing reaction on surface.....	113
B.21	Slag particle showing reaction on surface.....	113
B.22	Ettringite formed around surface of reacting slag particle.....	114
B.23	Close-up view of Figure B.22.....	114

Abstract of Dissertation Presented to the Graduate School
of the University of Florida in Partial Fulfillment of the
Requirements for the Degree of Doctor of Philosophy

**EFFECT OF HIGH CURING TEMPERATURES ON THE STRENGTH,
DURABILITY AND POTENTIAL OF DELAYED ETTRINGITE FORMATION IN
MASS CONCRETE STRUCTURES**

By

Lucy Acquaye

May 2006

Chair: Abdol Chini

Major Department: Design, Construction and Planning

The Florida Department of Transportation (FDOT) has in recent years recorded high core temperatures of 170°F - 200°F during curing of mass concrete elements. Frequent reports of such high temperatures have raised concerns of the strength and durability of concrete cured at such high temperatures. Additional concerns have been raised of the possibility of expansions of the hardened concrete from delayed ettringite formation (DEF) and its subsequent deterioration. FDOT specifies a maximum differential temperature of 35°F between the core and exterior of mass concrete elements during curing to avoid cracking from high thermal stresses and a shorter service life of the structure. However no limit is specified for the maximum curing temperature. This dissertation investigated the effects of high temperatures on the strength, durability and potential of delayed ettringite formation in mass concrete mixes.

Using typical FDOT Class IV mass concrete mixes it was found that elevated curing temperatures resulted in lower later-age strengths. Blending the cement with fly ash and slag resulted in increased strength and durability when compared to the plain cement mixes for all curing durations and temperatures.

Investigating the potential of delayed ettringite formation in the concrete mixes cured at elevated temperatures and the effect of permeability on the onset and amount of ettringite formed showed that:

1. At room temperature curing no ettringite was observed when samples were examined microscopically using a scanning electron microscope (SEM) at 7, 28 and 91 days, notwithstanding having the highest permeability values.
2. At elevated curing temperatures of 160 and 180°F, the plain cement mixes had high permeability values and microscopic examination showed ettringite crystals in void spaces at 28 days. At 91 days these samples showed voids almost filled with the crystals.
3. Concrete mixes containing 18% fly ash and 50% slag and cured at the elevated temperatures resulted in much lower permeability. The low permeability of the blends delayed the onset of ettringite formation as well as the amount formed when compared to the plain cement mixes. This was particularly evident in the slag mixes.

CHAPTER 1 INTRODUCTION

Background

In recent years, Florida Department of Transportation (FDOT) has recorded high core temperatures of 170 – 200°F during curing of mass concrete structures. Mass concrete structures as defined in the FDOT Structures Design Guidelines is “any large volume of cast-in-place or precast concrete with dimensions large enough to require that measures be taken to cope with the generation of heat and attendant volume change so as to minimize cracking” (FDOT, 2002). Although a definite size has not been determined, a concrete member, which is 2 ft to 3 ft thick, is considered to be mass concrete.

In its mass concrete specifications, FDOT does not set a limit on the maximum core temperature during curing. FDOT however in its specification for mass concrete, limits the differential curing temperature between the core and exterior of the mass concrete to 35°F. Limiting the differential temperature is specified to avoid cracking due to excessive thermal stresses in the concrete. Cracking due to thermal behavior may cause loss of structural integrity and monolithic action, or may cause excessive seepage and shortening of the service life of the concrete structure or may be esthetically objectionable (American Concrete Institute (ACI), 1999)

The high core temperatures were recorded in mass concrete structures cured in accordance with maintaining the maximum differential temperature of 35°F throughout the curing period. These high temperatures have raised concerns on the effects of high curing temperatures on the strength and durability of mass concrete structures. Of

additional concern is the potential of delayed ettringite formation (DEF) in the hardened concrete when cured at such high temperatures and its associated deterioration of the concrete structure. Ettringite in Portland cement systems is the first hydrate to crystallize during the first hour of placing the concrete. At high curing temperatures ($>160^{\circ}\text{F}$), the ettringite becomes unstable and decomposes only to reform later in the hardened concrete in the presence of moisture with associated cracking of the structure. Concretes cured at temperatures above 160°F are susceptible to DEF in the hardened concrete. Isolated cases of expansion and cracking from DEF have occurred in some in-situ concretes of large section and high cement content in the U.K. These in-situ concretes were cast in the summer months and the possible early peak temperature was between 185 and 200°F . The cracking took between 8 and 20 years to manifest itself (Hobbs, 1999). The cement-water reaction during the hydration of cement is an exothermic reaction. Due to the low diffusivity of heat from concrete, it acts as a insulator and in a large concrete mass, the heat liberated from the reaction can accumulate and lead to high temperatures.

A study by Tarkhan (2000) of mass concrete specifications used by state highway agencies in the United States found that nine highway agencies of the forty-three respondents had mass concrete specifications. Highway agencies of Illinois and Kentucky specified a maximum curing temperature of 160°F . A maximum differential temperature of 35°F was specified by eight of the nine highway agencies with mass concrete specifications. 65% of all respondents believed that there is a need for further research into the effects of high curing temperature on concrete properties. Reasons cited to limit the maximum curing temperature of mass concrete elements included:

- Avoid reduction of later age strength,

- Minimize swelling and shrinkage cracking,
- Increase the durability of the concrete and
- Decrease the formation of delayed ettringite (DEF) in the hardened concrete and its subsequent damage.

There are several known potential causes of cracking in concrete. One is excessive stress due to applied loads and another is cracks due to drying shrinkage or temperature changes in restrained conditions. Mass concrete is often subject to both of these stresses; therefore, prevention of cracking is a vital consideration in the design of these structures. However, during the construction process, the most pressing item is the control of drying shrinkage and differential temperature. The rise in temperature of mass concrete depends on the initial concrete temperature and volume to surface area ratio. Furthermore, the increase in temperature is affected predominantly by the chemical composition of cement, with C₃A (Tricalcium Aluminate) and C₃S (Tricalcium Silicate) being the compounds primarily responsible for elevated temperature development. The water-cement ratio, fineness of the cement, concrete mixture temperature and temperature of curing are also contributors to the development of heat. When the water-cement ratio, fineness, or curing temperature is increased, the heat of hydration is increased. The rate and amount of heat generated are important in any concrete construction requiring considerable mass. The heat accumulated must be rapidly dissipated in order to impede a significant rise in concrete temperature at the center of the structure. The excessive rise in concrete temperature is undesirable since the concrete will harden faster at an elevated temperature and any non-uniform cooling of the concrete structure may create stresses due to thermal contraction.

The current method of preventing cracking in mass concrete is to maintain a temperature differential (between the surface and the core) of no more than 35°F. Control of temperature gain is possible (Kosmatka and Panarese, 1994) through the following:

- Low-heat-of-hydration Portland or blended cement
- Reductions in the initial concrete temperature to approximately 50°F by cooling the concrete ingredients
- Cooling the concrete through the use of embedded cooling pipes during curing
- Low lifts: 5 ft or less during placement.
- Pozzolans: the heat of hydration of pozzolan is approximately 25 to 50% that of cement.

When the massive concrete specified has high cement contents (500 to 1000 lb. per cu yard), many of the above mentioned placing methods cannot be used. For concretes that are often used in mat foundations and power plants good placing methods (Kosmatka and Panarese, 1994), are the following:

- Place the entire concrete section in one continuous pour
- Avoid external restraint from adjacent concrete elements
- Control internal differential thermal strains by preventing the concrete from experiencing excessive temperature differential between the internal concrete and the surface.

In order to control the internal temperature differential, the concrete is insulated to keep it warm (tenting, quilts, or sand on polyethylene sheeting). Studies have shown that the maximum temperature differential (MTD) between the interior and exterior concrete should not exceed 35°F to avoid surface cracking.

The Florida Department of Transportation Standard Specifications Section 450 allows the maximum curing temperature of 158 to 176°F for accelerated curing of pre-

stressed concrete elements. However, accelerated curing is conducted under suitable enclosures with a controlled environment to avoid thermal shock and minimize moisture loss. These conditions do not exist in mass concrete operations and such high temperatures may have detrimental effects on concrete properties. It is therefore necessary to revisit the current specification for mass concrete, and examine the need for additional provisions. The provisions that need to be reconsidered are maximum internal concrete temperature and/or maximum concrete placing temperature.

Objectives and Scope of Research

The objectives of this dissertation were as follows:

- To determine the effects of concrete curing temperature on the strength and durability of concrete, using typical FDOT Class IV mass concrete mixes.
- To determine the effects of fly ash and slag on the strength and durability of concrete cured at elevated temperatures.
- To determine the propensity of typical FDOT class IV mass concrete mixes to DEF when cured at elevated temperatures.
- To determine the effect of permeability of the concrete microstructure on the onset and amount of ettringite formed.
- To determine the effect of replacing part of the cement with fly ash or slag on the onset and amount of ettringite crystals formed in samples cured at the elevated temperatures.

The concrete used for this research will be typical class IV FDOT mass concrete mixes. The use of fly ash and slag as partial replacement of cement is known to increase the durability and strength of concrete. There is little information available on its influence on ettringite formation in concrete cured at elevated temperatures. This

dissertation reports findings on how the strength and durability of concrete cured at the elevated temperatures. Additionally by the use of Scanning electron Microscope, this dissertation presents findings on ettringite formation in concrete curried at elevated temperatures and how this is influence by the addition of fly ash and slag.

Research Methodology

This dissertation was conducted by performing the following tasks:

1. Performed a state of the art review of work reported on heat generation in mass concrete and measures taken to avoid cracks and premature deterioration of concrete.
2. Evaluation of the effects of concrete temperature on the properties of hardened concrete. The evaluation included the following tests: compressive strengths, rapid chloride permeability, time to corrosion, volume of permeable voids, and microstructure analysis using the Scanning Electron Microscope (SEM).
 - a. Class IV - Structural concrete mixes, consisting of 18% replacement by weight of cement with class F fly ash, were used. Specimens required for the above mentioned tests were cast at room temperature and stored in water tanks where they were subjected to different curing temperatures (73 to 200°F).
 - b. Other mixes tested were similar to Part a, except that 50% of cement was replaced by slag. Molds were cast and stored as explained in part a.
3. Analyzed the test results and determine the maximum internal concrete temperature above which the concrete properties will be affected (later age strength reduction, durability problems, and DEF).

4. Examination of the current FDOT mass concrete specifications and suggest, if necessary, the requirement for maximum curing temperature or maximum concrete placement temperature.

Importance of Research

The research presented in this dissertation will provide information on the effect of elevated curing temperatures on the strength and durability of typical class IV FDOT mass concrete mixes. Additionally information from this research will serve as a basis to decide if the specification for mass concrete used by FDOT should specify a limit on the maximum curing temperature. Fly ash and slag are used in typical class IV mass concrete and this research will show their effect at high curing temperatures on the strength and durability of the concrete and the potential of DEF formation.

CHAPTER 2 LITERATURE REVIEW

Introduction

This chapter presents a state-of-the-art review of literature on how strength, durability and formation of delayed ettringite (DEF) in concrete are affected by high curing temperatures. In massive concrete structures, high curing temperatures result from a combination of heat produced by the hydration of concrete and the relatively poor heat dissipation of concrete. Although various measures are implemented to limit the maximum temperatures in mass concrete, a high core temperature of 200°F has been recorded in Florida for a mass concrete structure cast during the summer. While such concrete meets the specification of maintaining a maximum differential temperature of 35°F between the core and surface of the mass concrete structure, of major concern is what happens to the strength, durability and DEF in the concrete when subjected to such high curing temperatures.

This chapter reviews how heat is generated in concrete from the hydration of cement. Cracking of concrete due to the heat as well as the microstructure formed under such high temperature curing is examined. The influence of the microstructure formed under high curing temperatures on the strength and durability of concrete are presented. To improve the quality of concrete structures cured under high temperatures, other cementitious materials such as fly ash and blast furnace slag have gained increasing use in mass concrete structures. The effects on the microstructure of concrete due to the use of such materials and the influence on strength and durability of mass concrete structure

are reviewed. A final review is presented on how high curing temperatures makes hardened concrete structures susceptible to damage from the formation of delayed ettringite (DEF).

Cement Hydration

The compounds of Portland cement (see Table 2.1) are nonequilibrium products of high temperature reactions in a high-energy state. When cement is hydrated, the compounds react with water to acquire stable low-energy states, and the process is accompanied by the release of energy in the form of heat (Mehta and Monteiro, 1993). Cement acquires its adhesive property from its reaction with water by forming products, which possess setting, and hardening properties.

Table 2.1 Major Compounds of Portland Cement

Name of compound	Oxide composition	Abbreviation
Tricalcium Silicate	$3\text{CaO} \cdot \text{SiO}_2$	C_3S
Dicalcium Silicate	$2\text{CaO} \cdot \text{SiO}_2$	C_2S
Tricalcium Aluminate	$3\text{CaO} \cdot \text{Al}_2\text{O}_3$	C_3A
Tetracalcium Aluminoferrite	$4\text{CaO} \cdot \text{Al}_2\text{O}_3 \cdot \text{Fe}_2\text{O}_3$	C_4AF

The heat generated from the hydration of cement causes a rise in temperature of concrete. If this rise occurred uniformly throughout a given concrete element without any external restraint, the element would expand until the maximum temperature has been reached. The concrete will then cool down with uniform contraction as it loses heat to the ambient atmosphere. This uniform expansion and contraction will result in no thermal stresses within the concrete element. According to Neville (1997), restraint exists in all but the smallest of concrete members. These thermal restraints result in external and internal cracking of the concrete. Figure 2.1 shows an example of temperature change,

which causes external cracking of large concrete mass. The critical 20°C (35°F) temperature difference occurs during cooling (FitzGibbon, 1976).

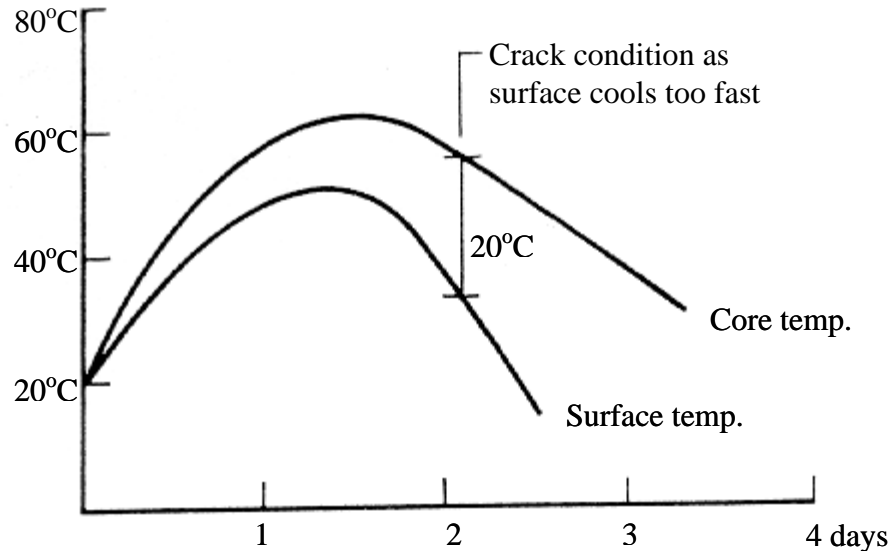


Figure 2.1 External thermal cracking

In massive concrete structures, internal restraint occurs from the inability of the heat to dissipate quickly from the core of the member due to the low thermal diffusivity of the concrete. A temperature differential is set up between the core of the concrete and the surface due to the accumulation of the heat from the hydration process. The unequal thermal expansion in the various parts of the concrete member results in stresses, compressive in one part and tensile in the other. Cracking of the surface results when the tensile stresses at the surface of the element due to the expansion of the core exceed the tensile strength of the concrete. According to FitzGibbon (1976), the cracking strain of concrete is reached when an internal thermal differential of 20°C (36°F) is exceeded.

Figure 2.2 shows a pattern of temperature change, which causes internal cracking of a large concrete mass. The critical 20°C (36°F) temperature is reached during heating but

cracks open only when the interior has cooled through a greater temperature range than the exterior.

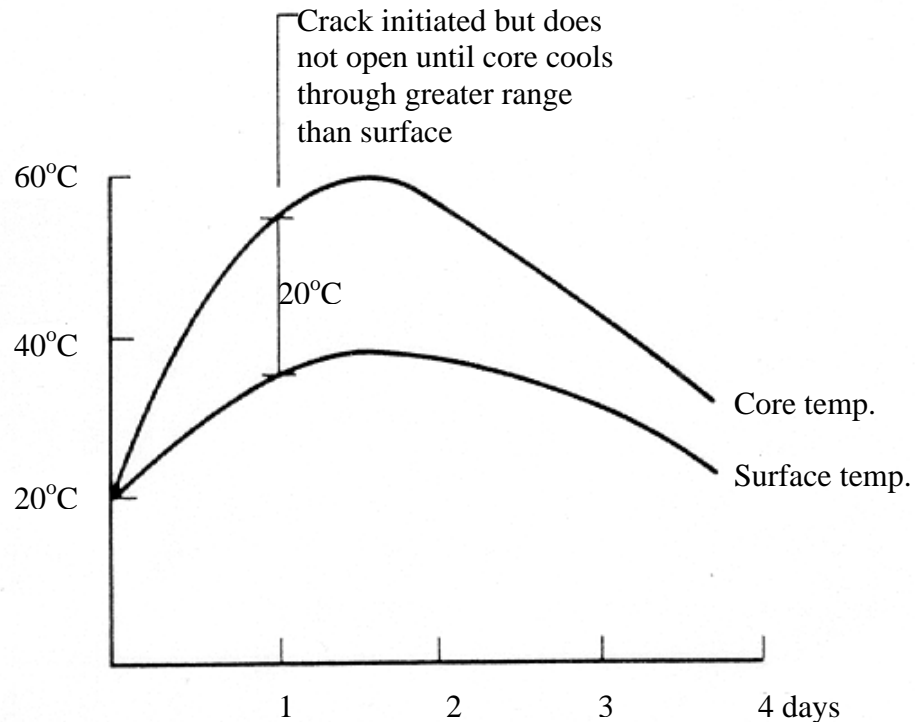


Figure 2.2 Internal thermal cracking

Cracking due to thermal behavior may cause loss of structural integrity and monolithic action or may cause extreme seepage and shorten the service life of the concrete structure. Various measures are undertaken to reduce the temperature rise in large concrete pours. Notable among these measures include:

- The prudent selection of a low-heat-generating cement system including pozzolans;
- The reduction of the cementitious content;
- The careful production control of aggregate gradations and the use of large-size aggregates in efficient mixes with low cement contents;

- The precooling of aggregates and mixing water (or the batching of ice in place of mixing water) to make possible a low concrete temperature as placed;
- The use of air-entraining admixtures and chemical admixtures to improve both the fresh and hardened properties of the concrete;
- Coordinating construction schedules with seasonal changes to establish lift heights and placing frequencies;
- The use of special mixing and placing equipment to quickly place cooled concrete with minimum absorption of ambient heat;
- Dissipating heat from the hardened concrete by circulating cold water through embedded piping;
- Insulating surfaces to minimize thermal differentials between the interior and the exterior of the concrete.

Despite the application of the above-mentioned measures to control temperature rise in concrete, maximum core temperatures of 200°F have been recorded in Florida. This high temperature have been reached while satisfying the specification for mass concrete of maintaining a maximum temperature differential of 35°F between the core and the surface of the concrete structure. Of increasing concern is the effect on the properties of concrete when subjected to such high curing temperatures. An examination of the microstructure of concrete formed at high curing temperatures is reviewed next.

Effect of Curing Temperature on the Microstructure of Hydrated Cement Paste

Verbeck and Helmuth (1968) found the reactions between cement and water to be similar to any other chemical reaction, proceeding at a faster rate with increasing temperature. This rapid initial rate of hydration at higher temperatures they theorize retards subsequent hydration of the cement producing a non-uniform distribution of the

products of hydration within the paste microstructure. At high temperatures, there is insufficient time available for the diffusion of the products of hydration away from the cement particles due to the low solubility and diffusivity of the products of hydration. This results in a non-uniform precipitation of the products of hydration within the hardened cement paste.

The results of a calorimetric study on the early hydration of cement as reported by Neville (1997) indicate that a heat evolution peak occurs at about 6 to 8 hours after the initialization of the hydration process at normal temperatures. This was revealed from early hydration reactions of cement, using the conduction calorimeter (Verbeck and Helmuth, 1968). During this period, the cement undergoes very rapid reactions with 20 percent of the cement hydrating over a 2 or 3-hour period. At an elevated temperature of 105°F, these reactions are accelerated with as much as 30 to 40 percent of the cement hydrating in a 2-hour period. At steam curing temperatures, 50 percent or more of the cement hydrates in an hour or less.

Products of cement hydration have low solubility and diffusivity and at high curing temperatures, the rapid hydration does not allow for ample time for the products to diffuse within the voids. This results in a high concentration of hydration products in a zone immediately surrounding the grain. This forms a relatively impermeable rim around the cement grain, which subsequently retards any subsequent hydration (Verbeck and Helmuth, 1968). This situation does not occur in normal temperature curing where there is adequate time for the hydration products to diffuse and precipitate relatively uniformly throughout the interstitial space among the cement grains. The coarse pore structure in

the interstitial space from the high temperature has a detrimental effect on the strength of concrete.

Further evidence from Goto and Roy (1981) confirms the observation by Verbeck and Helmuth (1968) of retardation of subsequent cement hydration at high temperatures. In an examination of the structure of the hydrated cement paste subjected to high temperatures in its early life, Goto and Roy (1981) found out that curing at 60°C (140°F) resulted in a much higher volume of pores larger than 150nm in diameter compared with curing at 27°C (81°F). These large pores make the concrete susceptible to deterioration from harmful substances, which are easily transported through the concrete structure.

A study by Kjelsen et al (1990) of the microstructure of cement pastes hydrated at temperatures ranging from 41 – 122°F (5 – 50°C) using backscattered imaging found that the low curing temperatures resulted in a uniform distribution of hydration products and fine self-contained pores. Elevated temperatures on the other hand resulted in a non-uniformly distributed hydration products and coarse, interconnected pores. The microstructure of the hydrated cement paste formed at high curing temperatures affect the strength and durability of the concrete. The large interconnected pores resulting from high temperature curing does not make for durable concrete structures. Since strength resides in the solid parts of a material, the presence of voids as a consequence of high curing temperature are detrimental to the strength of the concrete.

Dense Shell of Hydration Products

Kjellsen, Detwiler and GjØrv (1990) support the concept that a dense shell of hydration products surrounding the cement grains is formed at higher curing temperatures. Hydration products are more uniformly distributed at lower temperatures. In addition, at higher temperatures of curing there are five phases as opposed to the

standard four phases at lower temperatures. The five phases are unhydrated cement, calcium hydroxide, two densities of C-S-H and pores. The strength of the material is greatly affected by the uniformity of the microstructure. At the elevated temperatures the C-S-H close to the grains is much denser and stronger. However, the intervals between the cement grains determine the strength of the concrete. Therefore curing at elevated temperatures has a harmful effect on the later-age strength of concrete. Additionally elevated curing temperatures according to Kjellsen, Detwiler and GjØrv (1990) result in increased porosity. Kjellsen, Detwiler and GjØrv (1990) further noted that C₃S pastes that were cured at higher temperatures (50-100°C) had a coarser structure, including an increase of large pores, over those cured at 25°C. Even steam curing (97°C) resulted in coarser pore structure. The difference in porosity is attributed mostly to the difference in volume of pores of radius 750-2300 Å. For plain cement pastes of equal water-cement ratios cured to the same degree of hydration, the higher the curing temperature the greater the total porosity. The results indicate that large pores have the greatest effect on permeability. Permeability is a contributing component to most durability problems, therefore it is suggested that higher curing temperatures possibly reduce the durability of plain cement concretes.

Effect of Curing Temperature on Concrete Strength Development

The strength of concrete is its ability to resist stress without failure. Strength of concrete is commonly considered its most valuable property. Strength usually gives an overall picture of the quality of concrete because it is directly related to the structure of the hydrated cement paste (Neville, 1997).

A rise in curing temperature according to Neville (1997) speeds up the hydration process so that the structure of the hydrated cement paste is established early. Although a

higher temperature during placing and setting increases the very early strength, it may adversely affect the strength from 7 days (Neville, 1997). This is because the rapid initial hydration according to Verbeck and Helmuth (1968) appears to form products of a poorer physical structure, probably more porous, so that a proportion of the pores will always remain unfilled. Since the voids do not contribute to the strength of concrete, a low temperature with slow hydration will result in a uniform distribution of hydration products within the interstitial space and high strengths at latter ages.

A fast hydration of cement from high curing temperatures will result in a high early strength due to more hydration products being formed. At latter ages however, the retardation in hydration as a result of a dense shell around the hydrating cement grains will result in a more porous structure and reduced strengths as shown in Figure 2.3 (Verbeck and Helmuth, 1968).

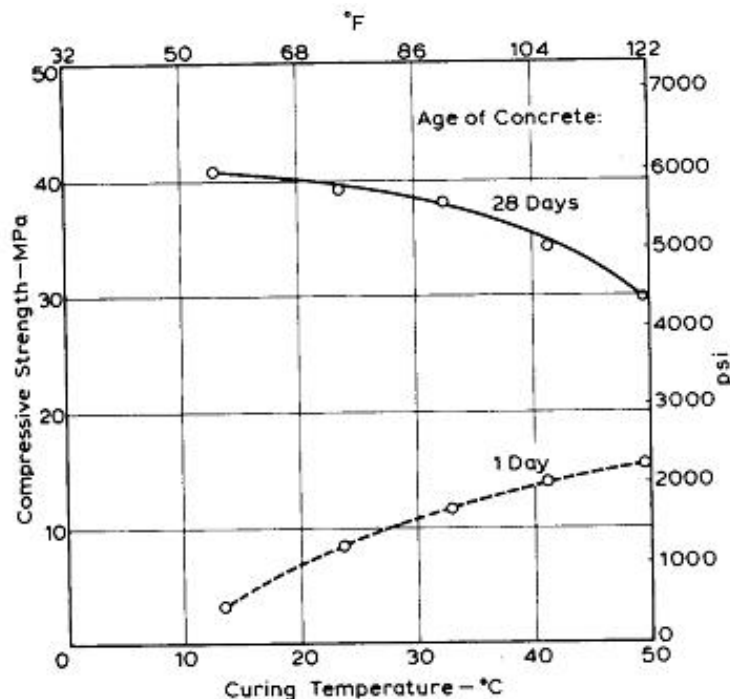


Figure 2.3 Effect of curing temperature on concrete strength development

Effect of Temperature on the Durability of Concrete

According to ACI Committee 201, durability of Portland cement concrete is defined as its ability to resist weathering action, chemical attack, abrasion, or any other process of deterioration. Durable concrete will retain its original form, quality, and serviceability when exposed to its environment. Although designers of concrete structures have been mostly interested in the strength characteristics of concrete, durability issues in concrete technology have been brought to the forefront in recent times as a result of the premature failure of nondurable concrete structures.

The pore structure of the concrete determines the ease with which deleterious harmful substances such as chloride ions are transported into the concrete. Harmful substance such as chloride ions in concrete attack and corrode the steel resulting in premature failure of the structure. High curing temperatures in concrete result in porous concrete. This is because the low diffusivity of the hydration products does not allow for uniform distribution at high curing temperatures due to the faster reaction rate. These hydration products precipitate in the vicinity of the cement grains resulting in a more porous concrete. At low curing temperatures, the hydration products are uniformly distributed within the interstitial spaces making it difficult for deleterious harmful substances to be transported into the concrete

Kjellsen et al. (1990) performed an investigation of the pore structure of plain cement pastes hydrated at 41, 68 and 122°F (5, 20 and 50°C respectively). The specimens were tested when they reached 70% hydration, a time marking adequate development of the microstructure. Two techniques used to measure porosity in this study were mercury intrusion and backscattered electron images. They theorized that during hydration at elevated temperatures cement hydration proceeds more rapidly. Subsequently since the

cement has low solubility and low diffusibility, cement hydration products are not able to disperse at a significant distance from the cement grain in the limited time provided at high temperature curing. This causes areas of dense hydration products that act as a barrier, preventing further hydration. When there is a development of dense hydration product there is also a development of greater volume of large pores and a coarser pore structure. The large pores correspond to a reduction in the modulus of elasticity of the concrete indicating increased cracking as it is exposed to structural stresses.

The curing temperature clearly affected the pore structure of hydrated cement paste as shown in Table 2.4. The higher curing temperature resulted in a greater quantity of larger pores as well as an increase in the total porosity. These results are in agreement with the observation by Goto and Roy (1981) that curing at 60°C (140°F) resulted in a much higher volume of pores larger than 150nm in diameter compared to curing at 27°C (81°F). These larger pores make the concrete more susceptible to attack by harmful substances since they provide an easier pathway through the concrete. Permeability is a contributing factor to various kinds of durability problems, therefore suggesting that high curing temperatures could reduce the durability of plain cement concretes. The increased permeability also leads to increased water intrusion to the reinforcing steel and promoting an increase to the rate of corrosion of the members.

Table 2.2 Measured Porosity

Curing temperature	Porosity (MIP + HP)	Porosity (BSEI)	Standard deviation
41°F	33.2%	4.27%	.818%
68°F	34.2%	10.93%	1.086%
122°F	35.7%	15.11%	1.881%

Campbell and Detwiler (1993) explain that the durability of concrete is a primary contributor to its satisfactory performance. Agencies typically control the durability of concrete by restricting the water-cement ratio to 0.45 or less. However, the curing process is often overlooked, though it also affects the durability of the concrete. A basic principle noted is that the Portland cement concretes resistance to penetration by chloride ions is reduced due to coarsening of the cement paste pore structure. Specifying a low water-cement ratio provides limited effectiveness in bettering the performance of the concrete.

Fly ash and Slag in Concrete

Class F fly ash is an artificial pozzolanic material, which possesses no cementitious value, but in finely divided form, in the presence of moisture, chemically reacts with calcium hydroxide from the Portland cement reaction to form compounds possessing cementitious properties. The fly ash reaction products closely resemble the calcium silicate hydrate produced by hydration of Portland cement (Neville, 1997). The fly ash reaction does not start until sometime after mixing. According to Fraay et al (1989), the glass material in fly ash is broken down only when the pH value of the pore water is at least about 13.2. The increase in alkalinity required for the fly ash reaction is achieved through the reaction of the Portland cement. At high temperatures, the fly ash reaction takes place sooner due to the increased hydration rate of the cement. Prior to the reaction of the fly ash particles, they act as nuclei for the precipitation of the cement hydration. When the pH of the pore water becomes high enough, the products of reaction of fly ash are formed on the fly ash particles and in their vicinity. With the passage of time, further products diffuse away and precipitate within the capillary pore system, this result in a reduction of the capillary porosity and consequently a finer pore structure (Fraay et al,

1989). Figure 2.8 shows the changes in pore size distribution determined by mercury porosimetry, in cement paste containing 30 percent of Class F fly ash by means of total cementitious material (Fraay et al, 1989). The cement paste becomes increasingly denser after the initiation of the pozzolanic reaction of fly ash.

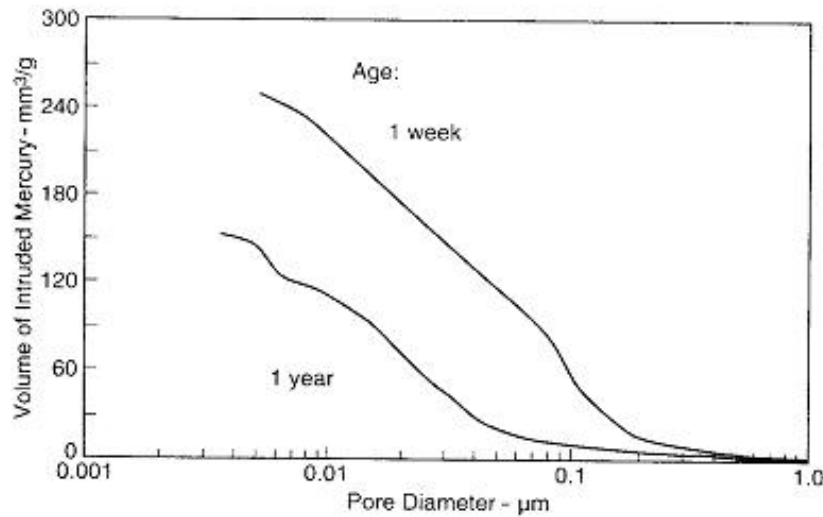


Figure 2.4 Pore size distribution with age for 30% Fly ash mix

Slag is a waste product in the manufacture of pig iron. Chemically, slag is a mixture of lime, silica and alumina, the same oxides that make up Portland cement (Neville, 1997). Compared to the fly ash, finely ground granulated blast-furnace slag is self-cementing. It does not require calcium hydroxide to form cementitious product such as calcium silicate hydrates. When used on its own, the amounts of hydration products formed by the blast-furnace slag is insufficient for application of the material to structural purposes. Used in combination with Portland cement, the hydration of the slag is accelerated in the presence of calcium hydroxide and gypsum (Mehta and Monteiro, 1993). The beneficial effects of slag arise from the denser microstructure of the hydrated cement paste, more of the pore space is filled with the hydration products than in cement only mixes.

Supplementary cementing materials are suggested to increase the performance of the concrete. Campbell and Detwiler investigated the optimum mix design for satisfactory strength and durability of steam-cured concrete with 0.45 water-cement ratio and various compositions of Canadian Type 10 cement (ASTM Type I) with slag and silica fume. The compressive strength of the cylinders after 18 hours of steam curing and one day of moist curing were compared. The results as shown in Table 2.5 reveal that slag is effective in reducing the rate of chloride ion diffusion and therefore increasing the durability of the concrete. However the mixes with silica fume and slag, or silica fume alone were more durable.

Table 2.3. Results of compressive strength and AASHTO T-277 test

Mix no.	Description	Compressive strength MPa	Total Charge passes, coulombs, average of three slices	Rating
M1	Control:100% PC	27.3	11130*	High
M2	30% Slag	25.3	7800	
M3	40% Slag	27.9	7690	
M4	50% Slag	28.9	4500	
M5	5.0% SF	32.6	1780	Low
M6	7.5% SF	33.3	910	Very Low
M7	10.0% SF	36.4	290	
M8	30% Slag; 7.5% SF	28.5	350	
M9	40% Slag; 7.5% SF	31.3	200	
M10	30% Slag; 10% SF	34.5	150	
*Extrapolated value.				

Detwiler, et al. (1994) investigated the chloride penetration of 0.4 and 0.5 water-cement ratio concretes containing either 5 percent silica fume or 30 percent slag (substitution by mass) cured at elevated temperatures. They found that higher curing temperatures resulted in greater penetration of chloride ions. In addition, at any given

temperature, both the silica fume and slag concretes performed better than the Portland cement concrete. Their studies showed that the use of pozzolanic materials is more effective than lowering the water-cement ratio from 0.5 to 0.4 in improving the resistance to chloride ions (Tables 2.6 and 2.7).

Table 2.4 AASHTO T-277 tests for charge passed

Mix	w/c	73°F	122°F	158°F
Portland Cement	.40 .50	5700 9800	12,000† 13,000†	18,000† 16,000†
5 % Silica Fume	.40 .50	1500 1800	3000 3400	4100 13,000
30% Slag	.40 .50	1300 1700	1500 2200	4300 5400

*Charge(coulombs) passed in 6 hr for concretes cured at constant temperatures indicated to degree of hydration of approximately 70 percent.

†Extrapolated values. These tests were terminated before the full 6 hr had elapsed due to excessive temperature increases.

Table 2.5 Rate of chloride diffusion ppm/day (average of three replicates, Norwegian test)

Concrete	w/c	73°F	122°F	158°F
Plain Cement	.40 .50	10 13	12 15	34 38
5 % Silica Fume	.40 .50	4 3	7 5	12 22
30% Slag	.40 .50	3 6	4 7	13 18

Delayed Ettringite Formation (DEF) in Concrete

In the early 1980's, Heinz and Ludwig (1987) observed that precast units made of high strength concrete that had been heat treated during production, showed damage of the structure connected with a loss of strength. These damages occurred in those building components which for several years had been subjected to open-air weathering and

therefore to frequent saturation. The damage was characterized by crack formation emerging from the edges of the building components as well as a loss of bond between the cement paste and the coarse aggregates. The damage was attributed to the late formation of ettringite in the hardened concrete. Delayed ettringite formation (DEF) is the destructive development of ettringite in concrete, months or years after placement in an environment where moisture exposure is frequent (Hime and Marusin, 1999). DEF is a worldwide phenomenon having been found in railway ties (sleepers) produced in Germany, Finland, The United States, Australia and South Africa (Hobbs 1999, Heinz & Ludwig 1987, Hime & Marusin, 1999).

Ettringite ($C_6\overline{ASH}_{32}$) in Portland cement systems is the first hydrate to crystallize during the first hour of placing the concrete. This is because of the high sulfate/aluminate ratio in the solution phase during the first hour of hydration. The precipitation of early ettringite contributes to stiffening (loss of consistency), setting (solidification of the paste) and early strength development. Later, after depletion of sulfate in the solution when the aluminate concentration goes up again due to renewed hydration of C_3S and C_4AF , ettringite becomes unstable and is gradually converted into monosulfate ($C_4\overline{ASH}_{18}$) which is the final product of Portland cements containing more than 5 percent of C3A (Mehta & Monteiro, 1993). At high curing temperatures, the decomposed ettringite reforms in the hardened concrete in the presence of moisture with the resultant expansion and deterioration of the concrete. In a study of expansions in mortar samples subjected to higher curing temperatures, Lawrence (1995) found that the minimum curing temperatures for expansion lie between 65 and 70°C. The primary ettringite is unstable when cured at this temperature due to the amount of alkalis in the

pore liquid. If the concrete is exposed to such temperatures, primary ettringite will not be formed and that which was formed prior to such a heat treatment will decompose (Stark & Seyfarth, 1999). Under moist conditions, at or below room temperature, ettringite again becomes the stable phase and may cause DEF (Heinz, Kalde, Ludwig & Ruediger, 1999).

The microstructure of concretes and mortars after expansion is characterized by the presence of bands of ettringite around aggregate particles and within cracks, pores and voids in the cement paste (Scrivener & Lewis, 1999). The expansive process in DEF is marked by enlargement of the affected concrete and the development of gross cracking. In extreme cases, the concrete becomes crumbly and soft, proving evidence of the destruction of the effectiveness of the cement paste binder (Diamond, 1996).

DEF is not only limited to precast concrete units, recent observations of DEF in large sections of in-situ concrete have been made in the U.K. (Johansen & Thaulow, 1999). DEF whether formed as a result of steam curing or from high core temperature from larger sections of concrete cast in-situ has been found by Diamond (1996) to exhibit similar crack patterns and microstructural features. The observed crack pattern is that of a network with component crack segments running partly along aggregate peripheries (rim cracks), but generally connecting through segments running through the cement paste (paste crack). Two opposing schools of thought exist as to how DEF leads to expansion of the concrete. The homogeneous paste expansion theory (Johansen & Thaulow, 1999), maintains that the paste expands and the DEF is deposited in the gaps created between the aggregates and the paste as the aggregates do not expand. This theory is refuted by many writers among them Diamond (1996) who maintain that crystal pressure from the

formation of ettringite better explains the expansion and subsequent deterioration of the concrete.

The expansion associated with the formation of ettringite is influenced by the microstructure of the material in which it is deposited and the amount of pore space available (Taylor, Famy & Scrivener, 2001). Some of the ettringite produced is deposited freely in available space and does not contribute to expansion. Thus, the expansion does not depend simply on the amount of ettringite produced. Additionally, expansion depends on the quality of the pore space. A given amount of ettringite will produce more expansion if the pores in which it is deposited are small and poorly connected than if they are large and more highly connected.

SEM examination at 180 days and 5 years of concrete cured at various temperatures showed the following (Stark & Seyfarth, 1999):

- For normally cured concrete, there was no evidence of ettringite at 180 days but at 5 years the concrete showed a dense structure with fine ettringite needles covered the pore surfaces, without filling the pores completely. An accumulation of ettringite in the available spaces due to transportation processes took place within the time interval.
- At 180 days samples cured at 60°C showed small needle-like crystals evenly distributed on pore surfaces and in interfaces between aggregate and hardened cement paste. At 5 years the ettringite found was in larger crystals and in substantially larger amounts than found at 180 days. The concrete was crack-free comparable to the normally cured concrete. The concrete was intact with no hint

of damage, indicating that the existence of ettringite in internal damages of hardened concretes is not an indication of damaging ettringite formation.

- Samples cured at 90°C showed large ettringite crystals in structurally damaged areas and on surfaces of pores. After 5 years, the concrete was completely interspersed with microcracks. Pores, microcracks and interfaces were completely filled with new phase formations of ettringite.

CHAPTER 3 RESEARCH METHODOLOGY

Introduction

This chapter presents the materials, mixtures, and test methods used to evaluate the effects of elevated curing temperatures on the strength, durability and formation of Delayed Ettringite (DEF) in mass concrete. The work was divided into three phases as follows:

- In phase 1, three mixes of pastes comprising plain cement, cement with 18% fly ash and cement with 50% fly ash were cured at temperatures of 73, 160 and 200°F for various durations to determine the age at which a maturity of 70% degree of hydration of the cement was attained. Once this age was determined for the various mixes and curing temperatures, mass concrete with binders in the same proportions as in the paste would be made and tested when they reached 70% degree of hydration. This would ensure that all the mass concrete properties would be determined at the same maturity and make for easy comparison. Difficulty in establishing and exact time to reach 70% degree of hydration as well as inability to reach this maturity in the cement/fly ash mixes resulted in using the curing durations of 7, 28 and 91 days as the bases of comparing the mass concrete properties.
- In phase II, four FDOT Class IV mass concrete mixtures were made and cured at temperatures of 73°F, 160°F and 180°F for durations of 7, 28 and 91 days. The concrete samples were tested to determine the following properties:
 - Compressive strength – ASTM C 39 (ASTM 1996)

- Resistance to chloride penetration – ASTM C 1202 (ASTM 1994)
- Time to Corrosion – FM 5-522
- Density and percentage of voids – ASTM C 642 (ASTM 1997)
- Phase III. This phase involved microstructure analysis of the mass concrete by the aid of a scanning electron microscope. Mortar samples sieved from the concrete mixes were subjected to the same curing regime. At each test age, the mortar samples were removed and placed in methanol to stop further hydration of the cement. After a minimum of 7 days in the methanol, $\frac{1}{4}$ inches thick wafers were cut from the samples. These wafers were fractured and examined to determine the presence or lack of ettringite crystals.

Degree of Hydration

Introduction

A well-hydrated Portland cement paste consists mainly of calcium silicate hydrates, calcium sulphoaluminate hydrates and calcium hydroxide (Metha and Monteiro, 1993). When the cement paste is ignited to a temperature of 1832°F (1000°C), the nonevaporable water chemically combine in the hydration products is released. The degree of hydration is a measure of the nonevaporable water content of the paste expressed as a percentage of the nonevaporable water content of fully-hydrated cement paste. The nonevaporable water content of fully-hydrated cement paste is 0.23 grams of water per gram of cement (Basma et al, 1999).

For this study a degree of hydration of 70% was decided as the maturity level at which the mass concrete properties would be determined. The choice of 70% degree of hydration was based on a study by Kjellsen et al (1990) who found that the time required to attain this level of maturity is not so long as to be impractical to replicate in the

laboratory. Additionally, by this point, the rate of hydration has slowed enough that small variations in curing time will not result in significant error making for easy comparison of the various samples.

Methodology

Tables 3.1 and 3.2 show the chemical composition and physical properties of the cement, fly ash and blast furnace slag used in the study. The Portland cement used was AASHTO Type II. Described here are the methods applied to determine the time to attain 70% degree of hydration for three paste mixes isothermally cured at temperatures of 73, 160 and 200°F. The three paste mix designs tested are as follows

1. Plain cement paste mix
2. Cement and 18% Fly ash paste mix
3. Cement and 50% Fly ash paste mix

Table 3.1 Properties of Cement and Fly ash

Chemical Composition	Portland Cement	Fly Ash
% Silicon Dioxide (SiO_2)	20.6	86.9
% Aluminum Oxide (Al_2O_3)	5.1	
% Ferric Oxide (Fe_2O_3)	4.7	
% Magnesium Oxide (MgO)	0.7	
% Sulfur Trioxide (SO_3):	3.2	0.2
% Tricalcium Silicate (C_3S)	50.0	-
% Tricalcium Aluminate (C_3A)	5.6	-
% Total Alkalies as Na_2O	0.52	-
% Insoluble Residue	0.12	-
Loss of Ignition (%)	1.5	3.2
Physical Properties		
Fineness:	Blaine (m^2/kg) - 341	#325 Sieve - 34%
Time of Setting (Gilmore):		Fly ash activity index:
Initial (Minutes)	145	7 Days – 69%
Final (Minutes)	235	28 Days – 78%
Compressive Strength (PSI) – ASTM C-150:		
3 Days	3200	-
7 Days	4070	-

Table 3.2. Properties of Blast furnace slag –ASTM C 989-97b, AASHTO M302

Chemical Analysis	
% Silicon Trioxide (SiO_3)	2.3
% Sulfide Sulfur	0.9
Slag Activity Index	
7 Days	96%
28 Days	132%
Physical Properties	
Fineness: #325 Sieve (45um)	2%
Compressive Strength (PSI):	
7 Days STD Average	4750
7 Days Slag Average	4380
28 Days STD Average	5900
28 Days Slag Average	7810
Blast furnace slag produced by Lafarge in Tampa	

Table 3.3. Mix proportions of paste mixes

Mix design	Cement (lbs)	Fly Ash (lbs)	Water (lbs)	w/b ratio	Mixing Water °F
18% fly ash at 73°F	3.540	.777	1.77	.41	73
18% fly ash at 160°F and 200°F	5.057	1.110	2.53	.41	136
50% fly ash at 73°F	2.467	2.467	2.02	.41	73
50% fly ash at 160°F and 200°F	3.083	3.083	2.53	.41	136

The proportions of materials used in the paste mixes are shown in Table 3.3. The pastes were made in accordance to ASTM C 305-99. The procedures followed to determine the degree of hydration were as follows:

- a. Three samples each was made of each paste mix to be tested at each curing period and temperature. Samples at 73°F were tested at ages of 1, 3, 7, 10, 14, 28 and 56 days. Samples at 160 and 200°F were tested at ages of 1, 3, 7, 10 and 14 days.
- b. The water used for samples cured at 160°F and 200°F was preheated to 136°F, to produce a cement paste with temperature of approximately 98°F. This was done to reduce the time for samples cured at 160 and 200°F to be in equilibrium in the curing environment.
- c. Samples were cast in 1-ounce polypropylene screw cap jars (1.78 cubic inches) as shown in Figure 3.1. The polypropylene jars offer high temperature resistance up to 275°F for short periods and 212°F continuously. Each jar was capped and placed in watertight bags, which were submerged in a bucket of water. The watertight bags were used to ensure that during the first 24 hours of curing no additional water was permitted to affect the designated water cement ratio. The water in the buckets for samples cured at 160 and 200°F was preheated to approximately 100°F to ensure a short time lag to attain the elevated temperatures in the ovens as shown in Figure 3.2.



Figure. 3.1 Paste samples cast in one-ounce polypropylene screw cap jars.

- d. The samples cured at 73°F were placed in watertight bags immersed in water and cured in a moisture room kept at 100% humidity and 73°F, water.



Figure 3.2. Oven used to cure samples at 200°F

- e. After 24 hours, the samples were demolded, placed in four-ounce polypropylene jars as shown in Figure 3.3 and placed in their curing environment to continue the isothermal curing for the remaining curing duration.



Figure 3.3 Samples cured in four-ounce polypropylene jars after demolding

- f. At the end of curing duration three samples for each mix and temperature were removed and placed in methanol. Samples cured at 160 and 200°F were cooled to room temperature before placing in the methanol. This was done to avoid igniting the methanol. The samples were placed in the methanol to stop further hydration of the cement.
- g. After at least 7 days in the methanol, the samples were removed and wiped clean. The samples were then crushed in a mechanical crusher (see Figure 3.4). The crushed sample was then pulverized.



Figure 3.4 samples crushed in mechanical crusher

- h. Approximately 3 grams of the pulverized sample was then weighed as shown in Figure 3.5. The scale used was accurate to 1/10,000 of a gram. The samples were dried for 24 hours in an oven maintained at $221\pm 5^{\circ}\text{F}$ (105°C) to remove the evaporable water from the sample. After removal from the oven the samples were cooled to room temperature and the weight was recorded as w1.
- i. The samples were then ignited for 45 minutes at 1832°F (1000°C) to remove the nonevaporable water chemically combined in the hydration products. The samples were cooled to room temperature and the weight recorded as w2. Figure 3.6 shows samples removed from the oven after ignition.



Figure 3.5 Approximately 3 grams of samples weighed.



Figure 3.6 Samples removed after ignition at 1832°F .

Calculations to Determine the Degree of Hydration

The calculation of the degree of hydration was based on the formula given by Zhang et al (2000).

The nonevaporable water content, w_n was calculated according to the following equation:

$$w_n = \frac{(w_1 - w_2)}{w_2} - \frac{r_{fc}}{(1 - r_{fc})}$$

$$r_{fc} = p_f r_f + p_c r_c$$

The degree of hydration was determined as a ratio of

$$w_n / w_{nu}$$

w_{nu} - nonevaporable water content per gram of fully hydrated cement 0.23

w_1 - weight of the sample after drying

w_2 - weight of the sample after ignition

p_f - weight percent of fly ash in the mix, 18% and 50%

p_c - weight percent of cement in the mix

r_f - loss of ignition of fly ash 4.7%

r_c - loss of ignition of cement 2.1%

Problems Encountered in the Experimental Process

Various problems were encountered during the experimental process to determine the degree of hydration of the paste samples. These problems and how they were resolved is presented below.

1. The oven used to cure samples at 160°F failed five days into the curing process requiring a new oven to be used.
2. Some of the samples kept cured in the ovens at 160 and 200°F lost the water in which they were immersed during the course of the curing duration. Cracking of the jar covers and evaporation of the water caused this.

3. To resolve the above problems, curing tanks as shown in Figure 3.7 were used in place of the ovens for the elevated temperature curing. These tanks were filled with water maintained at 160 and 200°F.
4. The degree of hydration tests were repeated based on curing for elevated temperatures in the curing tanks. The results of the degree of hydration are shown in Figure 3.8.

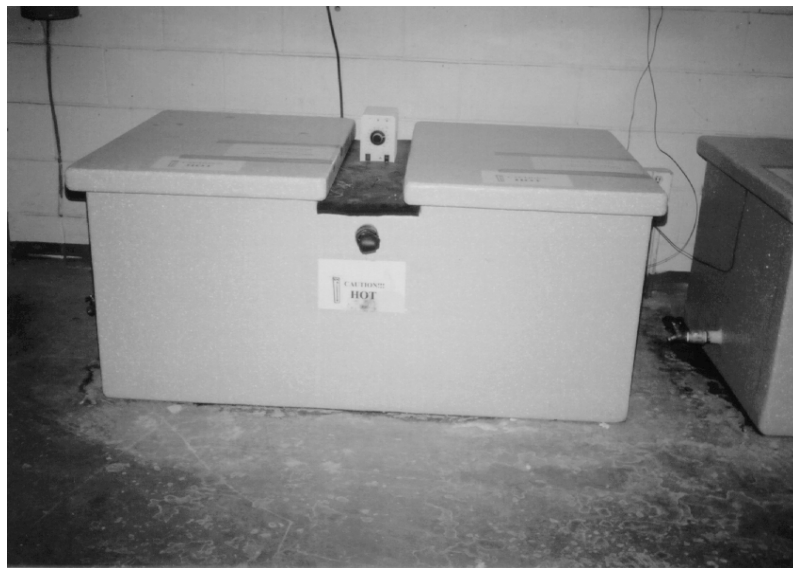


Figure 3.7 Curing tanks used for samples at elevated temperatures.

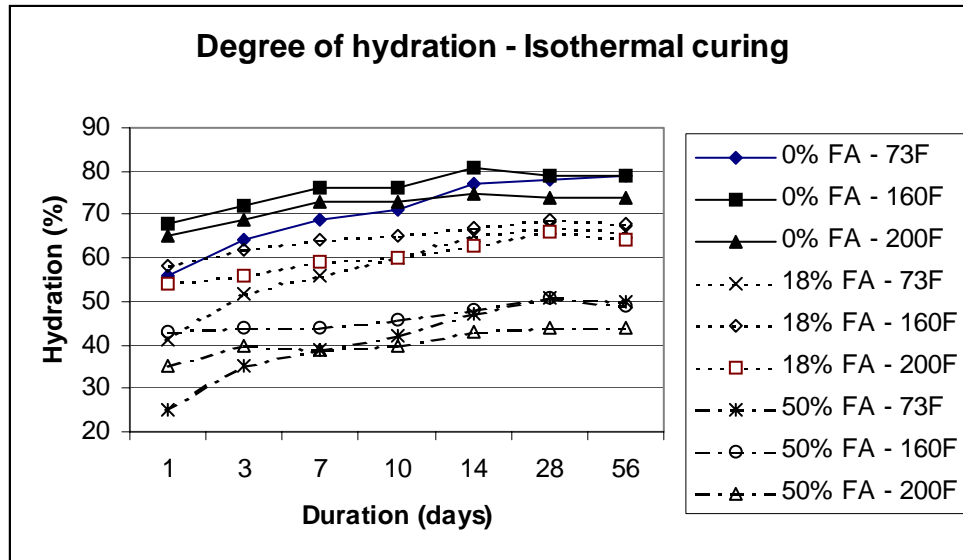


Figure 3.8 Degree of hydration ($w_{nu} = 0.23$)

Based on the results of the degree of hydration shown in Figure 3.8, samples made from the cement fly ash paste mixes did not attain a 70% degree of hydration for the temperatures and curing durations used in this test. The times to reach 70% degree of hydration in the plain cement mix was established as shown in Table 3.4.

Table 3.4 Time to 70% hydration in plain cement mix

Curing Temperature (°F)	Duration (approximate)
73	7
160	3
200	3

Based on the durations in Table 3.4, samples of FDOT Class IV mass concrete (Mix 1 – appendix) based on the paste mix were made and cured isothermally following the curing conditions used for the paste samples. Three samples were tested for each temperature to determine the compressive strength in accordance with ASTM C 39 – 96. Compressive strength results are presented in Table 3.5 and Figure 3.9.

Table 3.5 Concrete Mix 1 – 0% Fly Ash (Isothermal Curing)

Temp (°F)	Compressive strength (psi)				RCP (coulombs)	
	70% DH	28 Days	90 Days		70% DH	28 Days
73	6,839	7,472	8252		5,845	4,720
160	4,621	4,963	5616		8,763	7,110
200	2,910	2,872	2636		9,756	11,070

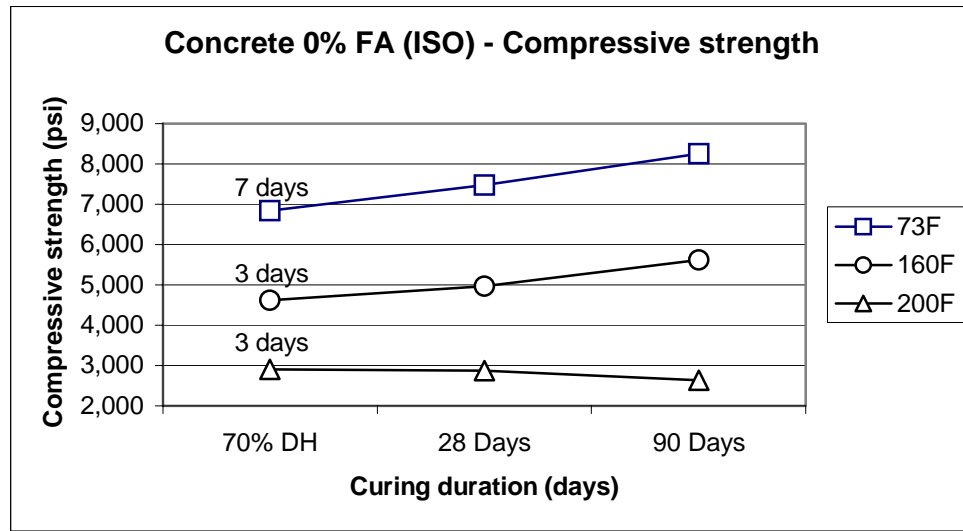


Figure 3.9. Compressive strength results

Figure 3.9 shows a substantial decrease in compressive strength of samples cured isothermally at 160 and 200°F compared to samples cured at room temperature. This is specially pronounced for 200°F curing temperature where compressive strength of a 90 days old sample is less than a 3 days old sample. The reduction in compressive strength of samples cured at elevated temperatures might be due to high temperature changes (100 to 200°F) as the freshly mixed concrete is introduced into the high temperature curing environment and thermal shock to concrete.

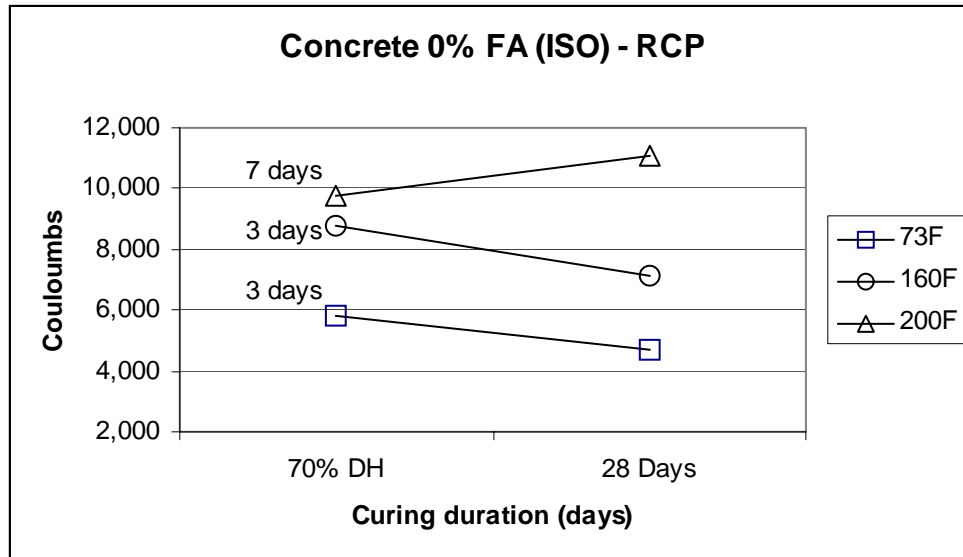


Figure 3.10 Rapid Chloride Permeability (RCP) results

Figure 3.10 shows the RCP results of the concrete samples cured isothermally at 160°F and 200°F compared to samples cured at room temperature (73°F). Samples cured at the high temperatures recorded high charges passing through the samples indicating reduced durability for the concrete. The samples cured at 200°F showed reduced durability from 7 days to 28 days as the charged passed increased over the curing duration. At 28 days, the samples cured at 73°F had the least current passing indicating better durability than the samples cured at 200°F, which recorded the highest charges passing at 28 days.

With the drastic reduction in compressive strength of the mass concrete samples cured at the elevated temperatures, the experimental set-up was changed as follows:

1. The curing was done adiabatically to simulate conditions as in mass concrete cured in the field. All the samples were introduced to the curing environment approximately 6 hours after the start of the mixing process. Samples at 160°F and 180°F were introduced into the curing tanks at 80°F after which the heat was

turned on. The curing temperature of 160°F was attained within 2 days after which the heat was turned off. The 180°F tank attained the maximum temperature after about 2½ days after which the heat was turned off. The lids of the curing tanks were kept on whilst the temperature cooled to 73°F within approximately two weeks of turning the heat off in both tanks.

2. The maximum temperature was reduced from 200 to 180°F.
3. A review of mass concrete mixes used by the FDOT, was undertaken to examine the proportions of binders commonly used by the department. The results as shown in Table 3.6, indicated that 80 percent of the cement/fly ash mixes had 0.18 and 0.20 of the cement replaced by fly ash. Two (2) per cent of the cement /fly ash mixes had a fly ash replacement of 0.40. Based on this review, the proportion of fly ash replacement for the mass concrete tests was limited to 18 percent
4. The samples were then transferred to the moisture room into curing baths, as were the 73 samples. Lime was then added to the water at this point in the curing cycle.
5. Following the change in the curing conditions, new tests were conducted to determine the time to achieve 70% degree of hydration for the mix. The results from this test are shown in Figure 3.11.
6. As can be observed in Figure 3.11, the curves were very erratic making it difficult to establish the duration to attain maturity of 70% degree of hydration in the various mixes. This led to the use of curing durations of 7, 28 and 91 days as the bases to compare the mass concrete properties in this study.

7. At specified curing durations, mass concrete samples described in the next section were tested and the degree of hydration of the cement was determined for that age and curing temperature.

Table 3.6 Binders used in mass concrete mixes by the FDOT

BINDERS USED IN MASS CONCRETE DESIGNS IN FLORIDA			
A. Cement mixes			
Proportion of Cement	Number of mixes	% Cement Mixes	% Total mixes
1.00	10	100	11
B. Cement / Fly Ash mixes			
Proportion of fly ash	Number of mixes	% Cement/ Fly ash Mixes	% Total mixes
0.18	18	32	21
0.19	6	11	7
0.20	21	37	24
0.21	1	2	1
0.22	5	9	6
0.30	1	2	1
0.35	2	4	2
0.39	2	4	2
0.40	1	2	1
Total	57	100	66
C. Cement / Blast Furnace Slag mixes			
Proportion of Slag	Number of mixes	% Cement/Slag Mixes	% Total mixes
0.50	11	55	13
0.60	2	10	2
0.70	7	35	8
Total	20	100	23
SUMMARY			
Binder	Number of Mixes	% of Mixes	
Cement	10	11	
Cement/ Fly Ash	57	66	
Cement/Slag	20	23	
Total	87	100	

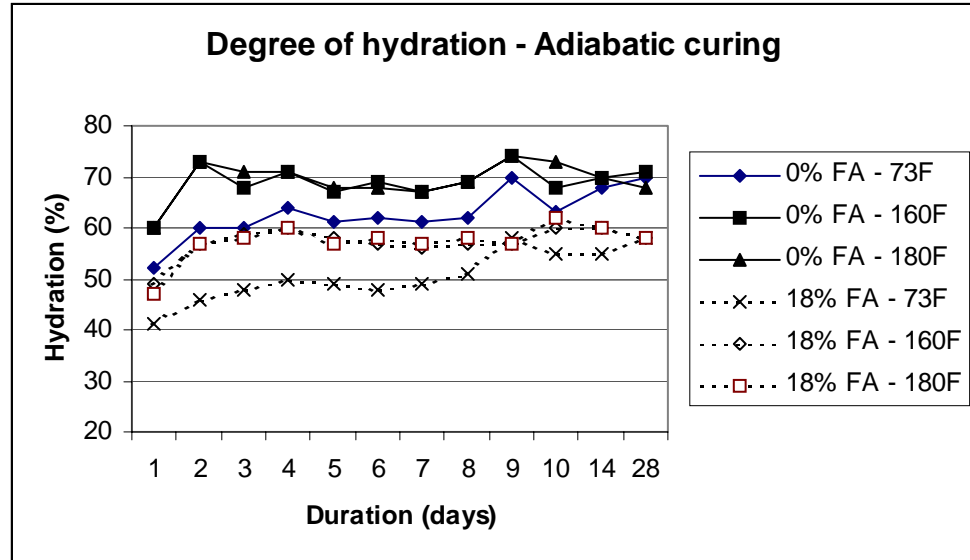


Figure 3.11 Degree of hydration based on adiabatic curing ($w_{nu} = 0.23$)

Mass Concrete Experiments

Two typical FDOT Class IV concrete with fly ash or slag as the supplementary cementitious material to cement were used in the mass concrete tests (See appendix A). The goal of the tests was to determine the effects of elevated curing temperate on the strength and durability of concrete properties. Four mixes with different proportion of cement, fly ash and blast furnace slag as shown in Table 3.7, were made and tested. The tests were repeated. The mixes tested were as follows:

- 0% Fly ash mixes (Mix 1 and Mix 3)
- 18% Fly ash mixes (Mix 2 and Mix 4)
- 0% Blast furnace slag mixes (Mix 5 and Mix 7)
- 50% Blast furnace slag mixes (Mix 6 and Mix 8)

Table 3.7. Mixture Proportions for FDOT Class IV mass concrete

Mixture	Saturated Surface-Dry Weights, lb/cu yd								
	Cement	Fly ash	Slag	Fine aggregate	Coarse aggregate	Air Entrainer (Darex)	Admixture (WRDA)	Water	w/b ratio
Mix 1 & 3	744	-	-	936	1746	4 oz	24.4 oz	305	0.41
Mix 2 & 4	610	134	-	918	1729	4 oz	24.4 oz	305	0.41
Mix 5 & 7	660	-	-	1076	1794	5 oz	33.0 oz	267	0.40
Mix 6 & 8	330	-	330	1066	1785	5 oz	33.0 oz	267	0.40

Samples made from the various mixes were cured adiabatically as before described.

All the samples were mechanically vibrated during their preparation. After casting in their molds, the samples were kept in watertight bags for 24 hours after which they were demolded and placed directly in the curing water. Samples cured at 73°F were kept in the moisture room. The heat in the 160 and 180°F tanks was turned off after the maximum temperature was attained. Cooling of the tanks to a temperature of approximately 73°F occurred over a 14-day period. The samples in the curing tanks were transferred into the moisture room and placed in limewater. Samples cured at 73°F were also places in limewater at this time.

Various tests were performed on the mass concrete samples after 7, 28 and 91 days of curing. The tests performed were:

1. Determination of degree of hydration
2. Compressive strength – ASTM C 39 (ASTM 1996)
3. Resistance to chloride penetration – ASTM C 1202 (ASTM 1994)
4. Time to Corrosion – FM 5-522
5. Density and percentage of voids – ASTM C 642 (ASTM 1997)

6. Microstructure analysis

Compressive Strength

The compressive strengths of the samples were determined at curing durations of 7, 28 and 91 days. The compressive strengths were determined according to ASTM C 39-93a, *Standard Test Method for Compressive Strength of Cylindrical Concrete Specimens*, by the FDOT physical laboratory. Twenty-seven 4" diameter x 8" cylinders were molded for each mix. Nine samples for each mix were tested at 7-, 14-, and 28-days age three for each curing temperature.

Resistance to Chloride Penetration

Each mix cured at the 73, 160 and 180°F was tested at 28-, and 91-days age to determine its ability to resist the chloride-ion penetration. The rapid chloride permeability for each sample was estimated following ASTM C 1202-94, *Standard Test Method for Electrical Indication of Concrete's Ability to Resist Chloride-Ion Penetration*. In this test, the chloride-ion penetrability of each sample was determined by measuring the number of coulombs that can pass through a sample in 6 hours. This provided an accelerated indication of concrete's resistance to the penetration of chloride-ions, which may corrode steel reinforcement or prestressed strands. Six 4" diameter x 8" cylinders of each mix, two for each curing temperature were tested at 28-, and 91-days age. A 2" thick disc was sawed from the top of each cylinder and used as the test specimen. It has been determined that the total charge passed is related to the resistance of the specimen to chloride-ion penetration. The surface resistivity of each sample to the penetration of chloride ions was measured at the curing durations from the remaining portions of the samples used in the rapid chloride permeability tests.

Time to Corrosion

The time to corrosion test determines the duration of time for reinforcement within a sample to corrode. The time to corrosion was determined according to *Florida Method of Test for An Accelerated Laboratory Method for Corrosion Testing of Reinforced Concrete Using Impressed Current*. The samples used in this test were cylinders of 4" diameter x 6" long. Nine samples were made for each mix three for each curing temperature. Each sample contained a #4 reinforcing bar, 12" long. The bottom of the reinforcing bar was elevated by 0.75" from the bottom of the mold. Fresh concrete was placed in each mold and each mold was overfilled. The apparatus that had the reinforcing bars attached to it was placed over the cylinders. The apparatus was then placed on an external vibrator that caused the reinforcing bars to submerged into the overfilled fresh concrete when the vibrator was turned on. After vibration, a trowel was used to slope the overfilled top of the mold at a 15-degree angle from the outer rim of the sample to the center of the sample. After 28 days of curing, the samples were further cured in a solution of 3% NaCl after which they were tested. The tests were performed at the Florida Department of Transportation Corrosion Laboratory.

Density and Percentage of Voids in Hardened Concrete

The density and percentage of voids for each mix and curing temperature were determined at curing durations of 7, 28 and 91 days. The tests were done according to ASTM C 642 - 97, *Standard Test Method for Density, Absorption, and Voids in Hardened Concrete*, by the FDOT physical laboratory. Approximately 800 grams of each sample was tested.

Microstructure analysis – Scanning Electron Microscope (SEM)

Introduction

A microscope provides the ability to see much finer details of an object than is possible to the naked eye. The scanning electron microscope (SEM), which became commercially available in the 1960s, permits the observation and characterization of heterogeneous organic and inorganic materials on a nanometer (nm) and micrometer (μm) scale (Goldstein et al, 1992). The resolution of a microscope is the smallest separation between two points in an object that can be distinctly reproduced in the image. Today's SEM has achieved a resolution better than 10nm, an improvement by a factor about 10³ relative to a light microscope (Sarkar, Aimin and Jana, 2001). The popularity of the SEM stems from its capability of obtaining three-dimensional-like images of the surfaces of a very wide range of materials.

Signals of Interest

In the SEM, the area to be examined or microvolume to be analyzed is irradiated with a finely focused beam, which may be swept in a raster across the surface of the specimen to form images or may be static to obtain an analysis at one position (Goldstein, Newbury, Joy, Lyman, Echlin, Lifshin, Sawyer and Michael, 1992). When a beam of primary electrons strikes a bulk solid, the electrons are either reflected (scattered) or absorbed, producing various signals (Figure 3.12)

The types of signals produced include secondary electrons (SE), backscattered electron (BSE), characteristic x-rays and other photons of various energies. These signals are obtained from specific emission volumes within the sample and can be used to examine many characteristics of the samples such as composition and topography. The intensity of the backscattered electrons is proportional to the atomic number of the

elements in the sample. More electrons are scattered from higher atomic number elements, and, in an image appear brighter than low atomic number elements which appear darker in an image. Backscattered electrons therefore respond to the compositional variations in the sample and enable the distinctions of the various phases based on the differences in their average atomic numbers.

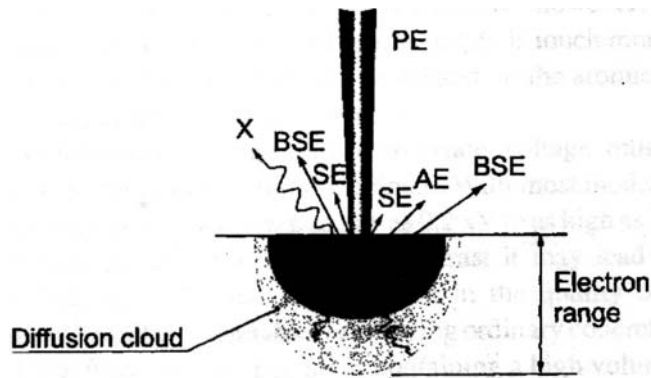


Figure 3.12. Different interactions of an electron beam (PE) with the solid target. BSE = backscattered electrons, SE = secondary electrons, X = x-ray, AE = auger electrons

Secondary electrons are loosely bound outer shell electrons from the sample atoms which receive sufficient kinetic energy during inelastic scattering of the beam electrons to be ejected from the atom and set in motion (Goldstein et al, 1992). Secondary electrons have a shallow escape depth and collecting them as an imaging signal enable high topographical resolution of the sample to clearly distinguish between the various shapes of the phases in the sample. Measuring the energy and intensity distribution of the characteristic x-ray signals generated by the focused electron beam enables chemical analysis of the specimen. This chemical analysis is done using the SEM's adjunct microanalytical unit, commonly known as the energy dispersive x-ray analyzer (EDAX), (Sarkar, Aimin and Jana, 2001). Characteristic x-rays are analyzed to yield both the

qualitative identification and quantitative compositional information from regions of the specimen as small as a micrometer in diameter.

SEM Use in Concrete

Most of the properties of concrete are evaluated according to standard procedures. The SEM does not fall under the realm of any standard procedure. It is a relatively new technique which is yet to be universally accepted by the concrete technologist. One of the first applications of SEM was in the study of concrete hydration in the early 1970s (Sarkar, Aimin and Jana, 2001). The chief interests one has in studying concrete under SEM are to study the effects of deterioration of concrete or its performance characteristics, qualitative phase identification, grain morphology, distribution pattern and association with other phases (Sarkar, Aimin and Jana, 2001).

Experimental Work

The scanning electron microscope used in this research was the SEM JSM 6400. All analyses were conducted at the Major Analytical and Instrumentation Center at the University of Florida. The SEM analysis was used to determine the presence of ettringite crystals in voids of mortar samples sieved from the concrete mixes. The signals of interest used in this study when the electron beam impinged on the specimen were secondary electrons and characteristic x-rays. Because of the different morphological features characteristic of the phases, they could be identified by secondary electron images. This avoided the use of thin or polished sections using backscatter (BS) electron which may wash out or grind out ettringite nests and introduce artifacts such as cracks. Moreover with SE techniques, crevices and both sides of “hills” are revealed. Fly ash particles used in some of the mixes are clearly revealed by SE techniques, while BS procedures may reveal them primarily as voids because of their poor backscattered

electron yield (Hime, Marusin, Jugovic et. Al, 2000). Measuring the energy and intensity distribution of the characteristic x-rays enabled a chemical analysis of the samples to confirm the various phases identified in the secondary electron image. Energy Dispersive Analysis of the X-rays (EDAX) was used to confirm or deny the presence of the ettringite. EDAX of an ettringite mass has a “step” pattern of the aluminum, sulfur and calcium peaks as shown in Figure 3.13 (Hime, Marusin & Jugovic, 2000).

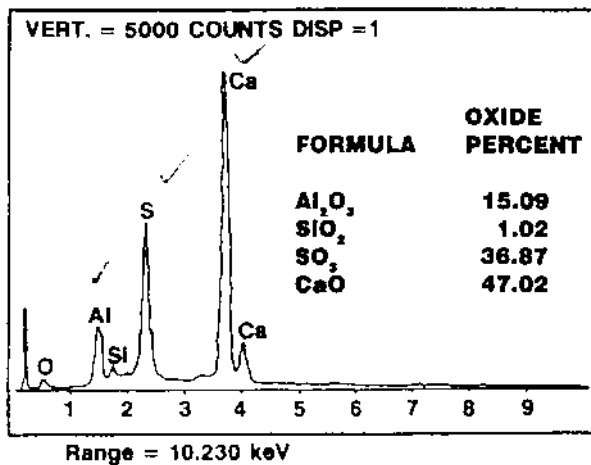


Figure 3.13 The EDAX analysis of “gel” showing calcium, sulfur, and aluminum peaks typical for ettringite

Sample Preparation for SEM Examination

The samples used for the microstructural analysis were made from mortar sieved from the concrete mixes. The samples were cured adiabatically as the mass concrete samples. After 24 hours in watertight bags, the samples were demolded from the two-ounce jar and placed directly in the curing environment. At the end of the curing period, the samples were removed from the curing tank and placed in methanol to stop further hydration. After at least 7 days in the methanol, the samples were removed and finely cut into $\frac{1}{4}$ " thick wafers. The samples were then placed in an oven maintained at a

temperature of 230 °F for 24 hours to remove all the evaporable water, not used in the hydration process. The samples were stored in a desiccator after removal from the oven.

To obtain very good images using the SEM and avoid the introduction of cracks or removal of any ettringite nests, cutting of the surface of the sample was avoided, instead pieces were fractured and the fractured surfaces were analyzed. The fractured pieces were cut and coated with carbon. Since the samples were non-conducting, coating was necessary to eliminate or reduce the electric charge that builds up rapidly in a non-conducting specimen when it is scanned by a beam of high-energy electrons. Figure 3.14 shows mortar samples mounted and ready for examination in the SEM



Figure 3.14. Mortar samples mounted on stubs for SEM examination

CHAPTER 4 TEST RESULTS AND DISCUSSION

Introduction

This chapter presents results of the experimental work conducted to determine the maximum curing temperature to avoid durability problems and the formation of delayed ettringite in mass concrete. The study was conducted in three phases:

1. Phase 1 involved tests to determine the time to achieve a maturity of 70% degree of hydration of cement in mass concrete mixes with cement, fly ash and blast furnace slag as the cementitious materials.
2. Phase 2 involved tests of two FDOT Class IV mass concretes at temperatures of 73, 160 and 180°F for 7, 28 and 91 days. Various tests were performed on the concrete to evaluate the effect of the curing conditions on the strength and durability of the concrete.
3. In phase 3, mortar samples prepared from the sieved mass concrete mixes were subjected to the same curing conditions. The samples were then examined under a scanning electron microscope to determine the formation or otherwise of delayed ettringite.

Phase 1 – Determination of Degree of Hydration

The results for the degree of the hydration for the different mixes tested are shown in Tables 4.2 through Table 4.5. Initially, all calculations for the degree of hydration were based on the fact that the nonevaporable water content for 1 gram of fully hydrated

cement was 0.23 grams of water. This value was found to be inapplicable to cement blends with fly ash or slag.

Scanning Electron Microscope (SEM) observations by Maltais & Marchand (1997) for pastes some incorporating fly ash as a 10, 20 and 30 per cent replacement of cement and cured at 68 and 104°F showed that the fly ash did not react before at least 28 days. Although the fly ash did not react during the first days of curing, their test results indicated that it could not be considered as a totally inert material. Despite the very little pozzolanic activity, Maltais and Marchand (1997) found out that the presence of fly ash appeared to increase the mortar nonevaporable water content at early days. This increase was attributed to an acceleration of the early cement hydration in the presence of fly ash.

Two reasons for the acceleration of cement hydration in the presence of fly ash are physical and chemical effects.

- Physical
 - The addition of fly ash tends to increase the number of fine particles in the system. The presence of these fine particles contributes to increase the density of the matrix making for better hydration of the cement.
 - The replacement of cement particles by fly ash is also believed to increase the available space in the floc structure created by the cement grains.
 - The fine particles provide additional nucleation sites for cement hydration products.
- Chemical
 - According to Maltais and Marchand (1997) the acceleration of cement hydration in the presence of fly ash is mainly related to the preferential

adsorption of calcium ions on the fly ash particles. The phenomenon contributes to decrease the calcium ion concentration in the liquid phase, which subsequently favors the dissolution of calcium phases from the cement grains.

Fly ash reacts with the calcium hydroxide formed from the hydration of the cement. The reduction in calcium hydroxide content from the pozzolanic reaction will not enable a value of 0.23 to be a good estimate of the degree of hydration. The pozzolanic reaction will reduce the amount of calcium hydroxide and replace it with hydrates formed by the pozzolanic reaction. The amount of water released from a mole weight of the hydrates is less than the amount of water released from a mole weight of calcium hydroxide due to its large molecular weight. A more reliable estimate was determined for the cement fly ash mixes after hydrating paste at 73°F in the moisture room for 1 year and calculating the nonevaporable water content. The new values for the nonevaporable water content for the cement and fly ash mixes were as follows:

- 0.19 for cement and 18% fly ash mix with w/b ratio of 0.41
- 0.15 for cement and 50% fly ash mix with w/b ratio of 0.41.

These values for the nonevaporable water content are comparable to that determined for various mixes of fly ash by Lam et al. (2000) and shown in Table 4.1 below.

Table 4.1. Nonevaporable water content for various Fly ash mixes Lam et al. (2000)

w/b	Fly ash replacement (%)	*Wn _u at 90 days
0.3	25	0.19
0.3	55	0.15
0.5	25	0.18
0.5	55	0.15
* Calculated from ratio of Wn / Degree of hydration		

Legend: Degree of Hydration results

- IOP –Isothermal curing of paste samples in oven
 - (Row # - 1, 6, 14, 16, 17, 24, 25, 36, 37, 40, 41, 44, 45, 48, 49)
- ITP –Isothermal curing of paste samples in tanks
 - (Row # - 2, 7, 15, 18, 19, 26, 27, 38, 39, 42, 43, 46, 47, 50, 51)
- ATM – Adiabatic curing of mortar samples in tank
 - (Row # - 3, 8, 11, 20, 21, 28, 29, 32, 33)
- ATC – Adiabatic curing of mortar sieved from concrete in tank
 - (Row # - 4, 5, 9, 10, 12, 13, 22, 23, 30, 31, 34, 35, 52, 53, 54)
- C & F - Calculation of degree of hydration based on total cement and fly ash content and the nonevaporable water content at full hydration after curing for 1 year at 73oF. the nonevaporable content for 1 gram of 18%FA mix was determined to be 0.19 and that for the 50%FA was determined to be 0.15.
- C – Calculation of degree of hydration based on cement solely responsible for the hydration products formed assuming no reaction of fly ash. NA designation is applied to durations and temperatures for which fly ash reaction is assumed to have started, invalidating an extension of this calculation.

- C & S - Calculation of degree of hydration based on total cement and blast furnace slag content and the nonevaporable water content at full hydration of 0.23 as for plain cement mixes.

Table 4.2. Degree of hydration results for plain cement mixes

Mix	Temp	Row	Mix design	Curing Duration (days)													
				1	2	3	4	5	6	7	8	9	10	14	28	56	91
73	0%	1	IOP – 0% .41w/c	58	-	67	-	-	-	70	-	-	71	71	73	74	-
		2	ITP – 0% .41 w/c	56	-	64	-	-	-	69	-	-	71	77	78	79	-
		3	ATM – 0% .41 w/c	52	60	60	64	61	62	61	62	70	63	68	70	-	-
		4	ATC – 0% .41 w/c	-	-	-	-	-	-	59	-	-	-	-	64	-	69
		5	ATC – 0% .40w/c	-	-	-	-	-	-	54	-	-	-	-	64	-	62
160	0%	6	IOP – 0% .41w/c	68	-	72	-	-	-	75	-	-	73	72	69	69	-
		7	ITP – 0% .41 w/c	68	-	72	-	-	-	76	-	-	76	81	79	79	-
		8	ATM – 0% .41 w/c	60	73	68	71	67	69	67	69	74	68	70	71	-	-
		9	ATC – 0% .41 w/c	-	-	-	-	-	-	61	-	-	-	-	61	-	66
		10	ATC – 0% .40w/c	-	-	-	-	-	-	62	-	-	-	-	59	-	61
180	0%	11	ATM – 0% .41 w/c	60	73	71	71	68	68	67	69	74	73	70	68	-	-
		12	ATC – 0% .41 w/c	-	-	-	-	-	-	59	-	-	-	-	63	-	69
		13	ATC – 0% .40w/c	-	-	-	-	-	-	60	-	-	-	-	59	-	60
200	0%	14	IOP – 0% .41w/c	73	-	75	-	-	-	80	-	-	78	75	75	76	-
		15	ITP – 0% .41 w/c	65	-	69	-	-	-	73	-	-	73	75	74	74	-

Table 4.3. Degree of hydration for 18% fly ash mixes

Mix	Temp	Row	Mix design	Curing Duration (days)														
				1	2	3	4	5	6	7	8	9	10	14	28	56	91	
73	16	IOP – 18% FA	C	63	-	65	-	-	-	75	-	-	78	76	79	NA	-	
				60		63				73			75	74	76	79	-	
		18	ITP – 18% FA	C	51	-	65	-	-	-	70	-	-	75	81	84	NA	-
		19		50	-	63	-	-	-	68	-	-	72	78	82	80	-	
	20	ATM – 18% FA	C	51	58	60	63	61	60	61	64	73	69	69	73	-	-	
				49	55	59	61	60	58	59	62	70	66	67	70	-	-	
		22	ATC – 18% FA	C	-	-	-	-	-	-	55	-	-	-	-	64	-	NA
		23		-	-	-	-	-	-	54					62		76	
18%	24	IOP – 18% FA	C	78	-	81	-	-	-	84	-	-	NA	NA	NA	NA	-	
				75	-	78	-	-	-	81			83	82	78	76		
		26	ITP – 18% FA	C	73	-	78	-	-	-	80	-	-	NA	NA	NA	NA	-
		27		70	-	75	-	-	-	77			79	81	83	82		
	28	ATM – 18% FA	C	61	71	74	75	73	71	70	NA	NA	NA	NA	NA	-	-	
				59	69	72	73	71	69	68	70	69	72	72	71	-	-	
		30	ATC – 18% FA	C	-	-	-	-	-	-	65	-	-	-	-	NA	-	NA
		31		-	-	-	-	-	-	63					64	-	73	
160	32	ATM – 18% FA	C	59	71	73	75	71	73	71	NA	NA	NA	NA	NA	-	-	
				56	69	72	73	69	70	69	70	69	75	73	71	-	-	
		34	ATC – 18% FA	C	-	-	-	-	-	-	63	-	-	-	-	NA	-	NA
		35		-	-	-	-	-	-	61	-	-	-	-	68	-	70	
180	36	IOP – 18% FA	C	80	-	84	-	-	-	84	-	-	NA	NA	NA	NA	-	
				78	-	81	-	-	-	81	-	-	83	82	81	84	-	
		38	ITP – 18% FA	C	68	-	70	-	-	-	74	-	-	NA	NA	NA	NA	-
		39		C&F	66	-	68	-	-	-	71	-	-	73	75	79	77	-
200	36	IOP – 18% FA	C	80	-	84	-	-	-	84	-	-	NA	NA	NA	NA	-	
				78	-	81	-	-	-	81	-	-	83	82	81	84	-	
		38	ITP – 18% FA	C	68	-	70	-	-	-	74	-	-	NA	NA	NA	NA	-
		39		C&F	66	-	68	-	-	-	71	-	-	73	75	79	77	-

Table 4.4. Degree of hydration for 50% fly ash mixes

Mix	Temp	Row	Mix design	Curing Duration (days)														
				1	2	3	4	5	6	7	8	9	10	14	28	56	91	
50%	73	40	IOP - 50% FA	C	58	-	68	-	-	-	80	-	-	82	84	86	NA	-
		41			44		53				61			63	65	66	64	
		42	ITP - 50% FA	C	50	-	70	-	-	-	78	-	-	84	94	102	NA	-
		43			38		53				60			65	71	78	76	
	160	44	IOP - 50% FA	C	80	-	80	-	-	-	82	-	-	NA	NA	NA	NA	-
		45			61		62				63			64	63	66	68	
		46	ITP - 50% FA	C	86	-	88	-	-	-	88	-	-	NA	NA	NA	NA	-
		47			65		67				67			71	74	78	75	
	200	48	IOP - 50% FA	C	86	-	88	-	-	-	86	-	-	NA	NA	NA	NA	-
		49			66		67				66			64	65	68	61	
		50	ITP - 50% FA	C	70	-	80	-	-	-	78	-	-	NA	NA	NA	NA	-
		51			53		61				59			60	66	67	68	

Table 4.5. Degree of hydration for cement and blast furnace slag mixes

Mix	Temp	Row	Mix design	Curing Duration (days)														
				1	2	3	4	5	6	7	8	9	10	14	28	56	91	
50%	73	52	ATC - 50% SL	C & S	-	-	-	-	-	-	69	-	-	-	-	78	-	81
		160	53	ATC - 50% SL	C & S	-	-	-	-	-	-	84	-	-	-	86	-	82
	180	54	ATC - 50% SL	C & S	-	-	-	-	-	-	82	-	-	-	-	85	-	84

Phase 2 – Tests of Mass Concrete

Table 4.6 provides a summary of the plastic properties of the mass concrete mixes tested. Tests for each mix included determination of the degree of hydration, compressive strength, time to corrosion, rapid chloride permeability, density and the percentage of voids at curing durations of 7, 28 and 91 days and curing temperatures of 73, 160 and 180°F. The test for each mix was repeated and the average results for each mix is provided in Tables 4.7 and 4.8.

Table 4.6. Summary of Plastic Properties of Fresh Concrete.

Test #	Mixture	Concrete Temperature (°F)	Air Temperature (°F)	Slump in	Air Content %	Workability	w/b ratio
1	Mix 1	75	72	6.50	4.0	Good	0.41
	Mix 2	75	72	5.00	2.0	OK	0.41
2	Mix 3	69	70	6.50	4.5	Good	0.41
	Mix 4	70	70	7.50	2.5	Good	0.41
3	Mix 5	74	72	5.25	6.0	Good	0.40
	Mix 6	74	72	3.25	3.9	Sticky	0.40
4	Mix 7	75	71	4.00	5.50	Good	0.40
	Mix 8	73	70	2.75	3.00	Stiff	0.40

Table 4.7. Results of concrete mixes M1 and M2

Test #	Mix ID	Temp (°F)	Duration (days)	Hydration (%)	Comp (psi)	Density (lbs/ft³)	Voids (%)	RCP (coulombs)	Resistivity (kohms/cm)	Corrosion (days)
1	M1 (0% Fly Ash) w/c = 0.41 slump = 6.5"	73	7	56	6048	-	-	-	-	-
			28	66	6860	155.70	16.00	5507	8.63	12
			91	70	7457	155.70	16.30	4456	11.07	-
		160	7	56	5992	-	-	-	-	-
			28	60	6051	157.10	16.70	8701	7.16	8
			91	63	6280	156.50	16.00	6693	8.28	-
		180	7	56	5761	-	-	-	-	-
			28	67	5790	159.05	15.95	9317	8.46	5
			91	66	6037	156.50	15.80	7695	8.27	-
		M2 (18% Fly Ash) w/c = 0.41 slump = 5.0"	73	7	49	6610	-	-	-	-
			28	58	7770	161.20	16.75	5014	9.04	14
			91	58	8517	159.90	15.90	2285	17.84	-
		160	7	62	6942	-	-	-	-	-
			28	61	7149	162.15	16.60	2470	21.33	9
			91	60	7810	160.30	16.70	1701	29.80	-
		180	7	57	6660	-	-	-	-	-
			28	62	7069	162.15	16.90	2646	19.42	9
			91	61	7437	160.70	16.20	1822	23.06	-

Table 4.8. Results of concrete mixes M3 and M4

Test #	Mix ID	Temp (°F)	Duration (days)	Hydration (%)	Comp (psi)	Density (lbs/ft ³)	Voids (%)	RCP (coulombs)	Resistivity (kohms/cm)	Corrosion (days)
2 (repeat of test 1)	M3 - same as M1 (0% Fly Ash) w/c = 0.41 slump = 6.5"	73	7	61	5800	154.20	16.30	-	-	
			28	61	6387	156.30	15.30	5616	11.22	15
			91	69	7043	152.20	14.50	4531	12.18	
		160	7	66	5567	155.30	15.90	-	-	
			28	62	5613	155.10	16.20	8565	8.42	5
			91	70	5957	155.20	15.80	6851	9.78	
		180	7	61	5323	155.80	16.00	-	-	
			28	59	5353	155.20	15.80	10459	8.85	7
			91	72	5343	154.10	15.50	7370	9.12	
	M4 - same as M2 (18% Fly Ash) w/c = 0.41 slump = 7.5"	73	7	58	6320	159.70	16.60	-	-	
			28	66	7173	159.40	16.00	5331	10.83	27
			91	93	8220	158.10	15.70	2272	18.95	
		160	7	64	6647	161.40	16.80	-	-	
			28	66	6570	160.40	17.40	2626	21.33	15
			91	86	7180	158.90	15.80	1872	26.09	
		180	7	64	6247	159.00	17.40	-	-	
			28	74	6643	158.70	17.10	2360	18.67	15
			91	90	7187	158.90	15.80	1923	22.13	

Table 4.9. Results of concrete mixes M5 and M6

Test #	Mix ID	Temp (°F)	Duration (days)	Hydration (%)	Comp (psi)	Density (lbs/ft ³)	Voids (%)	RCP (coulombs)	Resistivity (kohms/cm)	Corrosion (days)
3	M5 (0% Slag) w/c = 0.40 slump = 5.25"	73	7	50	4780	156.2	14.7	-	-	
			28	63	5673	150.0	14.0	5850	9.84	18
			91	63	6310	152.4	14.2	4105	12.1	
		160	7	54	4783	155.6	15.8	-	-	
			28	58	4673	152.9	15.1	10108	7.93	11
			91	62	4903	153.7	16.6	7770	8.45	
		180	7	55	4830	155.1	15.7	-	-	
			28	61	4673	151.9	14.9	8996	11.45	14
			91	65	4707	155.9	15.8	9233	9.65	
	M6 (50% Slag) w/c = 0.40 slump = 3.25"	73	7	69	5293	161.5	16.0	-	-	
			28	80	7165	158.5	14.7	2845	17.88	42
			91	83	8003	157.5	14.1	2114	24.50	
		160	7	80	6790	161.4	16.0	-	-	
			28	84	6877	159.3	15.1	1919	21.68	16
			91	84	7617	158.5	14.3	1662	25.90	
		180	7	80	5853	161.4	15.5	-	-	
			28	84	6273	158.7	14.7	2689	18.49	11
			91	87	7180	159.5	15.0	1753	25.00	

Table 4.10. Results of concrete mixes M7 and M8

Test #	Mix ID	Temp (°F)	Duration (days)	Hydration (%)	Comp (psi)	Density (lbs/ft ³)	Voids (%)	RCP (coulombs)	Resistivity (kohms/cm)	Corrosion (days)
4 (repeat of test 3)	M7 - same as M5 (0% Slag) w/c = 0.40 slump = 4.0"	73	7	57	5760	152.3	12.3	-	-	
			28	65	6733	155.7	13.6	4430	11.34	21
			91	61	7307	152.4	12.3	3960	12.5	
		160	7	69	5947	151.4	11.9	-	-	
			28	60	5653	156.3	14.3	8135	7.93	11
			91	60	5890	154.4	14.0	7119	8.45	
		180	7	64	5450	152.5	11.8	-	-	
			28	57	5430	154.8	14.7	6175	10.97	7
			91	54	5373	153.7	14.0	8347	9.05	
		M8 - same as M6 (50% Slag) w/c = 0.40 slump = 2.75"	73	7	69	5770	155.5	12.8	-	-
			28	75	8303	159.8	15.3	2540	19.45	85
			91	79	9003	155.7	12.6	1890	22.54	
		160	7	87	7307	156.3	12.0	-	-	
			28	87	7470	160.5	14.4	1943	23.67	22
			91	80	8230	156.1	12.9	1481	27.00	
		180	7	83	6567	155.4	11.8	-	-	
			28	85	6883	160.8	14.9	2105	20.55	44
			91	80	7370	157.3	12.1	1802	24.76	

Table 4.11. Summary of Results of concrete mixes M1 , M2, M3 and M4

Mix ID	Temp (°F)	Duration (days)	Hydration (%)	Comp (psi)	Density (lbs/ft ³)	Voids (%)	RCP (coulombs)	Resistivity (kohms/cm)	Corrosion (days)
M1 & M3 (0% Fly Ash) w/c = 0.41	73	7	59	5924	154.20	16.30	-	-	-
		28	64	6624	156.00	15.65	5562	9.93	14
		91	69	7250	153.95	15.40	4494	11.63	-
	160	7	61	5780	155.30	15.90	-	-	-
		28	61	5832	156.10	16.45	8633	7.79	7
		91	67	6119	155.85	15.90	6772	9.03	-
	180	7	59	5542	155.80	16.00	-	-	-
		28	63	5572	157.10	15.88	9888	8.66	6
		91	69	5690	155.30	15.65	7533	8.70	-

M2 & M4 (18% Fly Ash) w/c = 0.41	73	7	54	6465	159.70	16.60	-	-	-
		28	62	7472	160.30	16.38	5173	9.94	20
		91	76	8369	159.00	15.80	2279	18.40	-
	160	7	63	6795	161.40	16.80	-	-	-
		28	64	6860	161.30	17.00	2548	21.33	12
		91	73	7495	159.60	16.25	1787	27.95	-
	180	7	61	6454	159.00	17.40	-	-	-
		28	68	6856	162.15	17.00	2503	19.05	12
		91	70	7312	159.80	16.00	1873	22.60	-

Table 4.12. Summary of Results of concrete mixes M5, M6, M7 and M8

Mix ID	Temp (°F)	Duration (days)	Hydration (%)	Compressive (psi)	Density (lbs/ft ³)	Voids (%)	RCP (coulombs)	Resistivity (kohms/cm)	Corrosion (days)
M5 & M7 (0% Slag) w/c = 0.40	73	7	54	5270	154.3	13.5	-	-	
		28	64	6203	152.9	14.2	5140	10.59	20
		91	62	6808	152.4	13.3	4033	12.3	
	160	7	62	5363	153.5	13.9	-	-	
		28	59	5163	154.6	14.7	9122	7.93	11
		91	61	5397	154.1	15.3	7445	8.45	
	180	7	60	5140	153.8	13.8	-	-	
		28	59	5052	153.4	14.8	7586	11.21	11
		91	60	5040	154.8	14.9	8794	9.35	
M6 & M8 (50% Slag) w/c = 0.40	73	7	69	5532	158.5	14.4	-	-	
		28	78	7734	159.2	15.0	2693	18.67	64
		91	81	8503	156.6	13.4	2002	23.52	
	160	7	84	7049	158.9	14.0	-	-	
		28	86	7174	159.9	14.8	1919	21.68	19
		91	82	7924	157.3	13.6	1572	26.45	
	180	7	82	6210	158.4	13.7	-	-	
		28	85	6578	159.8	14.8	2689	18.49	28
		91	84	7275	158.4	13.6	1778	24.88	

Degree of Hydration Results

The degree of hydration was determined from mortar samples sieved from the concrete mixes. The samples were cured adiabatically for the same durations as the mass concrete samples. At the end of the curing durations, the hydration process was stopped by immersion in methanol and then tested to determine the degree of hydration. Figures 4.1 and 4.2 show the results of the hydration tests.

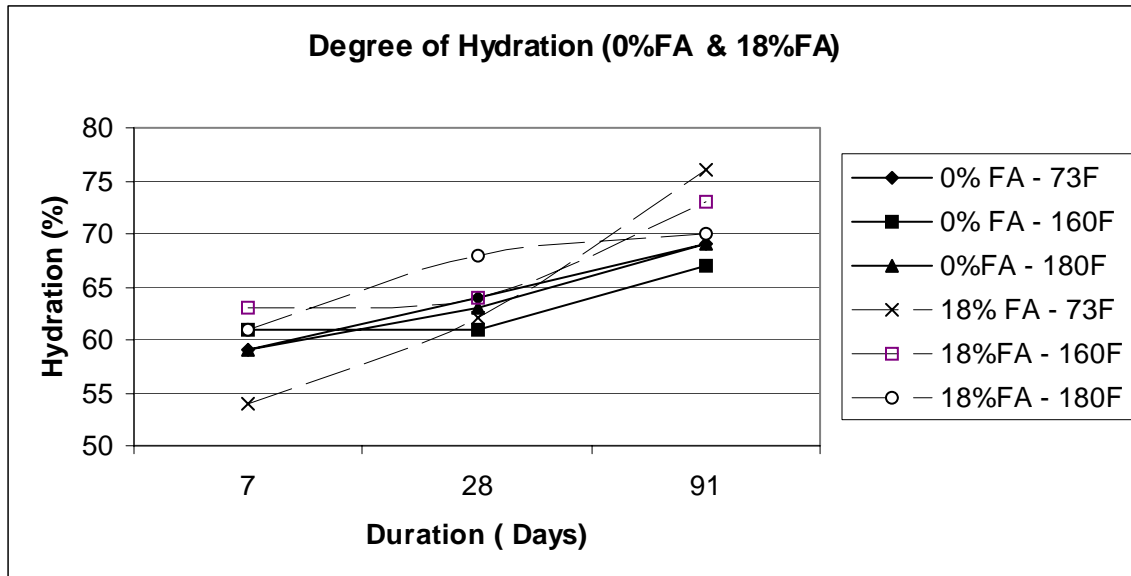


Figure 4.1. Degree of hydration for 0%FA and 18%FA mixes

Addition of Fly ash increases the degree of hydration at early ages for the samples cured at the higher temperatures. Higher curing temperatures have not been effective however in increasing the degree of hydration at early age for the mix without fly ash. At later ages, the degree of hydration for the fly ash mix is higher than that without fly ash at all curing temperatures. The degree of hydration for the fly ash mix at later ages is highest in the samples cured at 73oF and decreases with increasing curing temperature.

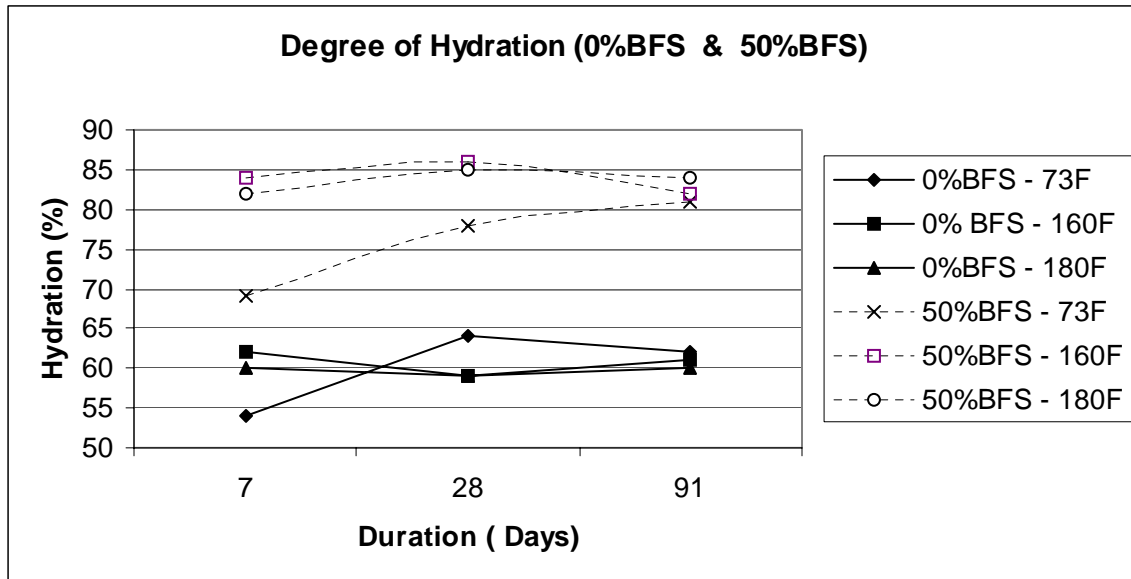


Figure 4.2. Degree of hydration for 0% BFS and 50% BFS mixes

Addition of slag as seen in Figure 4.2, resulted in a drastic increase in the degree of hydration over the mix without slag at both early and later ages for all curing temperatures. The slag mixes cured at higher temperatures showed a much higher degree of hydration at early ages, however at later ages all curing temperatures had reached to about the same degree of hydration.

Compressive Strength Results

The compressive tests were performed on twenty-seven different cylinders for each mix. Nine samples of each mix were tested at curing durations of 7, 28 and 91 days from the mixing date. Three samples each were tested for three different temperatures of 73, 160 and 180°F. The compressive strengths were determined in accordance with ASTM C39-93a. Figures 4.3 through 4.7 show the results of the compressive strength for the different mixes and curing conditions.

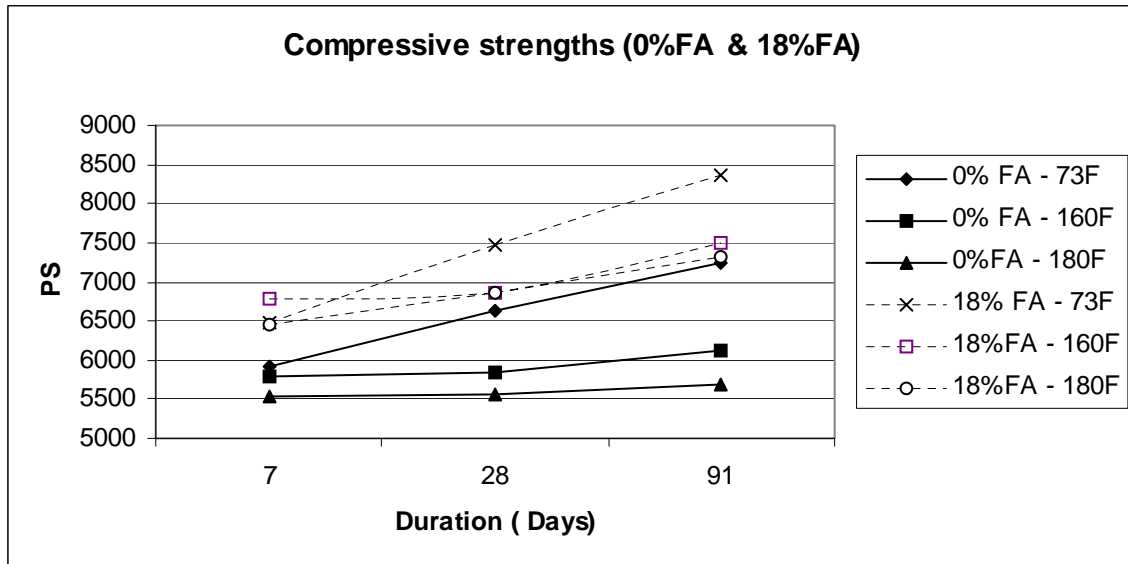


Figure 4.3. Compressive strengths for 0%FA and 18%FA mixes

Table 4.13. Compressive strength as a ratio of 28-day samples cured at 73oF

Mix	Duration (days)	Temperature (°F)		
		73	160	180
0% FA	7	0.89	0.87	0.84
	28	1.00	0.88	0.84
	91	1.09	0.92	0.86
18% FA	7	0.87	0.91	0.86
	28	1.00	0.92	0.92
	91	1.12	1.00	0.99

Higher curing temperatures resulted in lower strength for all ages and mixtures except fly ash mix at 7 days age, which had a higher strength at the 160F as shown in Figure 4.3 and Table 4.13. Addition of fly ash increased the strength at all ages and curing temperatures when compared to the mix without fly ash, mirroring the higher degree of hydration of the fly ash mixes over the plain cement mixes. The highest strength at later age was recorded for the fly ash mix cured at 73oF, which also had the highest degree of hydration at this age.

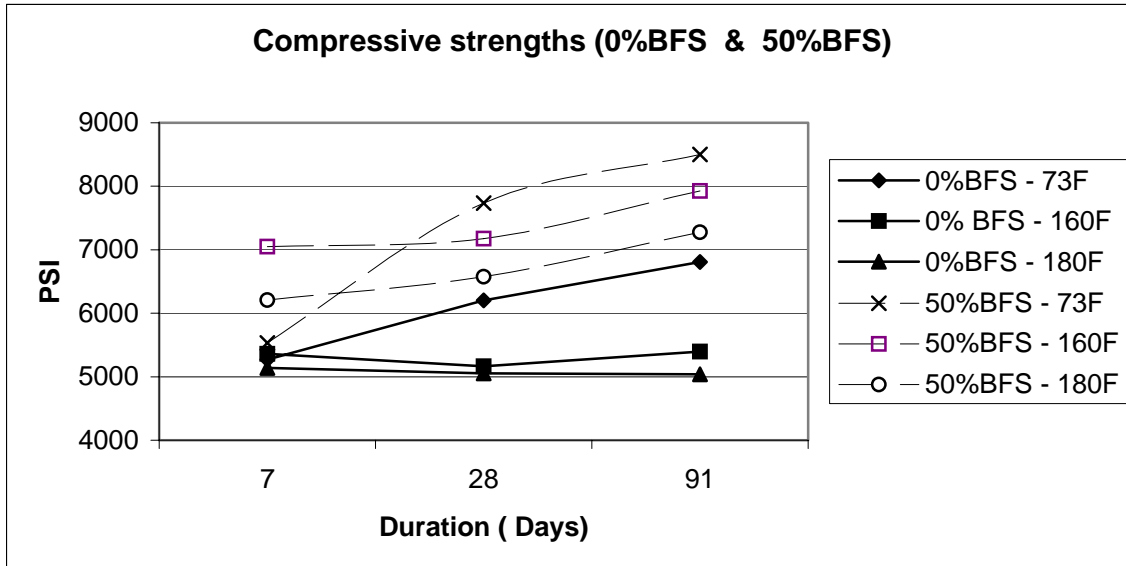


Figure 4.4. Compressive strengths for 0%BFS and 50%BFS mixes

Table 4.14. Compressive strength as a ratio of the 28-day samples cured at 73°F

Mix	Duration (days)	Temperature (°F)		
		73	160	180
0% Slag	7	0.85	0.86	0.83
	28	1.00	0.83	0.81
	91	1.10	0.87	0.81
50% Slag	7	0.71	0.91	0.80
	28	1.00	0.93	0.85
	91	1.10	1.02	0.94

Higher curing temperatures resulted in increased early age strength in the slag mix but reduced later age strength as seen in Figure 4.4 and Table 4.14. Higher curing temperatures in the mix without slag generally resulted in a decrease in both early and later age strength. The mix with slag had higher strengths at all curing durations and temperatures compared to the mix without the slag. This observation agrees with the higher degree of hydration in the slag mix over the mix without slag.

Resistance to Chloride Ion Penetration

Six samples of each mix were tested at 28 and 91 days, two for each curing temperature. The tests were done in accordance with ASTM C 1202-94. Results of this test are shown for the various mixes in Figures 4.5 and 4.6. The blended cement mixes were observed to have a higher resistance to chloride ion penetration than the plain cement mixes as shown by the lower charges passing through during the test.

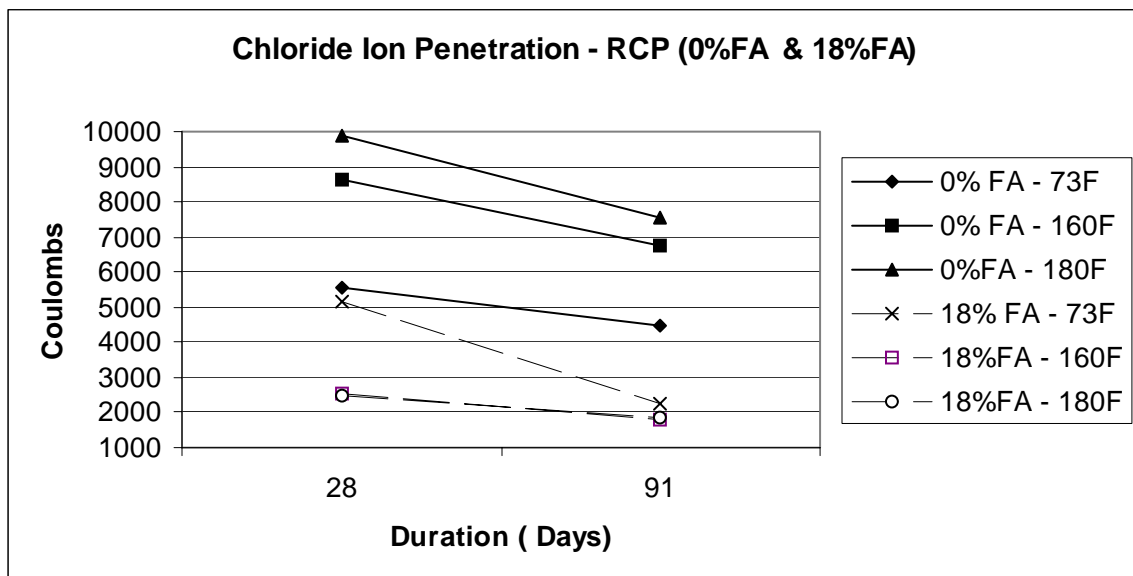


Figure 4.5 Chloride Ion Penetration results for 0%FA and 18%FA mixes

As shown in Figure 4.5 above, at higher curing temperatures, the mixes without fly ash, had higher chloride penetration at both 28 and 91 days. For the fly ash mixes however higher curing temperatures resulted at much reduced chloride ion penetration at 28 days although their influence on chloride penetration at 91 days was about the same as curing at 73°F. Overall, the fly ash mixes had lower chloride ion penetration at all curing durations and temperatures when compared to the mixes without fly ash.

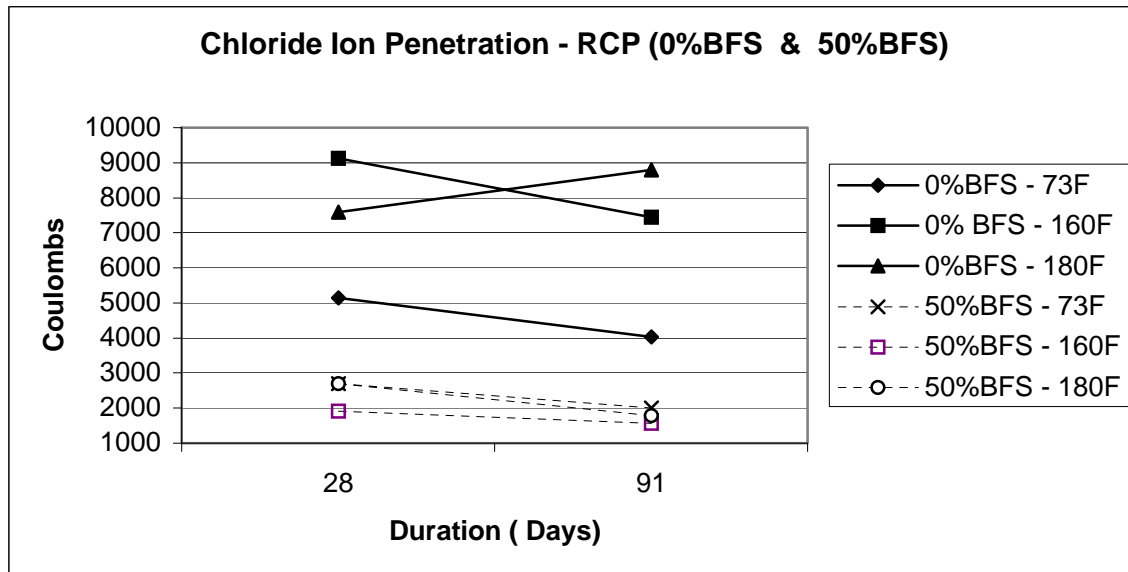


Figure 4.6. Chloride Ion Penetration results for 0%BFS and 50%BFS mixes

The mix without slag as seen in Figure 4.6, showed increased RCP values at higher temperatures. The RCP values for the slag mixes were not much affected by the curing temperatures. Overall, RCP values for the slag mixes were considerably reduced when compared to the mixes without slag at all curing temperatures and durations.

Density and Percentage of Voids Results

Two samples of each mix for each curing temperature weighing approximately 800g were tested at 7, 28 and 91 days to determine the density and percentage of voids. Figure 4.7 shows the density for the plain cement and fly ash mixes. Figure 4.8 shows the density for the blast furnace slag mix.

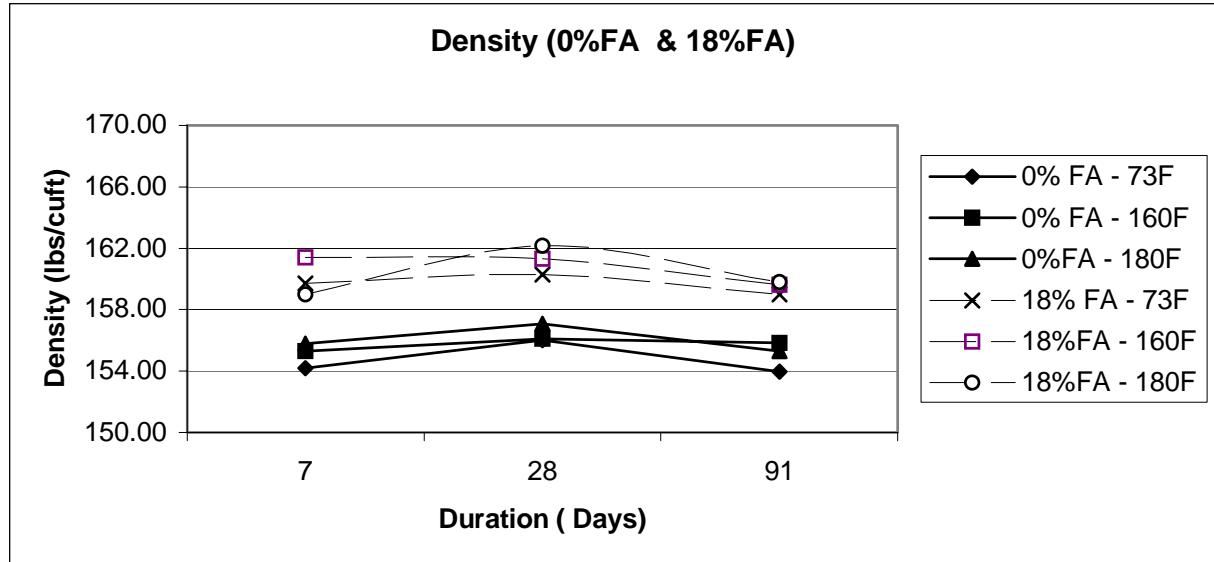


Figure 4.7 Density for 0%FA and 18%FA mixes

The mix with fly ash showed a higher density at all curing temperatures and curing durations, than the mix without it as seen in Figure 4.7. The curing temperature of the concrete had a minimal influence on the resulting density.

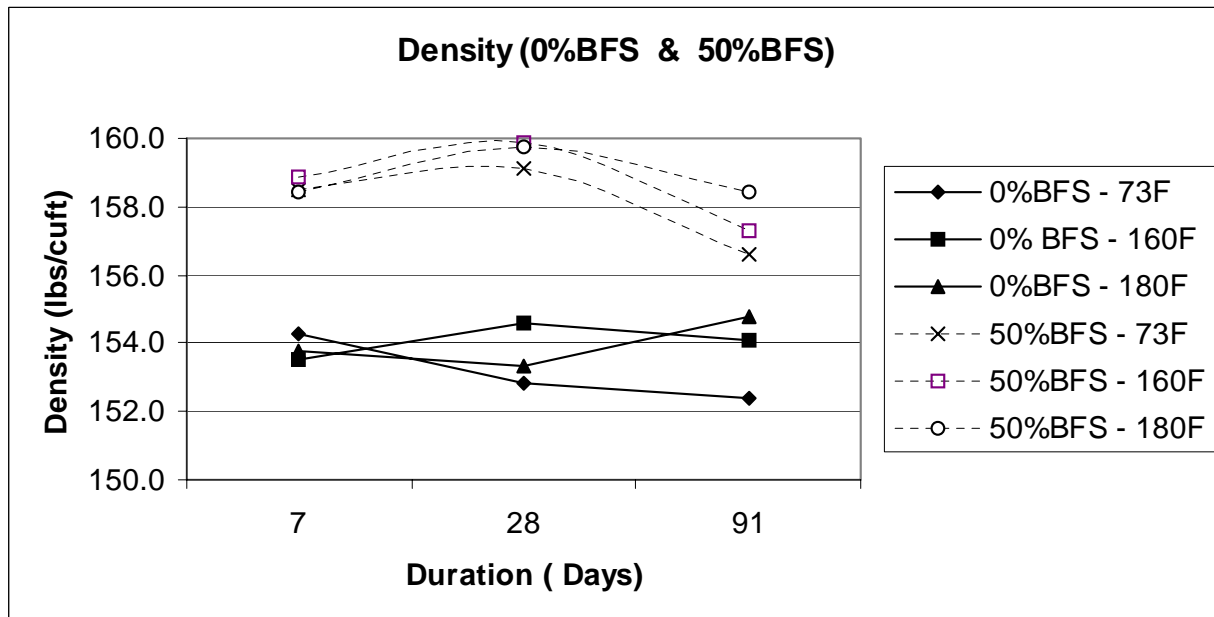


Figure 4.8. Density for 0% BFS and 50% BFS mixes

Addition of slag has increased density for all curing temperatures and ages. Higher curing temperatures have slightly increased density at 91 days for mixes with and without slag as seen in Figure 4.8.

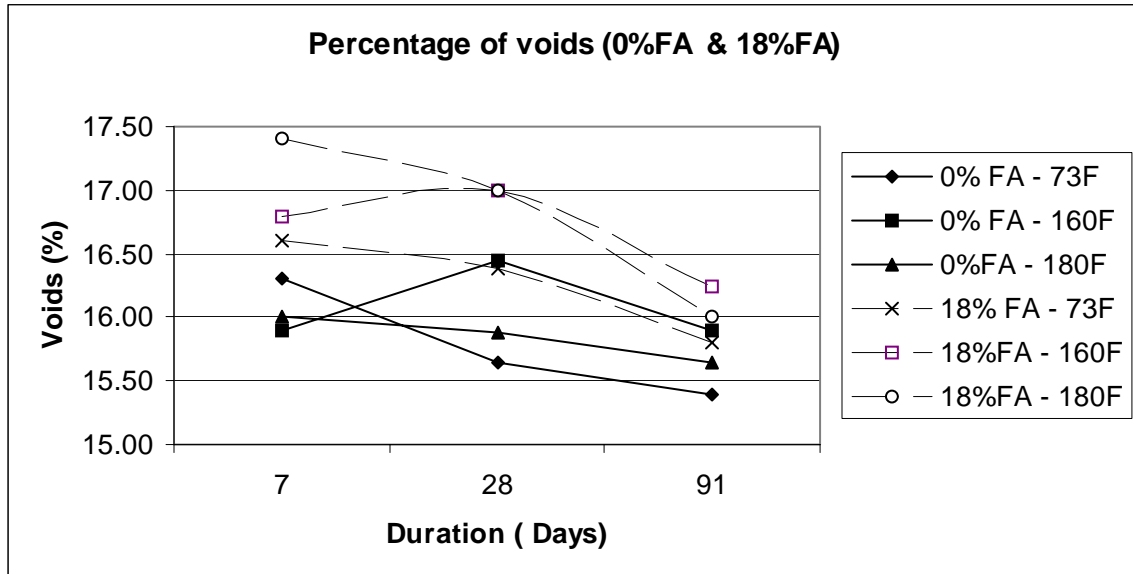


Figure 4.9. Percentage of voids for 0%FA and 18%FA mixes

At 7 days, the fly ash mixes had a higher percentage of voids at all curing temperatures when compared to the mix without fly ash as shown in Figure 4.9. The percentage voids in the fly ash mixes is higher in the samples cured at elevated temperatures. For both mixes with and without fly ash, the percentage of voids at 91 days was least in the samples cured at 73oF.

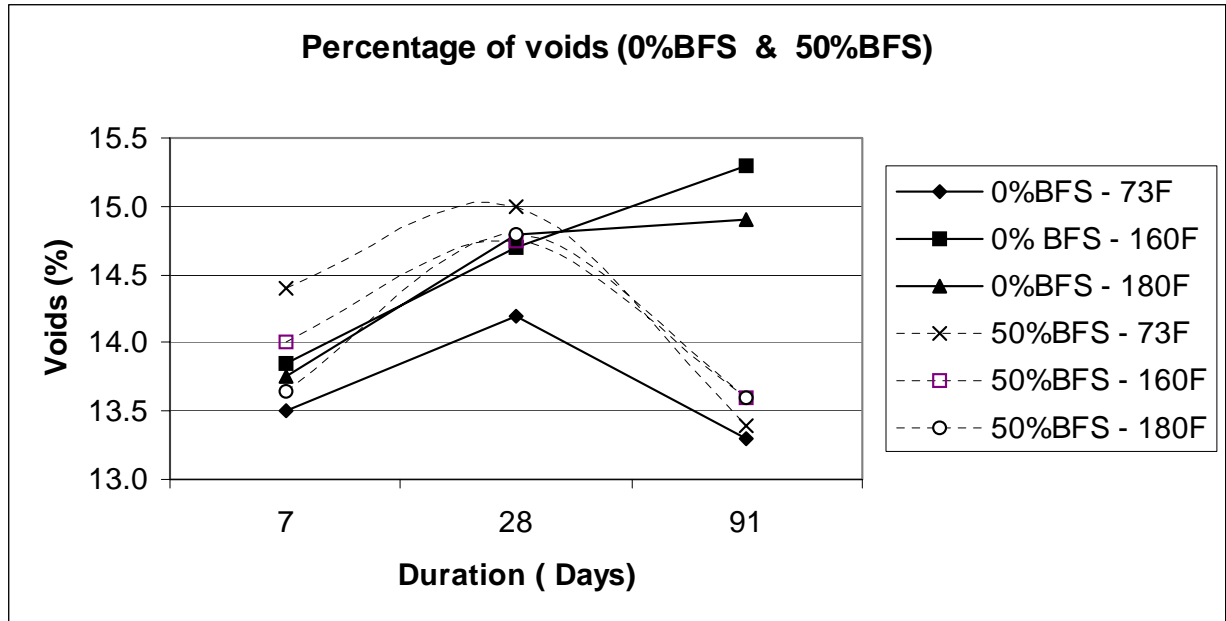


Figure 4.10. Percentage of voids for 0%BFS and 50%BFS mixes

At 7 days, the mixes with slag showed a lower percentage of voids in the samples cured at the elevated temperatures, however, this situation was reversed at 91 days in which the percentage of voids was lower in the samples cured at 73°F. At all curing temperatures and durations, the mix without slag cured at 73°F had the least percentage of voids as seen in Figure 4.10.

Time to Corrosion Results

The corrosion results for each mix and curing temperature is presented individually as an average of three samples. The results as shown in Figure 4.11 indicate the increase in the concrete durability by the use of slag. The use of fly ash also increased the time to corrosion when compared to the plain cement mixes, but to a smaller extent. Increasing the curing temperature for all the mixes resulted in reduction of time to corrosion.

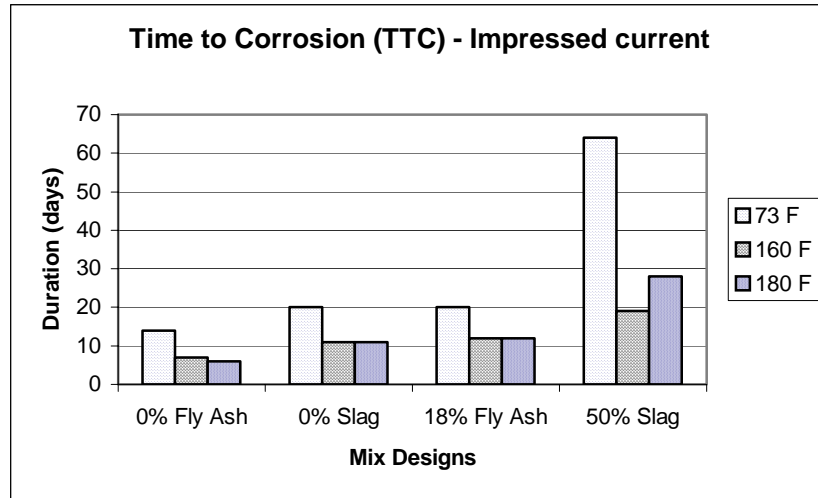


Figure 4.11. Time to Corrosion results for all mixes

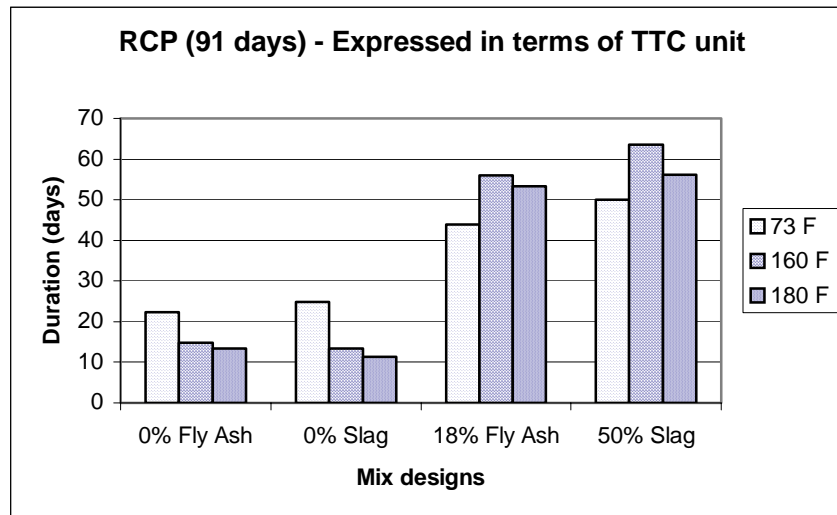


Figure 4.12. The RCP at 91days expressed in terms of Time to Corrosion unit

Three parameters were used in this research to study the durability of the concrete:

1. Percentage of voids
2. Rapid chloride permeability (RCP) and
3. Time to corrosion (TTC) – Impressed current

The following observations were made in relating these parameters:

- a. The percentage of voids determined for the various samples did not have much variation in the values and could not be used to establish differences in the durability of the mixes.
- b. The RCP and TTC tests exhibited similar results for the plain cement mixes (0% FA and 0% BFS), that is both tests showed reduction in durability when curing temperature increased (see Figures 4.11 and 4.12).
- c. The mixes with the Fly ash and slag showed conflicting durability results from the RCP and TTC tests as seen in Figures 4.11 and 4.12. The TTC test indicated better durability for the samples cured at 73oF (Figure 4.11), whereas the RCP test showed that the Fly ash and slag mixes had better durability at the higher curing temperatures.

Phase 3 – Microstructural Analysis

SEM Observations of Plain Cement Mixes

Effect of Curing Temperature on the Presence of Ettringite Crystals

1. None of the plain cement mixes cured at room temperature showed the presence of ettringite crystals (Figure 4.13). These samples had the highest permeability rates. However the high permeability values had no effect on ettringite formation. This observation agrees with a threshold temperature of 160°F is required during curing for ettringite to reform in the hardened concrete.
2. For the plain cement mixes cured at the elevated temperatures of 160 and 180°F, there was no observation of ettringite crystals when examined microscopically after 7 days of curing.

3. For the plain cement mixes cured at the elevated temperatures of 160 and 180°F, ettringite was present when they were examined at 28 and 91 days (Figures 4.14 & 4.16). These samples had higher permeability values when compared to the room cured samples.

Effect of Curing Duration on the Amount of Ettringite Crystals formed

1. At the elevated curing temperatures of 160 and 180°F well-formed balls of ettringite crystals were seen in the voids when examined at 28 days.
2. The high permeability of the samples cured at the elevated temperatures facilitated the formation and transportation of ettringite within the microstructure of the hardened samples. Voids observed partially filled with ettringite when examined at 28 days showed an increased amount of the ettringite crystals when examined at 91 days. Figures 5 and 7 show voids completely filled with ettringite when examined at 91 days, a direct consequence of the increased permeability.

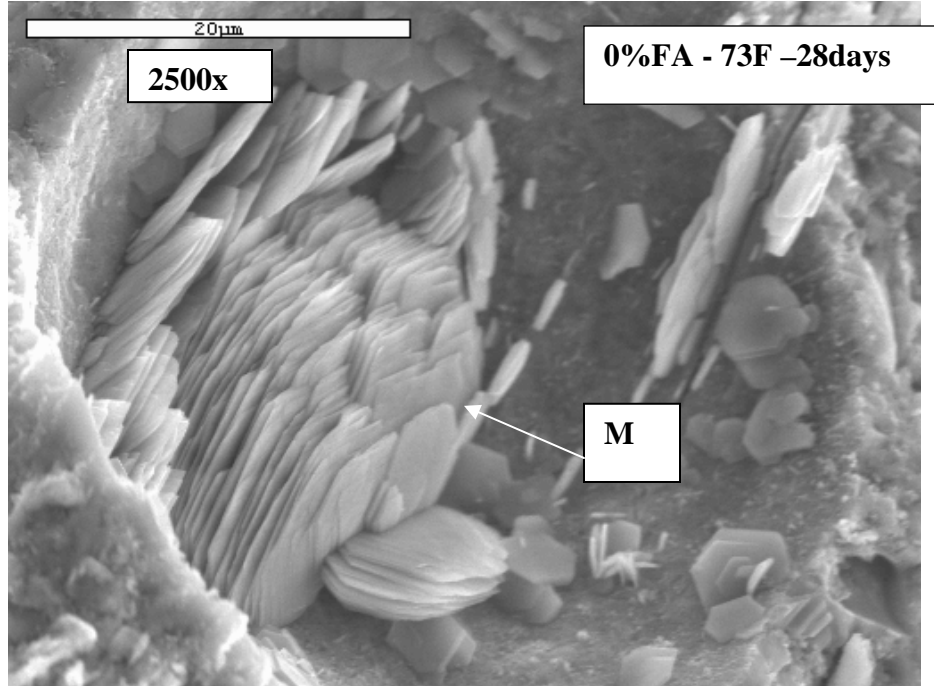


Figure 4.13 Well-defined Monosulphate (M) crystals in a void

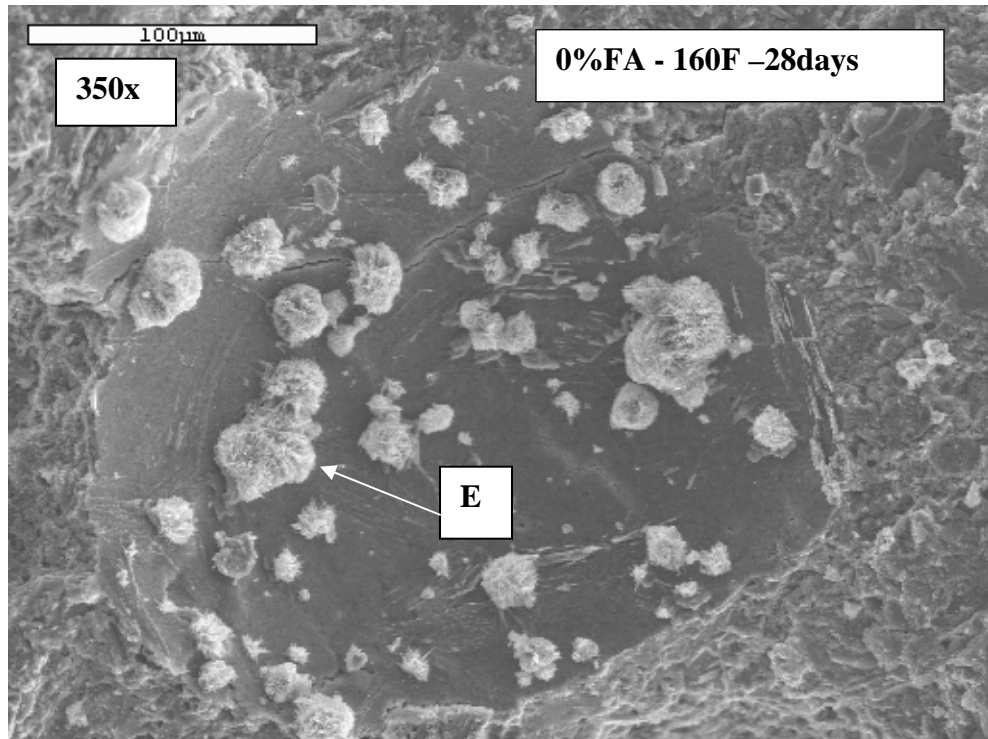


Figure 4.14. Void with clusters of Ettringite (E) crystals

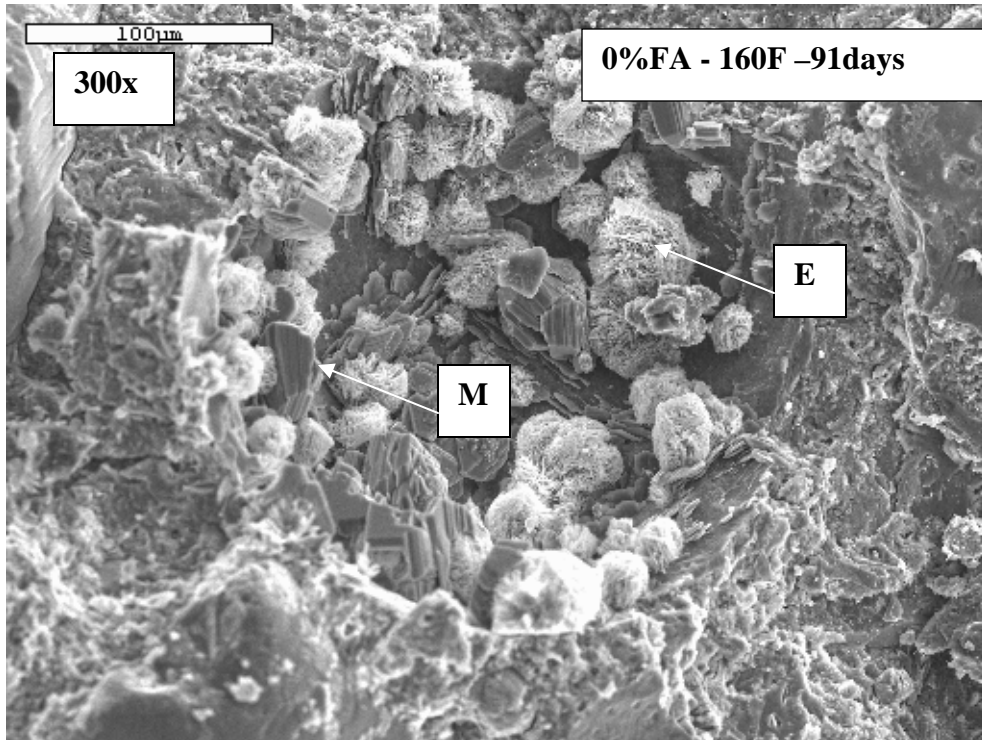


Figure 4.15. Void containing both Monosulphate (M) and Ettringite (E) crystals

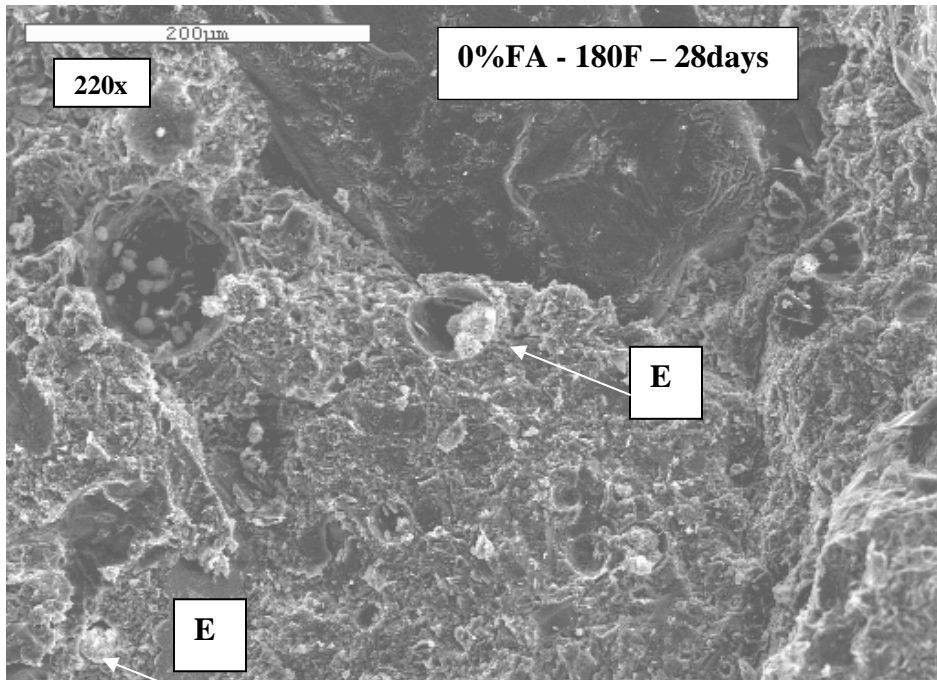


Figure 4.16. Voids containing Ettringite (E) some appear almost full of it.

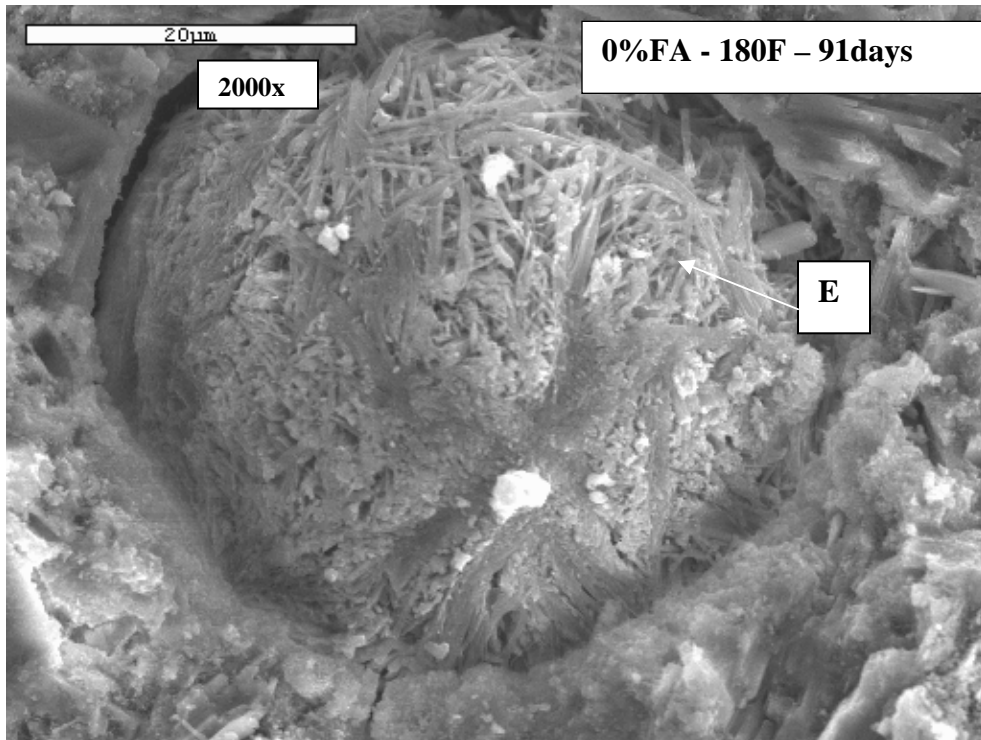


Figure 4.17. Void completely filled with fibrous Ettringite (E)

SEM Observations of Fly Ash Mixes

Introduction

Calcium hydroxide crystals formed by the hydrating cement constitute 20 to 25 percent of the volume of solid in the hydrated phase (Neville, 2004). Calcium hydroxide is water-soluble and may leach out of hardened concrete, leaving voids for ingress of water. Through its pozzolanic properties, fly ash chemically combines with calcium hydroxide and water to produce C-S-H, which fills in the spaces between hydrating cement particles, thus reducing the risk of leaching calcium hydroxide. The long-term reaction of fly ash refines the pore structure of concrete and reduces the permeability (ACI 232.2R-96, 1999). At normal temperatures, little pozzolanic activity from fly ash occurs after 28 days of curing (Malhotra and Ramezanianpour, 1994), this is evident in

the almost identical permeability values for the fly ash mixes and the plain cement mixes at 28 days cured at room temperatures. At the elevated temperatures however the pozzolanic activity occurs sooner and this is evident in the much lower permeability of the fly ash mixes cured at the elevated temperatures when compared to the plain cement mixes. At the elevated curing temperatures, the permeability values of the plain cement mixes is about 3 times more than those of the fly ash mixes.

Effect of Curing Temperature on the Presence of Ettringite Crystals

1. The fly ash samples cured at room temperature did not show the presence of ettringite even though the RCP test indicated the higher permeability values when compared to the fly ash mixes cured at the elevated temperatures.
2. At the elevated temperature curing of 160°F, ettringite was not present when examined at 28 days as shown in Figure 4.18. The low permeability of these samples will inhibit the ingress of water and the formation of ettringite. At 91 days however these samples showed the presence of ettringite crystals in the void spaces.
3. Ettringite was observed at 28 days in the fly ash samples cured at 180°F (Figure 4.19) just as in the plain cement mixes. These samples have almost identical permeability values to the fly ash samples cured at 160°F. While the samples cured at 160°F did not show ettringite at 28 days, the higher curing temperature of 180°F will account for the observation of the ettringite in the higher cured samples.

Effect of Curing Duration on the Amount of Ettringite Crystals formed in Voids

1. At 28 days, the ettringite formed in the voids of samples cured at 180°F was not as big and in well-formed balls as the crystals seen in the equivalent plain cement mixes.
2. At 91 days, examination of the fly ash samples cured at 180°F showed ettringite crystals in pore spaces (Figure 4.20). The amount of ettringite observed was increased from that observed in these samples at 28 days. These pores however were not entirely filled with the ettringite when compared to the equivalent plain cement mixes.

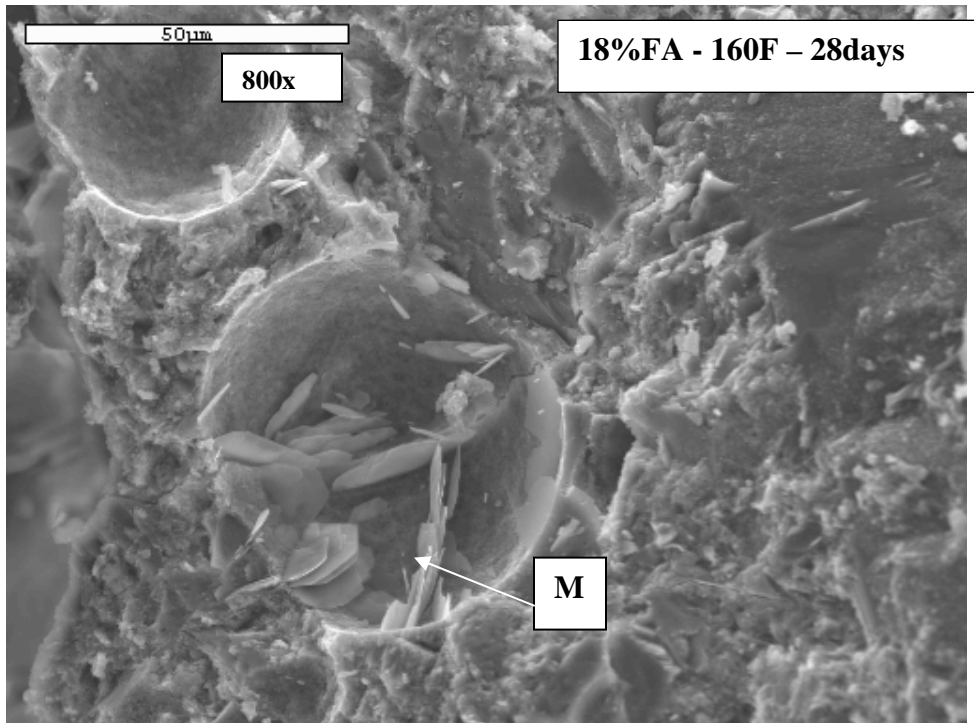


Figure 4.18. Void containing hexagonal plates of Monosulphate (M).

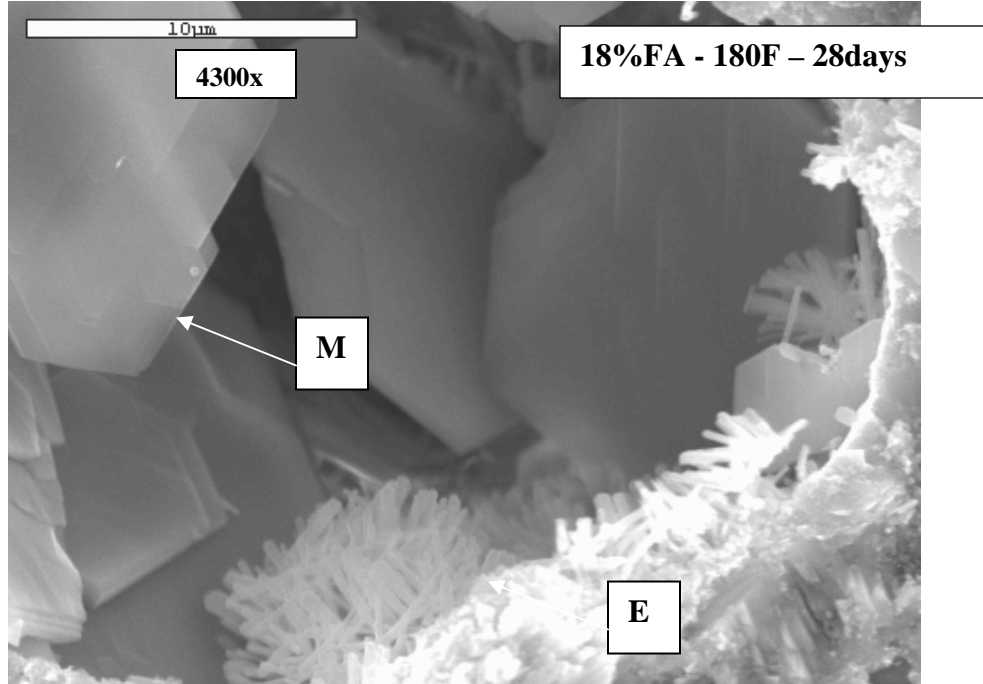


Figure 4.19. Void showing Monosulphate (M) transformed into Ettringite (E)

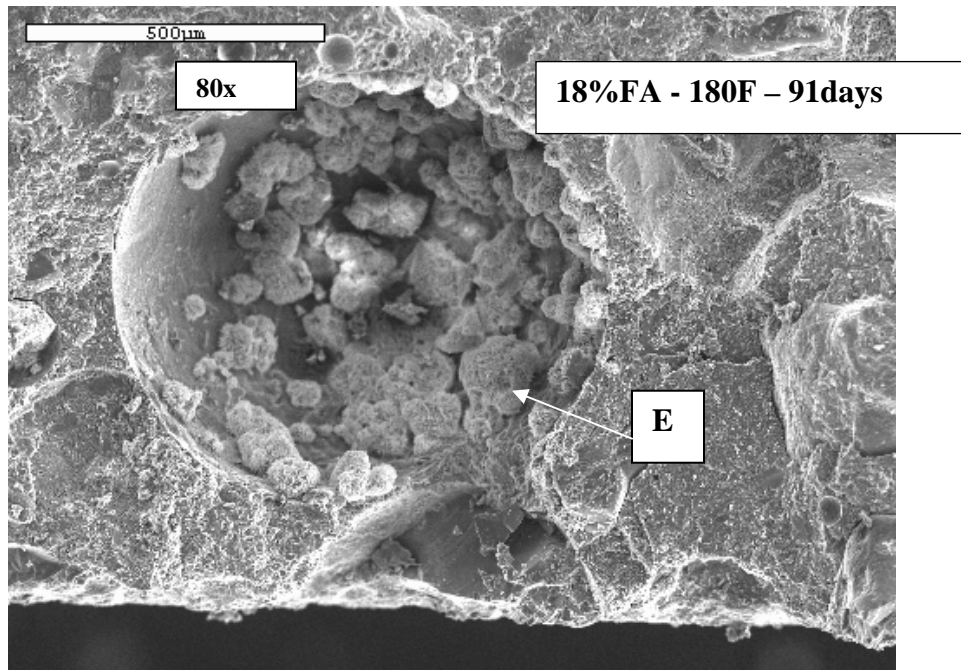


Figure 4.20. Clusters of Fibrous Ettringite (E) in void

SEM Observations of Slag Mixes

Introduction

Slag is a waste product in the manufacture of pig iron. Chemically, slag is a mixture of lime, silica, and alumina, the same oxides that make up Portland cement, but not in the same proportions (Neville, 2004). The permeability of mature concrete containing slag is greatly reduced when compared with concrete not containing slag. As the slag content is increased, permeability decreases. The pore structure of the cementitious matrix is changed through the reactions of slag with the calcium hydroxide and alkalis formed during the Portland cement hydration. Pores in concrete normally containing calcium hydroxide in part get filled with calcium silicate hydrate. Permeability of concrete depends on its porosity and pore-size distribution. Where slag is used, reduction in the pore size has been noted prior to 28 days after mixing (ACI 233R-95, 1999).

Miller and Conway (2003) examined the effectiveness of using slag to prevent DEF expansions in mortar made from expansive cements. One year into the study, they found that 5% slag substitution reduced or delayed, but did not eliminate expansions at curing temperatures above 167°F (75°C). Expansion was however completely absent when 17.5% slag substitution was used. Substitution of the cement by slag did not have any adverse effect on the strength of the mortar cured at 194°F (90°C) which showed superior strength at all ages for all mixes with 30% slag substitution (Miller and Conway, 2003). This was also evident in compressive strength tests of the mixes used in this study which showed higher strengths for the slag mixes cured at elevated temperatures (Chini and Acquaye, 2005). The beneficial effect of added slag in reducing expansions from DEF may have to do with the reduced pH of the pore solution. Ettringite is more stable below

pH of 12.5 and the slag may reduce the pH to the region where ettringite stability is enhanced. If there is less decomposition at the elevated temperature, less ettringite may potentially form later, when its formation may lead to volume instability (Miller and Conway, 2003).

Effect of Curing Temperature on the Presence of Ettringite Crystals

1. At all curing temperatures, the slag mixes had the lowest permeability values of the mixes tested.
2. No ettringite was observed at 28 days in the slag samples cured at the elevated temperatures (Figures 4.21 and 4.23). The slag samples had the least permeability values when compared to equivalent plain cement and fly ash mixes.
3. At 91 days, slag mixes cured at the elevated temperatures showed the presence of ettringite. Inclusion of 50% slag was the most effective at delaying the onset of the ettringite. However by 91 days, these ettringite crystals were observed in the void spaces

Effect of Curing Duration on the Amount of Ettringite Crystals formed

1. The amount of ettringite in the voids observed at 91 days in the elevated cured samples was in much smaller amounts than in the fly ash or plain cement mixes. They could only be seen at very high magnifications as shown in Figure 4.22.
2. Some ettringite crystals were formed on the surfaces of slag particles as seen in Figures 4.24 and 4.25

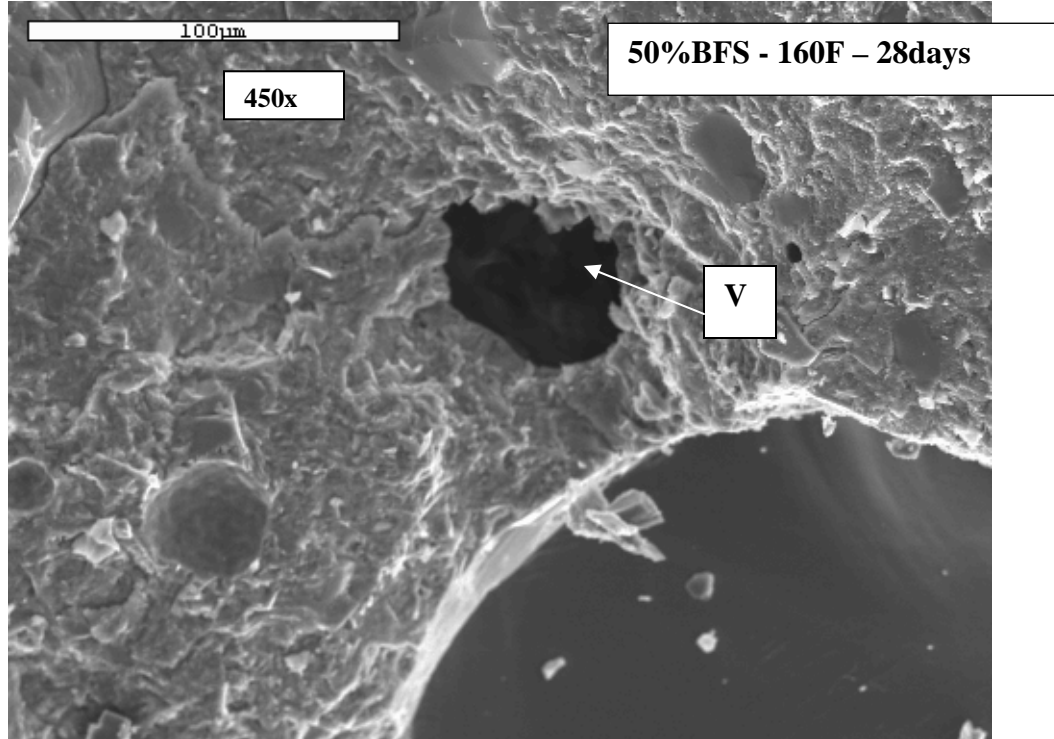


Figure 4.21. Sample with empty air Voids (V)

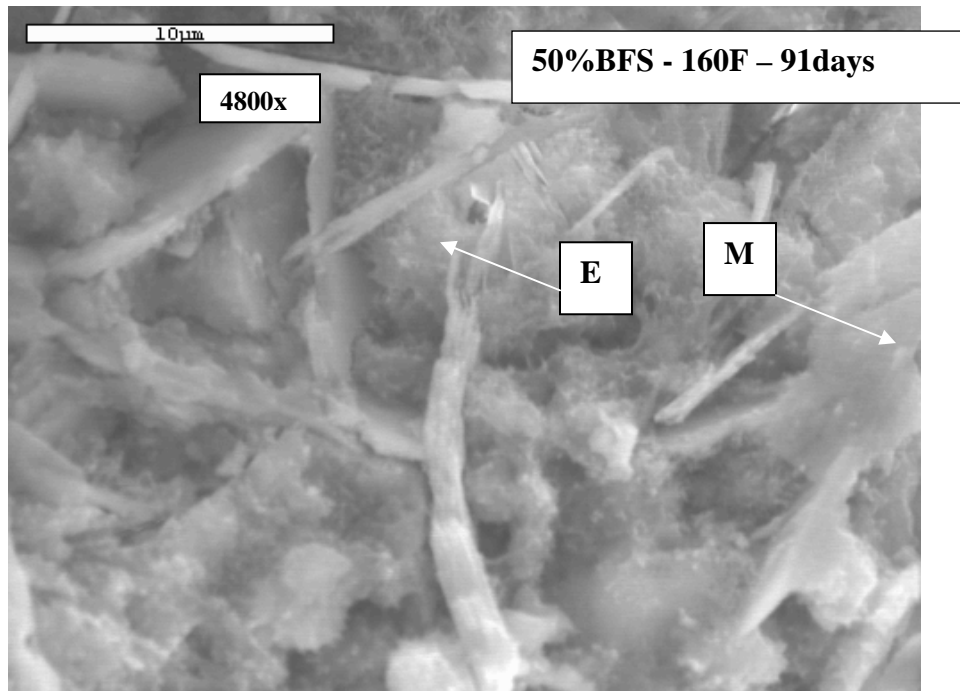


Figure 4.22 Higher magnification of Figure 4.32

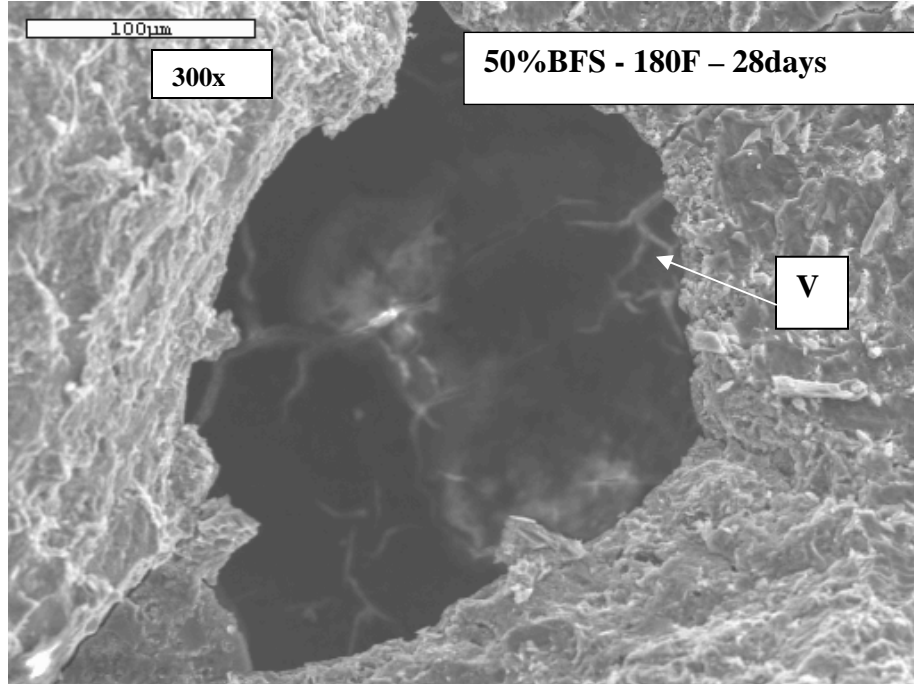


Figure 4.23. Sample with empty air Void (V)

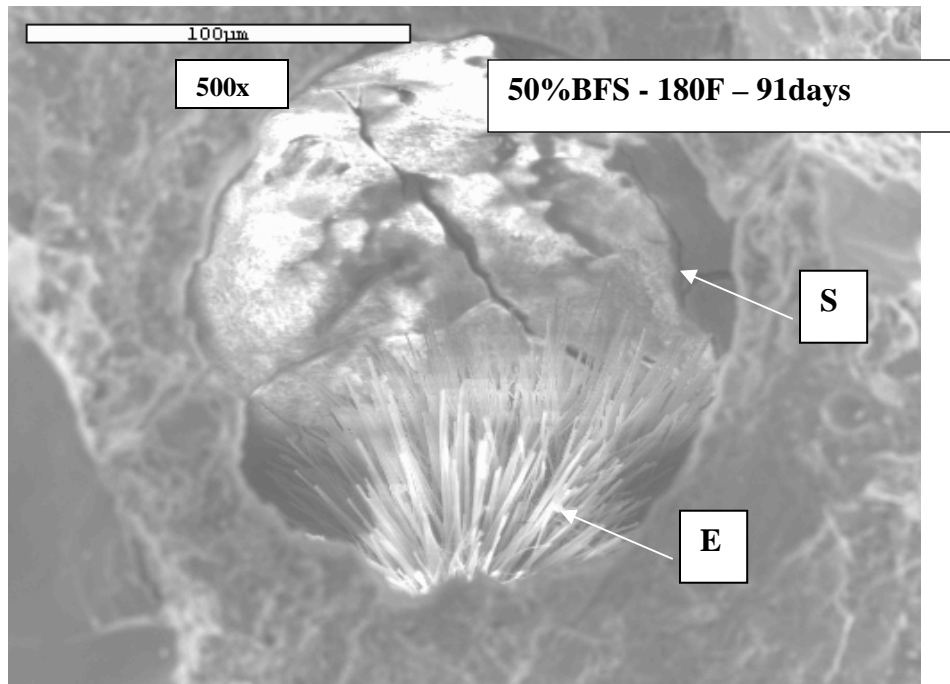


Figure 4.24. Reacting Slag (S) particle with Ettringite (E) formed

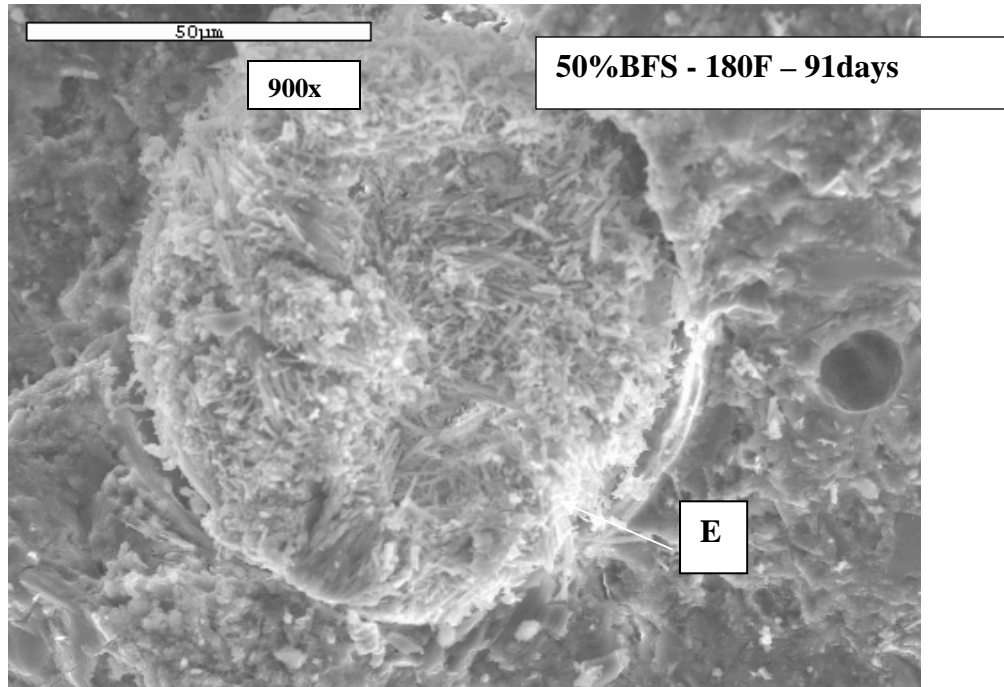


Figure 4.25 Slag particle completely covered with Ettringite (E)

CHAPTER 5 CONCLUSIONS AND RECOMMENDATIONS

Introduction

This dissertation investigated the effects of elevated curing temperatures on the strength, durability and potential of delayed ettringite formation (DEF) in typical FDOT Class IV mass concrete mixes. The three concrete mix designs tested were plain cement mixes, mixes with 18% fly ash and mixes with 50% slag. The durability of the concrete was evaluated through a measure of the permeability of the concrete. Higher permeability values indicated a greater ease of ingress of deleterious material and a less durable concrete. Two curing cycles were used for the elevated temperature curing- isothermal and adiabatic curing. Samples cured isothermally at the elevated temperatures were placed in tanks set at the elevated temperatures immediately after casting. In the adiabatic curing cycle, samples were introduced to the elevated curing temperature environment, 6 hours after casting. In the adiabatic curing cycle, the tanks were initially set at 80°F and the elevated temperatures of 160 and 180°F were attained within 2 and 2½ days respectively. The adiabatic curing cycles were set to simulate approximate conditions of mass concrete cured in the field.

Conclusions

Table 5.1 is a summary of the compressive strengths of plain cement mixes cured isothermally and Table 5.2 gives the permeability values of these samples. Summaries of results of the compressive strength, permeability and ettringite formation in samples cured adiabatically are shown in Tables 5.3 and 5.4. Comparing the strength and

permeability of the isothermally and adiabatically cured samples, the following conclusions were observed:

1. There was a substantial decrease in compressive strength of plain Portland cement concrete samples cast and stored immediately in water tanks under isothermal curing temperatures of 160 and 200°F compared to samples cured at room temperature 73°C. This reduction was 34 and 62% for 28-day compressive strength for samples cured at 160 and 200°F, respectively. In addition, RCP test of these samples showed a significant increase in permeability of concrete cured at high temperature.
2. When plain Portland cement concrete samples were subjected to the adiabatic curing cycle, there was a moderate reduction in 28-day compressive strength of samples cured at elevated temperatures compared to samples cured at room temperature. The reduction was approximately 15% and 18% for samples cured at temperatures of 160 and 180°F, respectively. However, there was still a significant increase in permeability of concrete measured through the RCP test.
3. Adiabatic curing of fly ash cement concrete samples (18% fly ash by weight) resulted in 8% reduction of 28-day compressive strength for samples cured at 160°F and 180°F compared to those cured at room temperature. However, permeability of concrete measured by RCP test improved noticeably at higher curing temperatures suggesting that at higher temperatures the fly ash becomes effective much earlier and reduces the

RCP values. At normal curing temperature the RCP reducing effect of fly ash becomes effective after approximately two months.

4. When 50% (by weight) of Portland cement is replaced by blast furnace slag, the 28-day compressive strength of samples cured adiabatically at elevated temperatures reduced by 7.and 15% for curing temperatures of 160°F and 180°F compared to those cured at room temperature. Results of compressive strength tests and RCP tests revealed that addition of blended cement improves strength and durability of concrete.

Table 5.1. Compressive strength samples cured isothermally

COMPRESSIVE STRENGTH (PSI)			
Temp (F)	Value	Plain cement mix	
		28 days	91 days
73	Avg*	7472	8252
	StaDev	304	276
	95%C.I.	±348	±319
<hr/>			
160	Avg*	4963	5616
	StaDev	276	624
	95%C.I.	±319	±711
<hr/>			
200	Avg*	2872	2636
	StaDev	276	406
	95%C.I.	±319	±464

Avg* – Average of 3 samples, SD – Standard Deviation, C.I. – 95% Confidence Interval

Table 5.2. RCP for samples cured isothermally

RAPID CHLORIDE PERMEABILITY (RCP)			
Temp (F)	Value	Plain cement mix	
		28 days	
		Coulomb	Rate
73	Avg*	4720.0	High
	SD	74.0	
	95% C.I.	±103	
160	Avg*	7110.0	High
	SD	410.0	
	95% C.I.	±568	
200	Avg*	11070.0	High
	SD	503	
	95% C.I.	±698	

Avg* – Average of 2 samples, SD – Standard Deviation, C.I. – 95% Confidence Interval

Table 5.3. Compressive strength for adiabatically cured samples

COMPRESSIVE STRENGTH (PSI)										
Temp (F)	Value	Plain cement mix			18% Fly ash mix			50% Slag mix		
		7 days	28 days	91 days	7 days	28 days	91 days	7 days	28 days	91 days
73	Avg*	5924	6624	7250	6465	7472	8369	5532	7734	8503
	SD	363.0	363.0	290.0	305.0	406.0	232.0	348.0	638.0	595.0
	95% C.I.	±290	±290	±232	±247	±319	±189	±290	±508	±479
160	Avg*	5780	5832	6119	6795	6860	7495	7049	7174	7924
	StaDev	305.0	334.0	305.0	334.0	406.0	406.0	348.0	392.0	392.0
	95% C.I.	±247	±276	±247	±261	±334	±334	±276	±319	±305
180	Avg*	5542	5572	5690	6454	6856	7312	6210	6578	7275
	StaDev	261.0	348.0	435.0	247.0	276.0	218.0	450.0	406.0	305.0
	95% C.I.	±203	±276	±348	±203	±218	±174	±363	±319	±247

Avg* – Average of 6 samples, SD – Standard Deviation, C.I. – 95% Confidence Interval

Relating the mix design, curing temperature, duration of curing and the concrete permeability to the amount and onset of formation of ettringite crystals in the samples cured adiabatically, the following conclusions were drawn from Table 5.4:

1. Samples cured at room temperature, resulted in high permeability values for each respective mix. However no ettringite crystals were observed in these samples when examined microscopically. This observation agrees with the fact that a threshold curing temperature of about 160°F is needed for ettringite to reform in the hardened concrete in the presence of moisture.
2. For samples cured at the elevated temperatures, the plain cement mixes had the highest permeability values and the largest amount of ettringite crystals observed in void spaces when examined at 28 and 91 days. The amount of ettringite increased with increased curing temperature and duration.
3. Addition of 18% fly ash and 50% slag reduced the permeability of the concrete mixes. At room temperature the slag mixes had the least permeability values at 28 days due to the early reaction of slag within this time. The fly ash mixes did not show much reduction in permeability values at 28 days when cured at room temperature.
4. Addition of fly ash and slag resulted in much reduced permeability values for samples cured at the elevated temperatures. The reduced permeability resulted in the delay of the onset of the ettringite and the amounts formed in the blended mixes.
5. The 50% slag was better at delaying the onset on the ettringite in the samples cured at 180°F so that at 28 days no ettringite was observed. At

160°F however, both the 18% fly ash and 50% slag were effective at delaying the onset of ettringite prior to 28 days.

Research Implications for Mass Concrete Structures.

This research has very important implications for mass concrete structures. These include:

- a. The samples used in this study were smaller allowing for easier penetration of water.
- b. This fact notwithstanding, the fly ash and slag were beneficial in delaying as well as limiting ettringite formation in the hardened concrete.
- c. In mass concrete structures, the high temperatures will be at the core of the structure and the dense structures resulting from the addition of slag and fly ash may prevent the ingress of water to such potential spots for ettringite formation in the hardened structure.
- d. Additionally, the modification of the pore solution by adding fly ash and slag may prevent ettringite formation in the hardened concreted and the associated expansion and deterioration.

Table 5.4. RCP and Ettringite Formation for adiabatically cured samples

RAPID CHLORIDE PERMEABILITY (RCP) and ETTRINGITE FORMATION (EF)														
Temp (°F)	Value (RCP)	Plain cement mix				18% Fly ash mix				50% Slag mix				
		28 days		91 days		28 days		91 days		28 days		91 days		
		RCP (Coulomb)	EF #	RCP (Coulomb)	EF #	RCP (Coulomb)	EF #							
73	Avg*	5,562	No	4,494	No	5,173	No	2,279	No	2,692	No	2,002	No	
	SD	236		159.0		205		135		239		290		
	95%C.I.	±231		±156		±201		±132		±234		±284		
	Rate	High		High		High		Mod		Mod		Mod		
160	Avg*	8,633	Yes <50%	6,772	Yes <50%	2,548	No	1,787	Yes <50%	1,931	No	1,572	Yes <50%	
	SD	1,189		348		242		176		164		182		
	95%C.I.	±1165		±341		±237		±173		±160		±178		
	Rate	High		High		Mod		Low		Low		Low		
180	Avg*	9,888	Yes >50%	7,532	Yes >50%	2,503	Yes <50%	1855**	Yes <50%	2,329	No	1,778	Yes <50%	
	SD	1,270		1,236		221		64		283		204		
	95%C.I.	±1245		±1211		±217		±72		±278		±200		
	Rate	High		High		Mod		Low		Mod		Low		

RCP Avg* –Average of 4 samples, SD – Standard Deviation, C.I. – 95% Confidence Interval

** – Average of 3 samples

EF # - Presence of ettringite in sample and percentage of void space filled with crystals formed:

< 50% - less than 50% of a void filled with ettringite

> 50% - greater than 50% of a void filled with ettringite

Recommendations

The objective of this dissertation was to investigate the performance of Portland cement concretes cured at elevated temperatures using typical FDOT Class IV concrete mixes. This was to determine if reported high curing temperatures (170 to 200°F) in FDOT mass concrete projects have detrimental effects on strength, durability and other physical/chemical properties of concrete. This research was also conducted to determine if limits placed on the differential temperatures curing should be extended to include

limits on the maximum core curing temperature. Based on findings of this dissertation it is recommended that:

1. Use of fly ash or slag as a cement replacement should be required in mass concrete since these fly ash and slag reduce the detrimental effect of high curing temperature on strength and durability of pure cement concrete.
2. When fly ash and slag are used as a cement replacement, based on ideal laboratory conditions and accurate batching proportions there was an 8 to 15% reduction in compressive strength due to elevated curing temperatures. However, this loss could be inflated considerably if the concrete was produced at a batch plant with wider mixer proportions tolerances and the ever-present potential of unmetered water in the mix.
3. This research also showed that when the pure cement concrete specimens were placed in preheated curing tanks as soon as they were molded and cured under constant temperatures of 160 and 200°F, their compressive strengths were significantly decreased (34 and 62% for 160 and 200°F, respectively) and their permeability were increased.
4. Use of fly ash or slag as a cement replacement in the blended concretes cured at the elevated temperatures resulted in low permeability values, which delayed the onset and amount of ettringite formed in the microstructure.
5. Formation of delayed ettringite in samples 28 days and older where temperature was 160 and 180°F is a point of concern and more study is needed to look at the microstructural analysis of samples cured at

temperatures more than 160°F, specifically for detection of delayed ettringite formation.

6. More research is needed to evaluate the effects of other proportions of fly ash and slag. Future research should also evaluate the effect of varying sample sizes on the observations made as well as observing the samples over a much longer study period.

APPENDIX A CONCRETE MIX DESIGNS

Mix 1 – Plain Cement Mix

TRAIL BATCH- DATA AND CALCULATIONS

(Saturated, Surface-dry Aggregates)

0% Flyash

Date: Nov. 19, 2001

Project: Jeeps at Hockessin - Mix No.1

Aggregate Properties: Grade *57
specific gravity: Fine 2.64 Coarse 2.42
Moisture Calculations:
FA= 0.00-0.50=0.50
CA= 1.6-2.60=3.05

Weights By: Lucy, Matt, and Richard
R. Delorenzo
Mixing By: R. Delorenzo
Air Content 1 to 6 %

Specifications:
Cement content 744 lb. Cement Type T#1

Slump range 3" in. ± 1.5"

Batch 6.0 Cu.Ft. CP= 6.222

MATERIAL	SOURCE	WT. PER CU.YD.(LB)	VOL. PER CU.YD.(CF)	WT. PER BATCH(LB)	ADJ. WT. PER BATCH(LB)	REMARKS
Cement	Southdown	<u>744</u>	<u>3.79</u>	<u>165.2</u>	<u>165.2</u>	
FLYASH						
WATER	G.Ville	<u>305</u>	<u>4.81</u>	<u>67.2</u>	<u>57.0</u>	<u>-10.8</u>
FINE AGG.	76-137	<u>936</u>	<u>5.68</u>	<u>208.0</u>	<u>207</u>	<u>+1.0</u>
COARSE AGG.	08-005	<u>1746</u>	<u>11.56</u>	<u>383.5</u>	<u>399.8</u>	<u>+11.8</u>
AIR ENTRAINER	DrexelSEA	<u>4 oz</u>	<u>1.06</u>	<u>26.3 ml</u>	<u>26.3 ml</u>	
ADMIXTURE	WITA 64	<u>24.4 oz</u>		<u>16.2</u>	<u>16.2</u>	
TOTAL				<u>27.0</u>		

SLUMP(IN) 6 1/2 AIR(%) 4.0 MIX TEMP 71°F WORKABILITY Good AIR TEMP 72°F
SLUMP BY: Fitzgerald AIR BY: Delorenzo CYLS. BY: J.C. Pizz. Refid. START TIME: 8:24
W/C RATIO .41 H2O HELD OUT ✓ ADDED ✓ END TIME: 8:32

CYLINDERS-COMPRESSIVE STRENGTH

TIME OF SET

(/ /) INITIAL SET: _____ / /
3 DAYS- _____

(/ /) FINAL SET: _____
7 DAYS- _____

(/ /) REMARKS: _____
28 DAYS- _____

DESIGNED BY: _____

WITNESSED BY: _____

Mix 2 – 18% Fly Ash Mix**TRAIL BATCH-- DATA AND CALCULATIONS**

(Saturated, Surface-dry Aggregates)

18% FlyAshDate: Nov. 19, 2007Project: Degree of Hydration - Mix No. 2

Aggregate Properties: Grade #57
 Specific gravity: Fine 2.64 Coarse 2.42
 Moisture Calculations:
 $FA = 0.00 - 0.50 = 0.50$
 $CA = 5.65 - 2.60 = 3.05$

Weights By: Ley, Matt and Richard
 Mixing By: R. DeLorenzo
 Air Content 1 to 6 %

Specifications:
 Cement content 744 lb. Cement Type I/II
 Slump range 3" in. $\pm 1.5"$

Batch 60 Cu.Ft. CF= 1.7222

MATERIAL	SOURCE	WT. PER CU.YD. (LB)	VOL. PER CU.YD. (CF)	WT. PER BATCH(LB)	ADJ. WT. PER BATCH(LB)	REMARKS
Cement	Costladow	610	3.10	125.5	125.5	
FLYASH	Excel	134	0.91	29.8	29.8	
WATER	G-Ville	205	4.29	67.8	57.1	-10.7
FINE AGG.	76-127	918	5.57	204.0	203.0	-1.0
COARSE AGG.	08-005	1729	11.45	384.2	395.9	+11.7
AIR ENTRAINER	Latex AFA	4 oz	1.08	26.3 ml	26.3 ml	
ADMIXTURE	MILA 64	24.4 oz		160.3 ml	160.3 ml	
TOTAL			27.0			

SLUMP(IN) 5 AIR(%) 2.0 MIX TEMP 75°F WORKABILITY OK AIR TEMP 72SLUMP BY: Thomas AIR BY: DeLorenzo CYLS. BY: Joe, Matt, Richard START TIME: 8:25W/C RATIO .41 H2O HELD OUT / ADDED / END TIME: 9:28

CYLINDERS-COMPRESSIVE STRENGTH

TIME OF SET

(/ /)	INITIAL SET:	(/)
3 DAYS-		
(/)	FINAL SET:	
7 DAYS-		
(/ /)	REMARKS:	
28 DAYS-		

DESIGNED BY: _____

WITNESSED BY: _____

Mix 3 – Plain Cement Mix

TRAIL BATCH-- DATA AND CALCULATIONS
 (Saturated, Surface-dry Aggregates) **(0% Fly Ash)**

Date: Feb 5, 2002 Project: Test of Hydration - Mix 3

Aggregate Properties: Grade 57 Weights By: Ley, Richard & Matt
 Specific gravity: Fine 2.64 Coarse 2.42 Mixing By: L. DiLorenzo
 Moisture Calculations:
 $FA = 0.00 - 0.50 = 0.50$ Air Content 1-6%
 $CA = 4.90 - 2.60 = 2.30$

Specifications:
 Cement content 744 lb. Cement Type F/A Slump range 3" in. ± 1.5"

Batch 6.0 Cu.Ft. CF= 0.2222

MATERIAL	SOURCE	WT. PER CU.YD. (LB)	VOL. PER CU.YD. (CF)	WT. PER BATCH(LB)	ADJ. WT. PER BATCH(LB)	REMARKS
Cement	Southdown	744	3.79	16.5.3	16.5.2	
FLYASH	-					
WATER	Gville	305	4.89	67.8	58.7	-9.1
PINE AGG.	76-137	936	5.62	208.0	207	+1.0
COARSE AGG.	OB-005	1746	11.56	388.0	398.1	+10.1
AIR ENTRAINER	Dairy AEA	4 oz	1.08	26.3 mL	26.3 mL	
ADMIXTURE	WLA 64	24.40z		160.3 mL	160.3 mL	
TOTAL			27.0			

JUMP (IN) 6 1/2 AIR(%) 4.5 MIX TEMP 69°F WORKABILITY Good AIR TEMP 70°F
 SLUMP BY: L. Fitzgerald AIR BY: T. Thomas CYLS. BY: Bob Fitzgerald START TIME: 9:07^A
 W/C RATIO 0.41 H2O HELD OUT — ADDED — END TIME: 9:15^A

CYLINDERS-COMPRESSIVE STRENGTH

TIME OF SET

<u>1 / 1</u> 3 DAYS-	INITIAL SET:	<u>1 / 1</u>
<u>1 / 1</u> 7 DAYS-	FINAL SET:	<u>1 / 1</u>
<u>1 / 1</u> 28 DAYS-	REMARKS:	<u>1 / 1</u>

DESIGNED BY: _____

WITNESSED BY: _____

Mix 4- 18% Fly Ash Mix**TRAIL BATCH-- DATA AND CALCULATIONS**

(Saturated, Surface-dry Aggregates)

Date: Feb 5 2022

(18% Fly Ash)

Project: Degree of Hydration - Mix 4

Aggregate Properties: Grade 57
 Specific gravity: Fine 2.64 Coarse 2.42
 Moisture Calculations:
 $FA = 0.00 - 0.50 = 0.50$
 $CA = 1.90 - 2.60 = 2.30$

Weights By: Lucey, Richard, & Matt
 Mixing By: R. Delorenzo
 Air Content 1.6 %

Specifications:
 Cement content 744 lb. Cement Type I/II Slump range 3" in. ± 1.5"

Batch 6.0 Cu.Ft. CF= 0.2222

MATERIAL	SOURCE	WT. PER CU.YD. (LB)	VOL. PER CU.YD. (CF)	WT. PER BATCH(LB)	ADJ. WT. PER BATCH(LB)	REMARKS
Cement	Southdown	610	3.10	135.5	135.5	
FLYASH	Royal	134	0.91	29.8	29.8	
WATER	G.Ville	305	4.89	67.8	58.8	-9.0
FINE AGG.	76-127	918	5.57	204.0	203.0	-1.0
COARSE AGG.	DF-005	1729	11.45	384.2	394.2	+10.0
AIR ENTRAINER	Dow AEA	4 oz	1.08	26.3 ml	26.3 ml	
ADMIXTURE	WPOT 64	24.4 oz		160.3 ml	160.3 ml	
TOTAL			27.0			

JMP(IN) 7.5 AIR(%) 2 1/2 MIX TEMP 70.0 WORKABILITY Good AIR TEMP 70°F
 SLUMP BY: Fitzgerald AIR BY: Delorenzo CYLS. BY: Roberts, Fitzgerald START TIME: 10:04 AM
 W/C RATIO 0.41 H2O HELD OUT — ADDED — END TIME: 10:12 AM

CYLINDERS-COMPRESSIVE STRENGTH

TIME OF SET

<u>1 / 1 / 1</u>	INITIAL SET: _____	(/)
<u>3 DAYS-</u>	FINAL SET: _____	
<u>7 DAYS-</u>	REMARKS: _____	
<u>(/ /)</u>		
<u>28 DAYS-</u>		

DESIGNED BY: _____

WITNESSED BY: _____

Mix 5 – Plain Cement Mix

TRAIL BATCH-- DATA AND CALCULATIONS

(Saturated, Surface-dry Aggregates)

0% Slag

Date: 2-13-02

Aggregate Properties: Grade #57
 Specific gravity: Fine 2.64 Coarse 2.42
 Moisture Calculations:
 $FA = 0.00 - 0.50 = 0.50$
 $CA = 4.59 - 2.68 = 1.91$

Project: Degree of Hydration-Mix 5Weights By: Richard L. KeyMixing By: Delorme / RentsAir Content 1-6 %

Specifications:
 Cement content 660 lb. Cement Type I/II Slump range 3" ± 1.5"

Batch 6.0 Cu.Ft. CF= 0.2222

MATERIAL	SOURCE	WT. PER CU.YD. (LB)	VOL. PER CU.YD. (CF)	WT. PER BATCH(LB)	ADJ. WT. PER BATCH(LB)	REMARKS
CEMENT	Cemex- (Southdown)	<u>660</u>	<u>2.36</u>	<u>146.7</u>	<u>146.7</u>	
SLAG/ASH	—					
WATER	G.Ville	<u>267</u>	<u>4.26</u>	<u>59.3</u>	<u>52.6</u>	<u>- 6.7</u>
FINE AGG.	76-137	<u>1076</u>	<u>6.53</u>	<u>239.1</u>	<u>227.9</u>	<u>+ 1.2</u>
COARSE AGG.	08-005	<u>1794</u>	<u>11.88</u>	<u>398.6</u>	<u>406.5</u>	<u>+7.9</u>
AIR ENTRAINER	Duck AER	<u>5.0 oz</u>	<u>0.95</u>	<u>32.9 mL</u>	<u>32.9 mL</u>	
ADMIXTURE	WRDA 64	<u>33.0 oz</u>	<u>—</u>	<u>216.9 mL</u>	<u>216.9 mL</u>	
ADMIXTURE	—					
ADMIXTURE	—					
TOTAL			<u>27.00</u>			

SLUMP(IN) 5.25 AIR(%) 6.0 MIX TEMP 74°F WORKABILITY Fluid AIR TEMP 72°FSLUMP BY: Richie AIR BY: Richie CYLS. BY: Richie START TIME: 09:00W/C RATIO 0.40 H2O HELD OUT — ADDED — END TIME: 09:18

CYLINDERS-COMPRESSIVE STRENGTH

REMARKS:

DESIGNED BY: _____

WITNESSED BY: _____

Mix 6 – 50% Slag Mix

TRAIL BATCH-- DATA AND CALCULATIONS

Saturated, Surface-dry Aggregates

Date: 3-13-02

aggregate Properties: Grade #57
 specific gravity: Fine 2.64 Coarse 2.42
 Moisture Calculations:
 FA = 0.00 - 0.50 = 0.50
 CA = 4.59 - 2.64 = 1.95

50% Slag

Project: Degree of Hydration - Mix 6

Weights By: Richard A Lucy

Mixing By: DeLorenzo / Robert,

Air Content 1-6 %

Specifications:

Cement content 660 lb. Cement Type I/II

slump range 3" ± 1.5"

Batch 6.0 Cu.Ft. CF= 0.2222

MATERIAL	SOURCE	WT. PER CU. YD. (LB)	VOL. PER CU. YD. (CF)	WT. PER BATCH(LB)	ADJ. WT. PER BATCH(LB)	REMARKS
CEMENT	Cemex - (Gardnrum)	330	1.68	73.3	73.3	
FLYASH/SLAG	Lafarge - SugaCem	320	1.80	73.3	73.3	
WATER	G.Ville	267	4.28	59.3	52.6	- 6.7
FINE AGG.	76-137	1066	6.47	236.9	235.7	-1.2
COARSE AGG.	08-005	1785	11.82	396.6	404.5	+7.9
AIR ENTRAINER	Drex AEA	5.0 oz	0.95	32.9 mL	32.9 mL	
ADMIXTURE	WHLA 64	33.0 oz	-	216.1 mL	32.9 mL	
ADMIXTURE						
TOTAL			27.00			

SLUMP (IN) 3.25 AIR (%) 3.9 MIX TEMP 74°F WORKABILITY *stiff* AIR TEMP 72°F

SLUMP BY: Roberts AIR BY: Roberts CYLS. BY: Roberts START TIME: 0755

W/C RATIO 0.40 H2O HELD OUT — ADDED — END TIME 12:03

CYLINDERS, COMPRESSIVE STRENGTH

REMARKS.

SIGNED BY:

WITNESSED BY:

Mix 7 – Plain Cement Mix**TRAIL BATCH-- DATA AND CALCULATIONS**
(Saturated, Surface-dry Aggregates)

0% Slag

Date: 5-8-02Project: Degree of Hydration-Mix 7

Aggregate Properties: Grade #57
 Specific gravity: Fine 2.64 Coarse 2.42
 Moisture Calculations:
 $FA = 0.00 - 0.50 = 0.50$
 $CA = - - -$

Weights By: DaleenzoMixing By: DaleenzoAir Content 1-6%

Specifications:
 Cement content 660 lb. Cement Type I/II

Slump range 3" ± 1.5"

Batch Cu. Ft. CF=

MATERIAL	SOURCE	WT. PER CU.YD. (LB)	VOL. PER CU.YD. (CF)	WT. PER BATCH(LB)	ADJ. WT. PER BATCH(LB)	REMARKS
CEMENT	Cemex- (Southdown)	<u>660</u>	<u>3.36</u>	<u>116.7</u>	<u>116.7</u>	<u>SL7 + b3</u>
FLYASH/SLAG	-					
WATER	Giville	<u>267</u>	<u>4.28</u>	<u>59.3</u>	<u>52.6</u>	<u>-6.7</u>
FINE AGG.	76-137	<u>1076</u>	<u>6.53</u>	<u>239.1</u>	<u>237.7</u>	<u>-1.2</u>
COARSE AGG.	08-005	<u>1794</u>	<u>11.88</u>	<u>398.6</u>	<u>406.5</u>	<u>+7.9</u>
AIR ENTRAINER	Dalek AEK	<u>5.0 oz</u>	<u>0.75</u>	<u>32.9 ml</u>	<u>32.9 ml</u>	-
ADMIXTURE	WRDA 64	<u>33.0 oz</u>	-	<u>216.9 ml</u>	<u>216.9 ml</u>	-
ADMIXTURE	-					
TOTAL			<u>27.00</u>			

SLUMP (IN) 4.0 AIR (%) 5 1/2 MIX TEMP 75 WORKABILITY Good AIR TEMP 71°F

SLUMP BY: _____ AIR BY: _____ CYLS. BY: _____ START TIME= _____

W/C RATIO _____ H2O HELD OUT _____ ADDED _____ END TIME= _____

CYLINDERS-COMPRESSIVE STRENGTH

REMARKS: _____

SIGNED BY: _____

WITNESSED BY: _____

APPENDIX B
ADDITIONAL SEM IMAGES

Part 1 - Mix 1:Plain Cement Only Mix (0%FA)

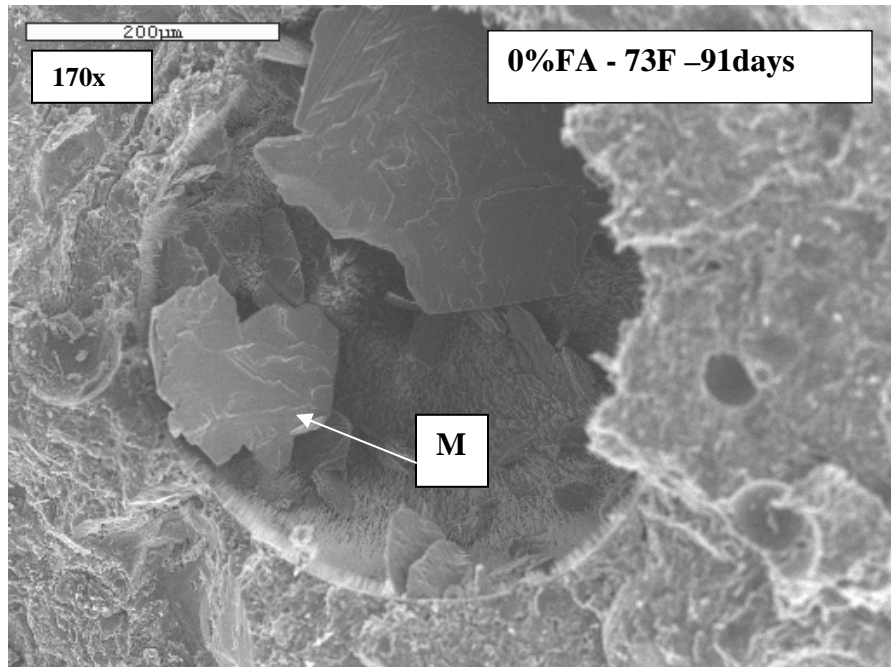


Figure B.1 Void with monosulphate (M), no ettringite found

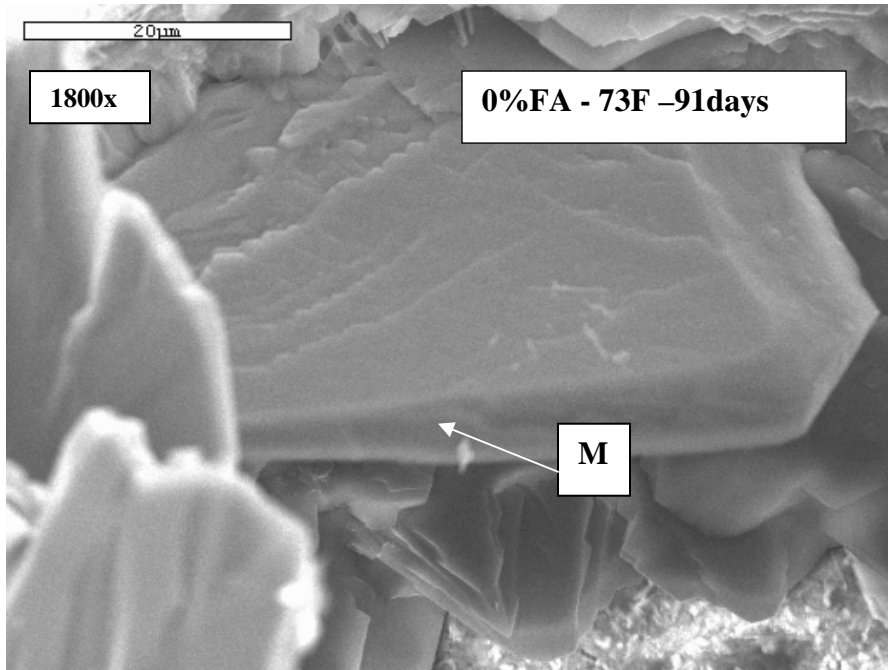


Figure B.2 Close-up view of Figure B.1

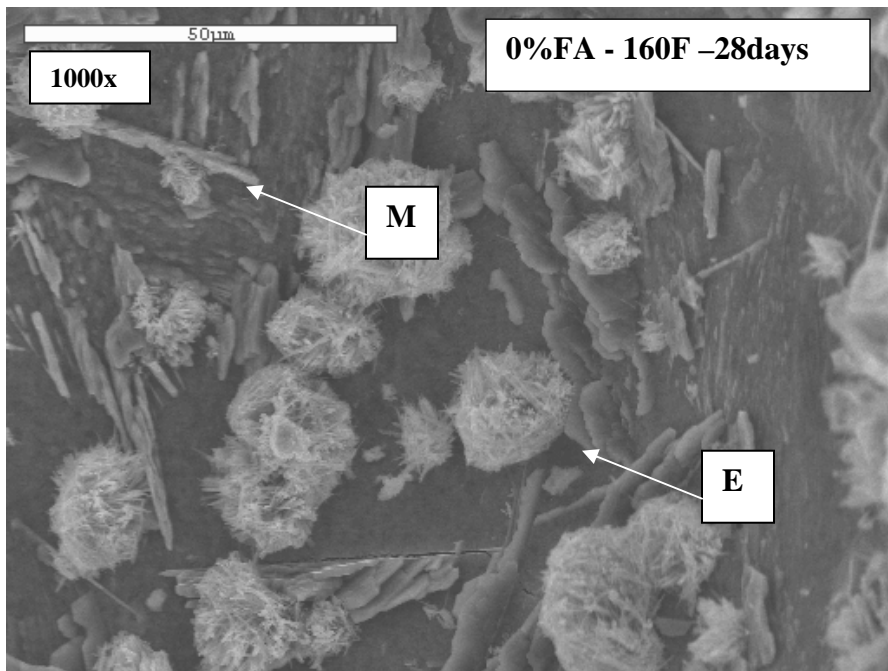


Figure B.3 Void with ettringite (E) and monosulphate (M)

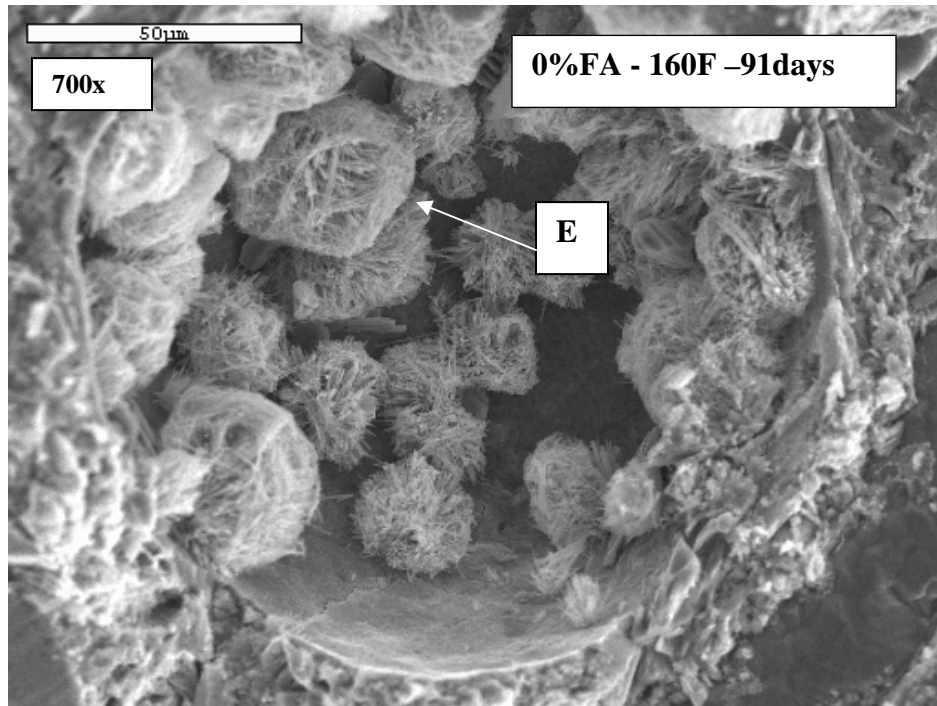


Figure B.4 Void with ettringite (E) crystals

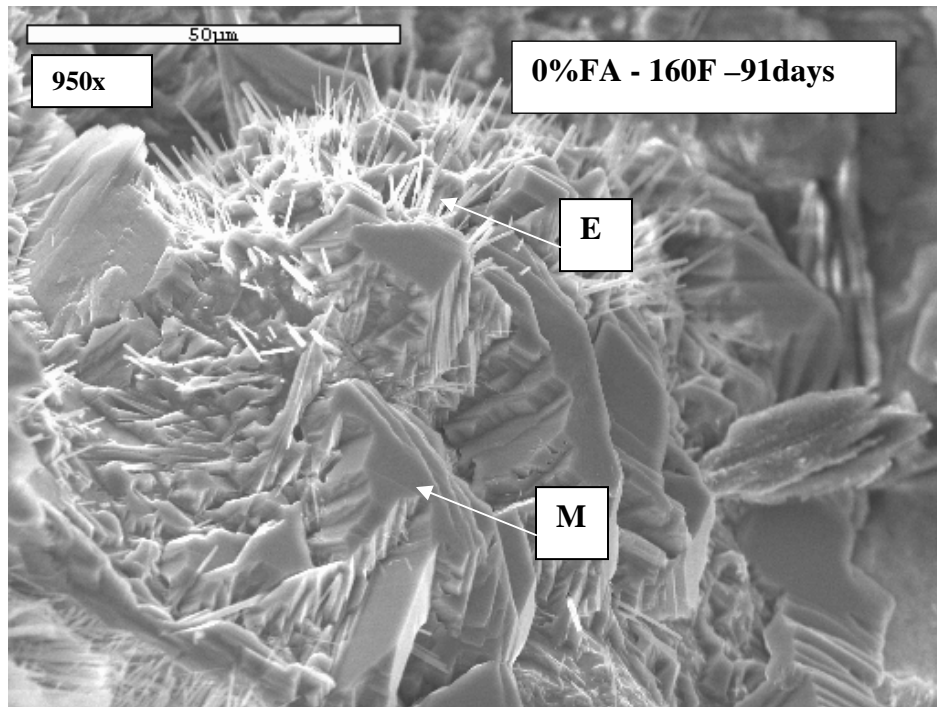


Figure B.5 Void showing monosulphate and the early formation of ettringite (E) crystals

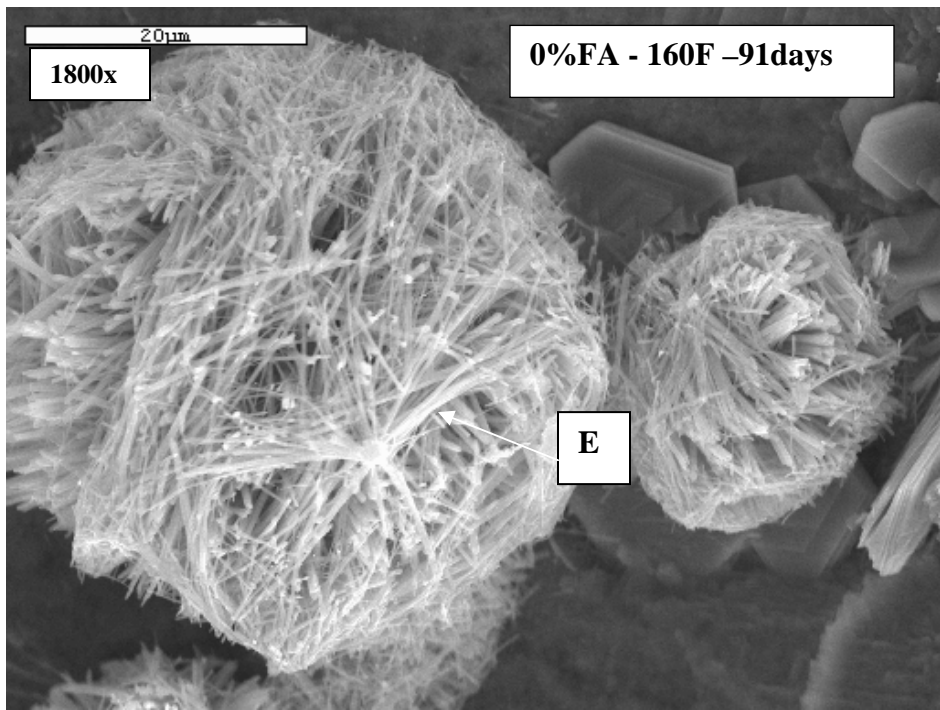


Figure B.6 Void showing ball of ettringite (E) crystals

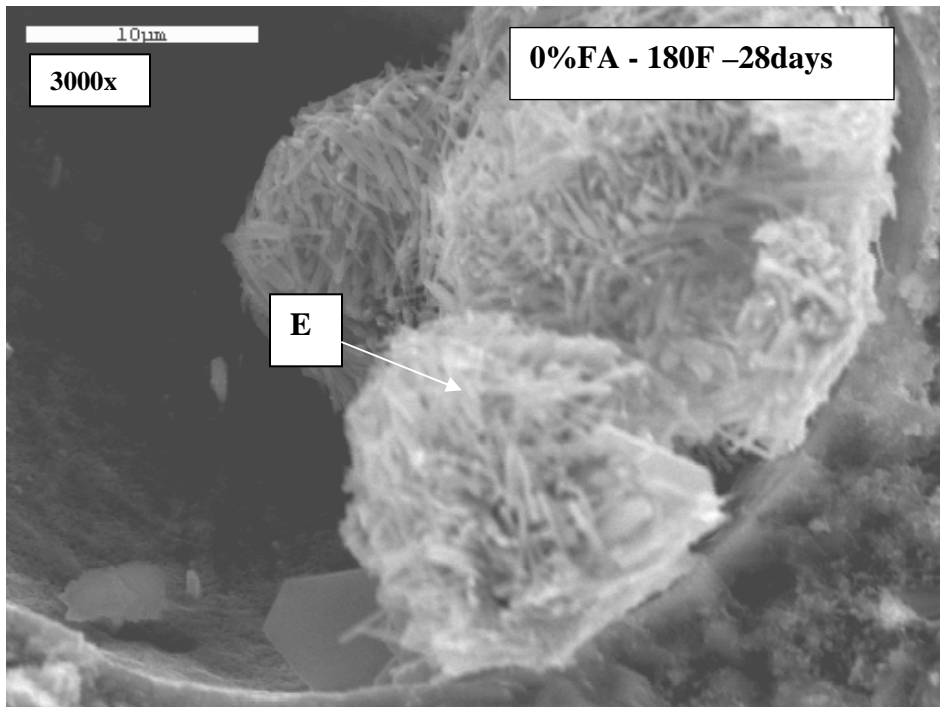


Figure B.7 Void showing balls of ettringite (E) crystals

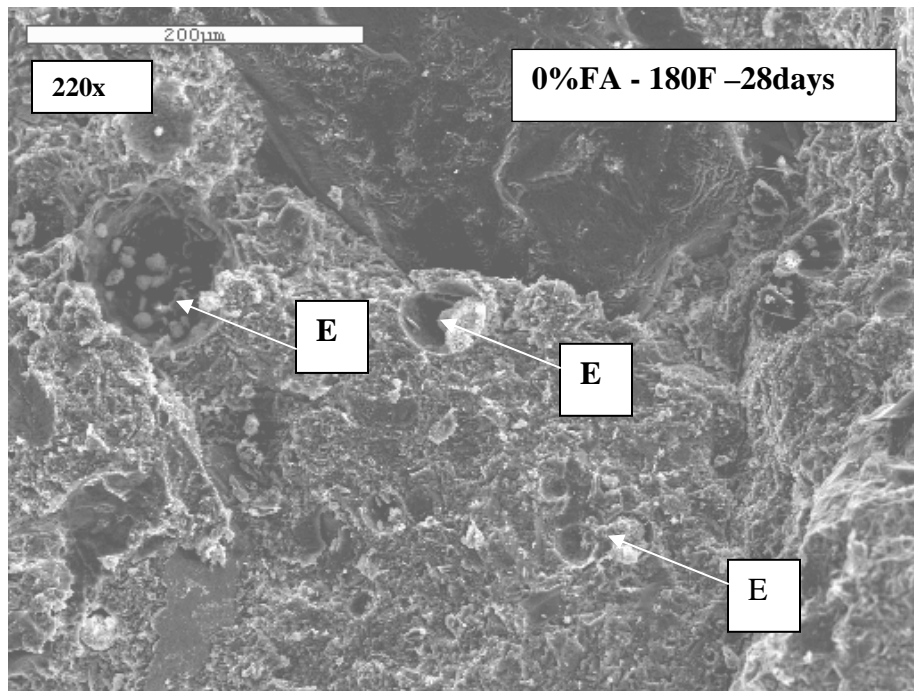


Figure B.8 Voids showing ettringite (E) crystals some almost full

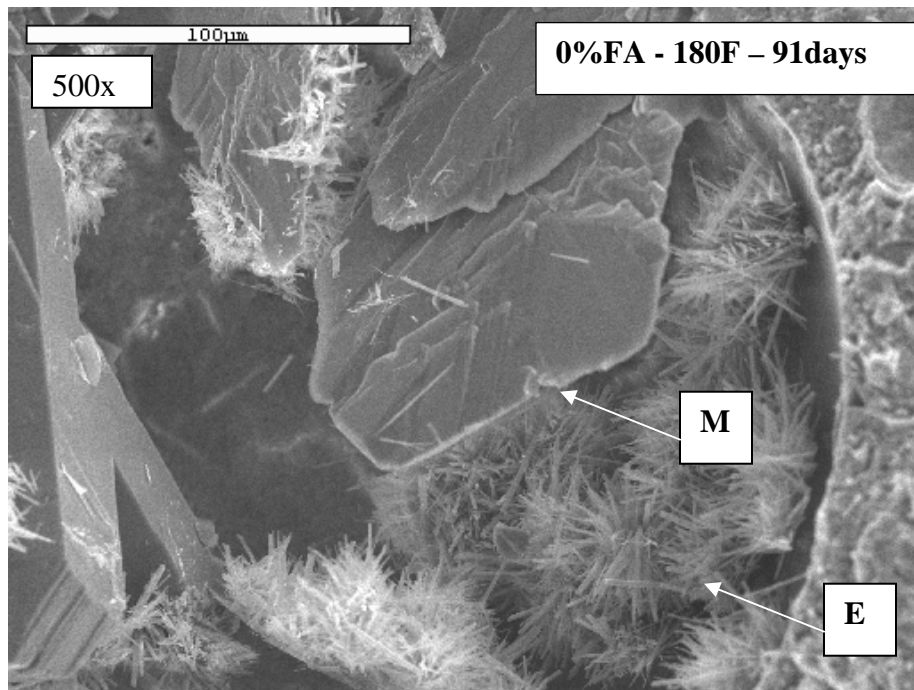


Figure B.9 Voids showing ettringite (E) and monosulphate crystals

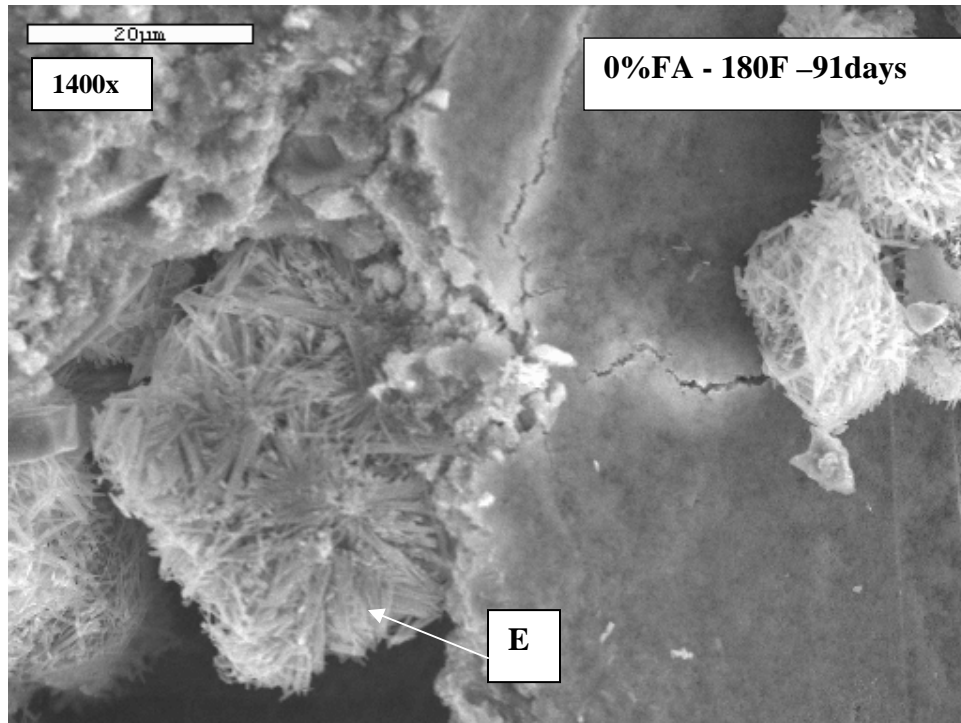


Figure B.10 Ettringite (E) crystals in and around vicinity of void

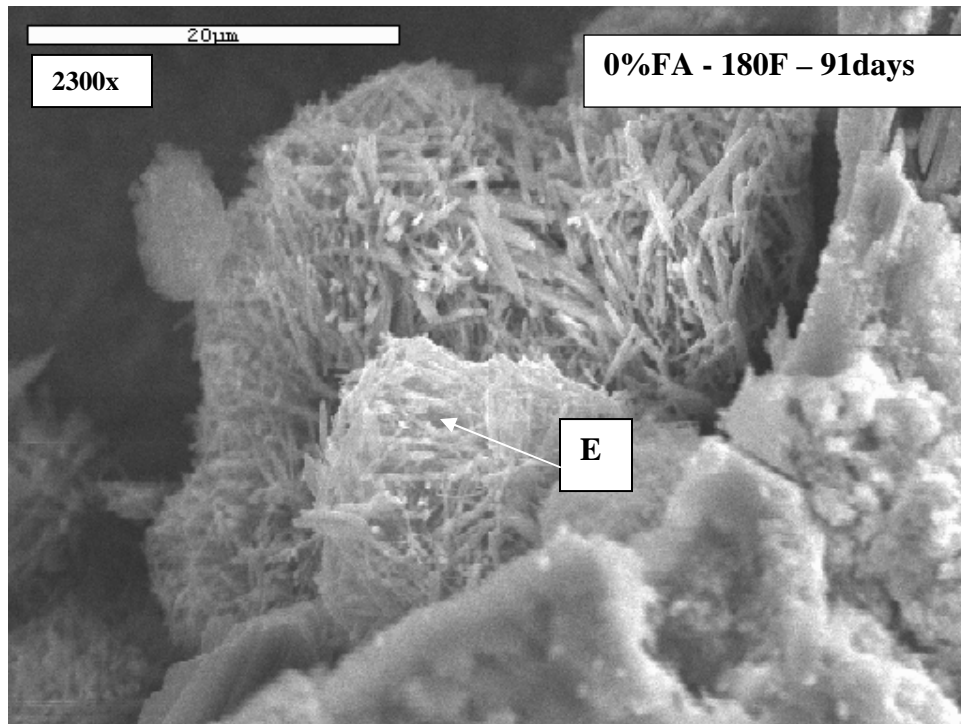


Figure B.11 Ettringite (E) crystals in void

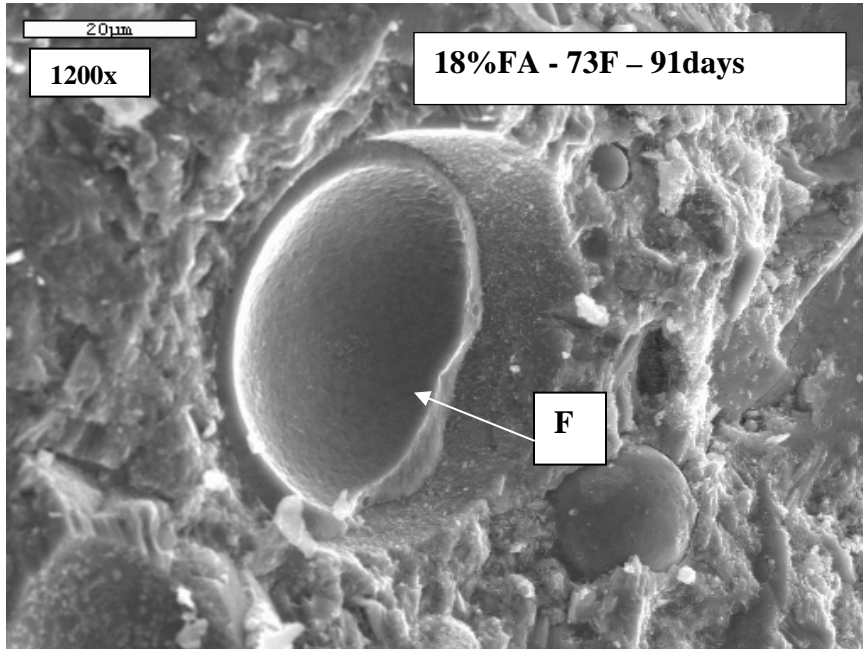
Part 2 - Mix 2: 18% Fly Ash Mix

Figure B.12 Fly ash particle with reaction around rim

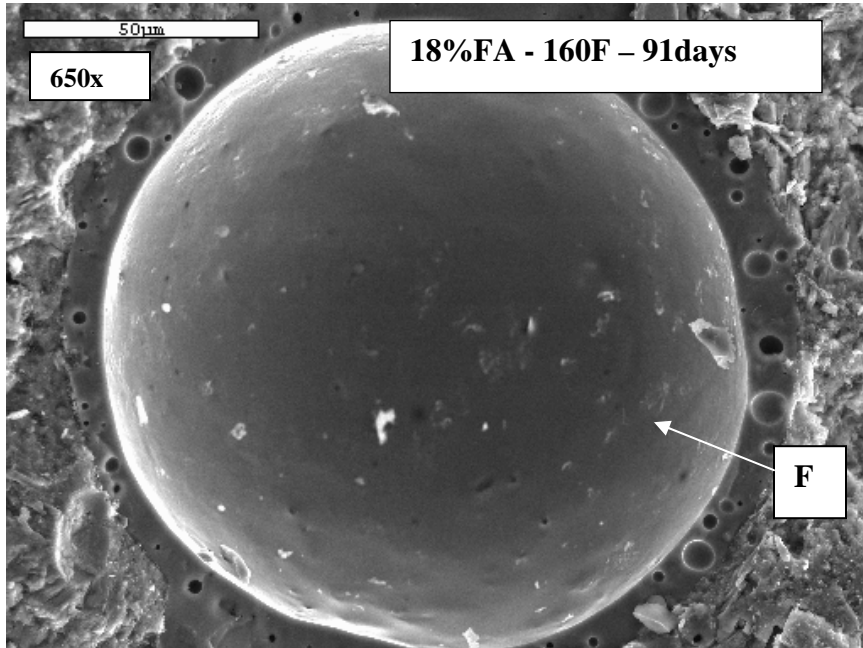


Figure B.13 Fly ash particle with reaction around rim

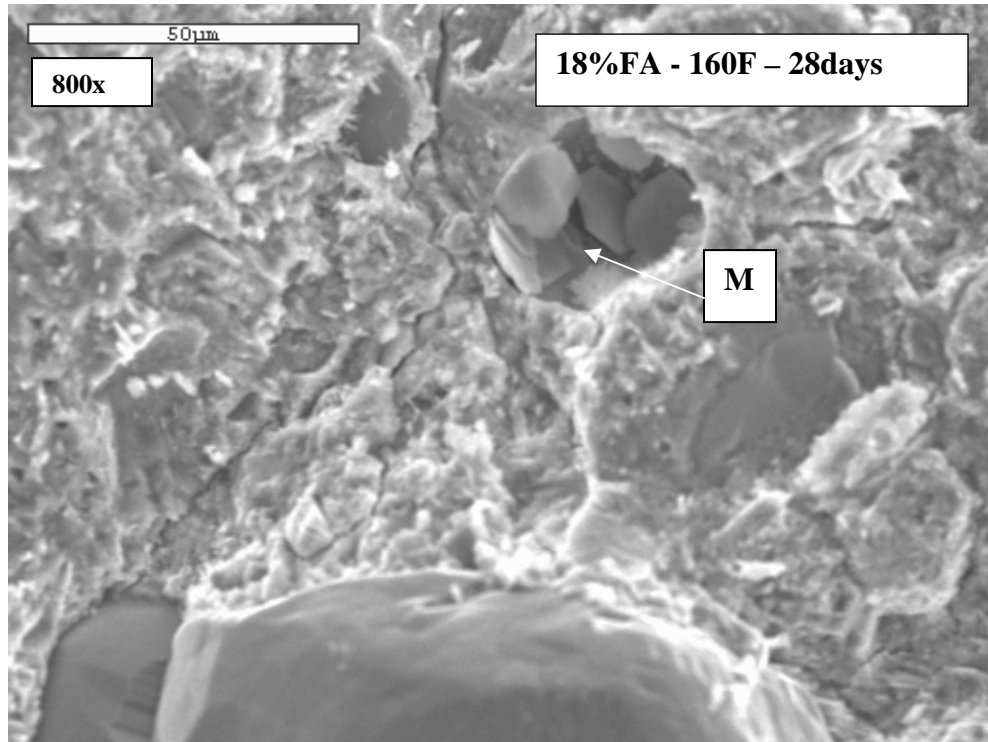


Figure B.14 Void containing monosulphate

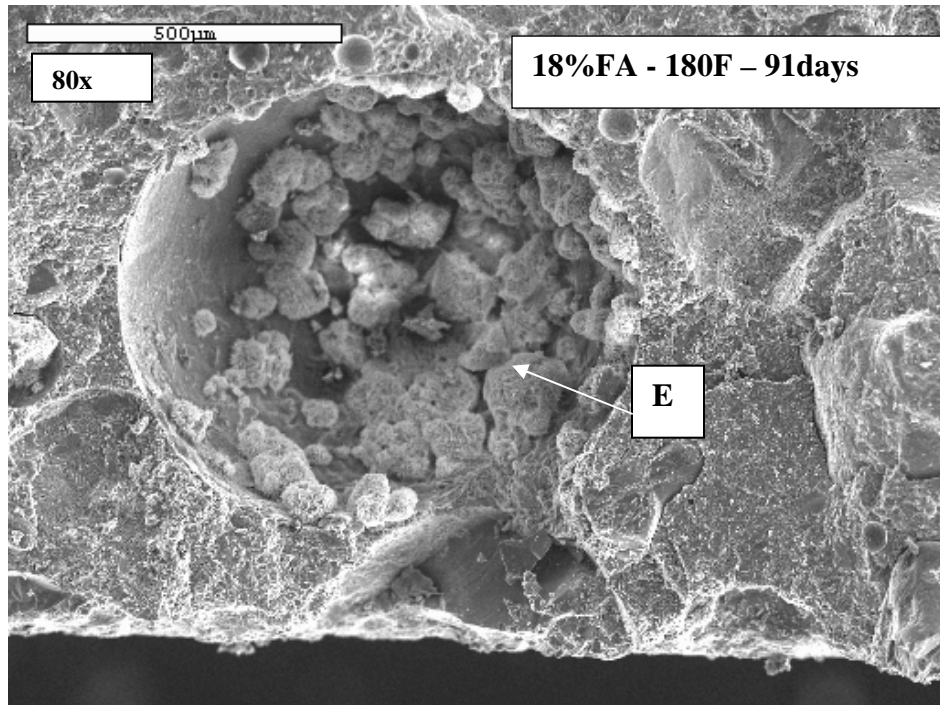


Figure B.15 Void containing ettringite crystals

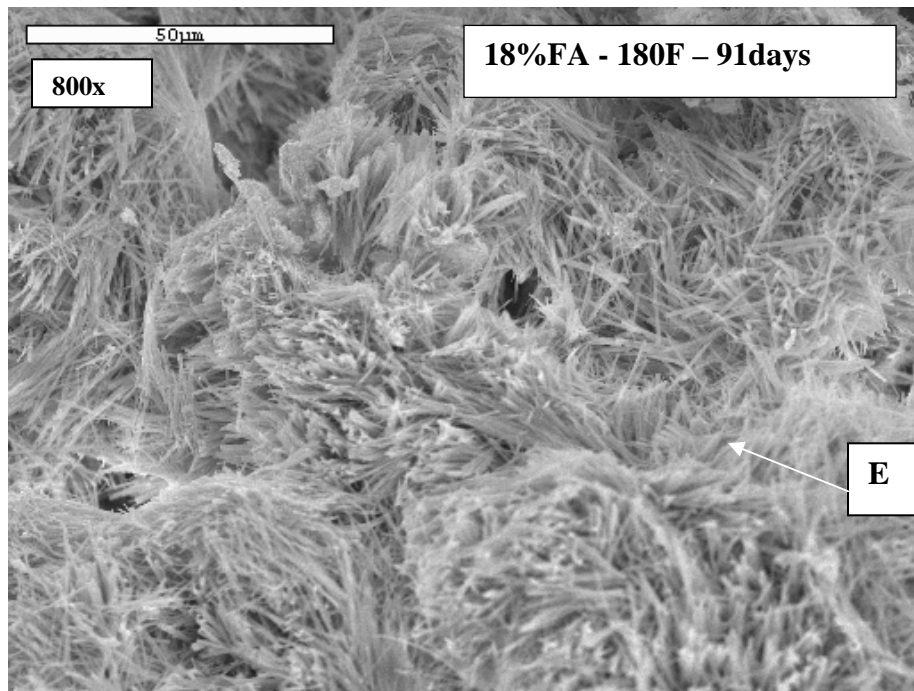


Figure B.16 Close up view of ettringite crystals in Fig B.15

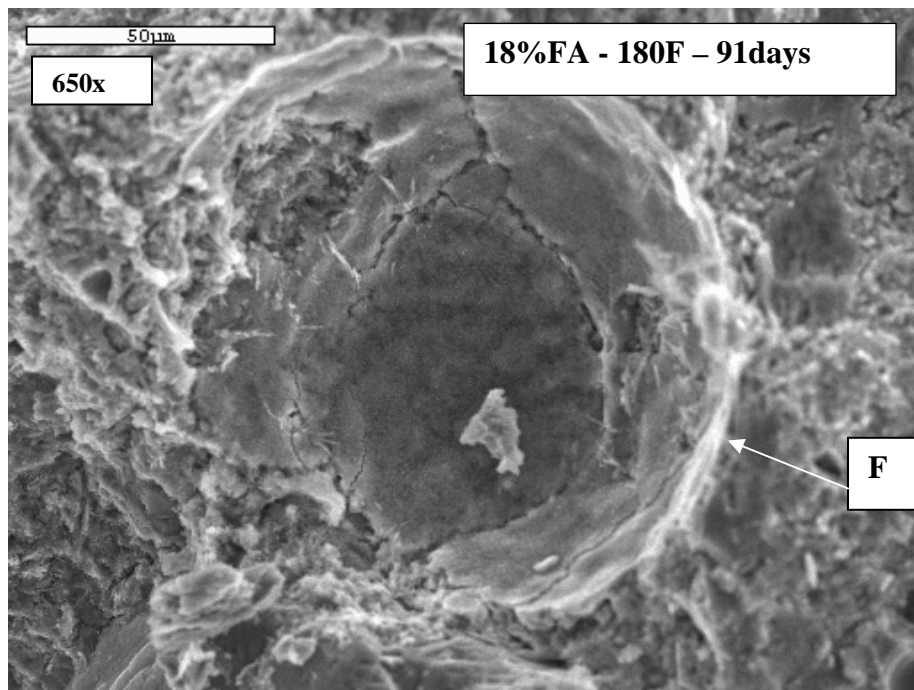


Figure B.17 Reacting fly ash particle

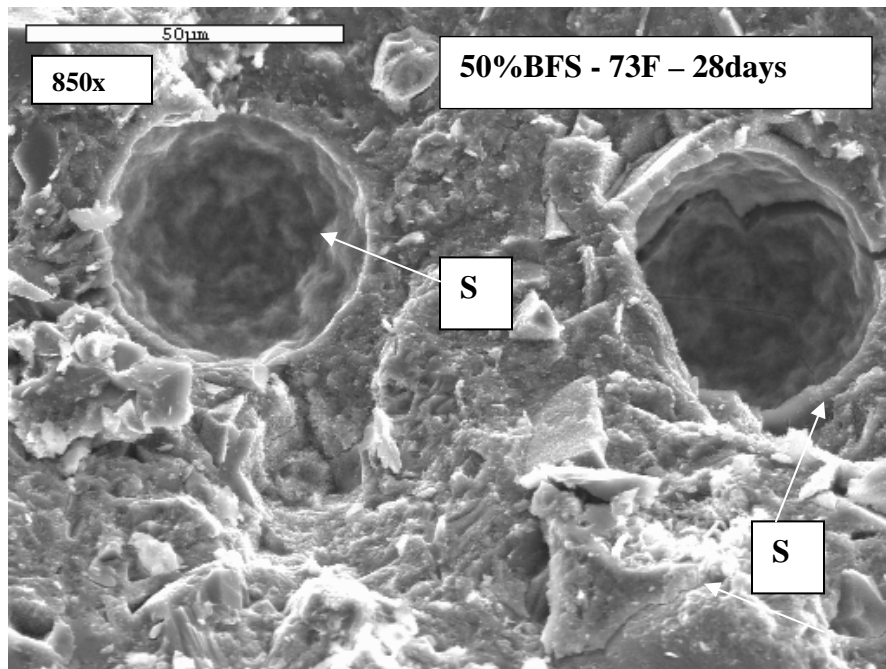
Part 3 - Mix 3: 50% Slag Mix

Figure B.18 Slag particles showing some early reaction

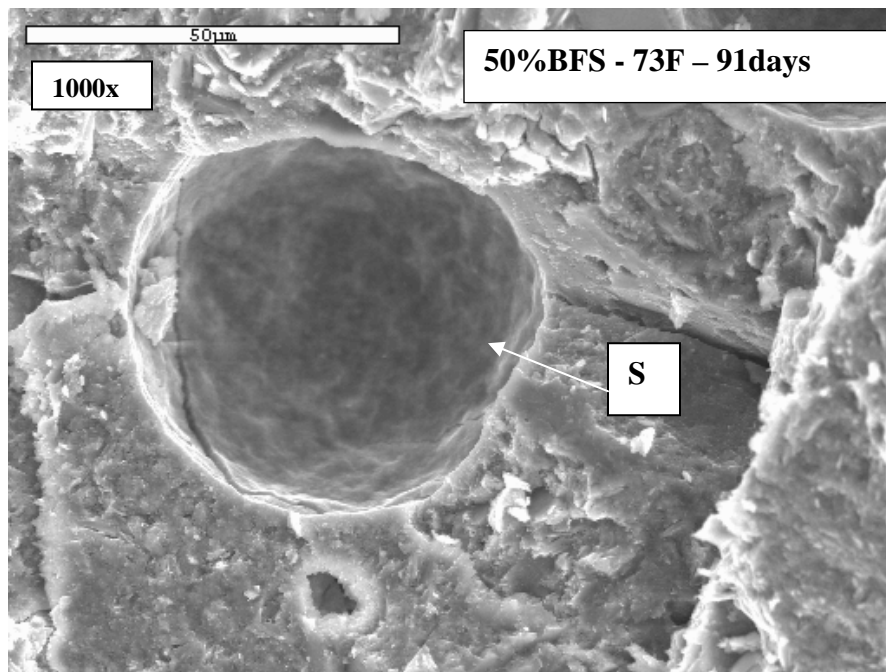


Figure B.19 Slag particles showing reaction on surface

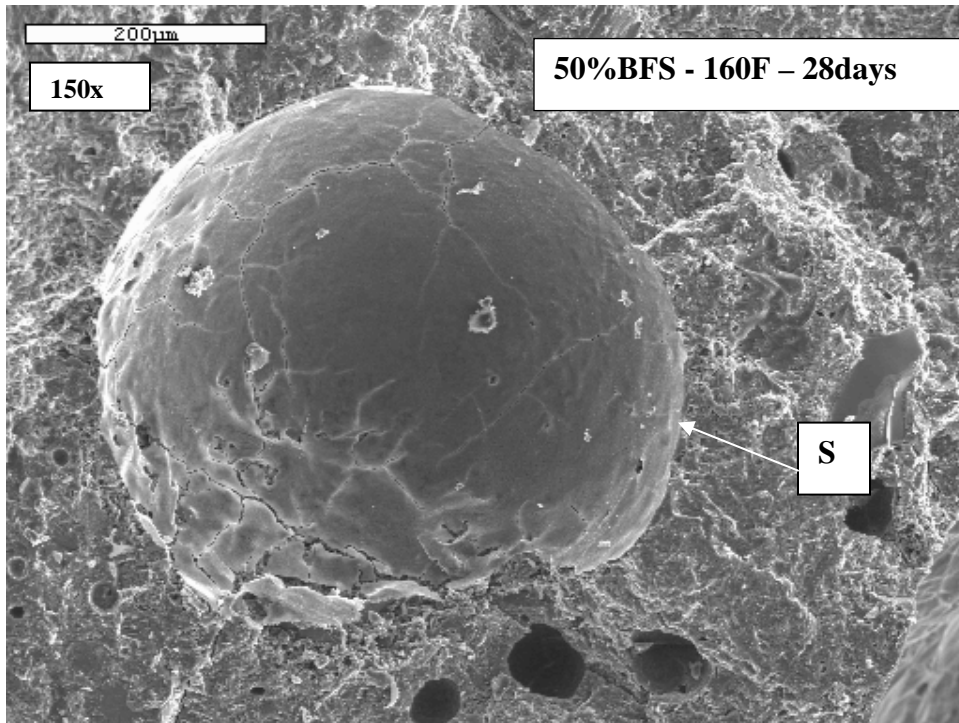


Figure B.20 Slag particle showing reaction on surface

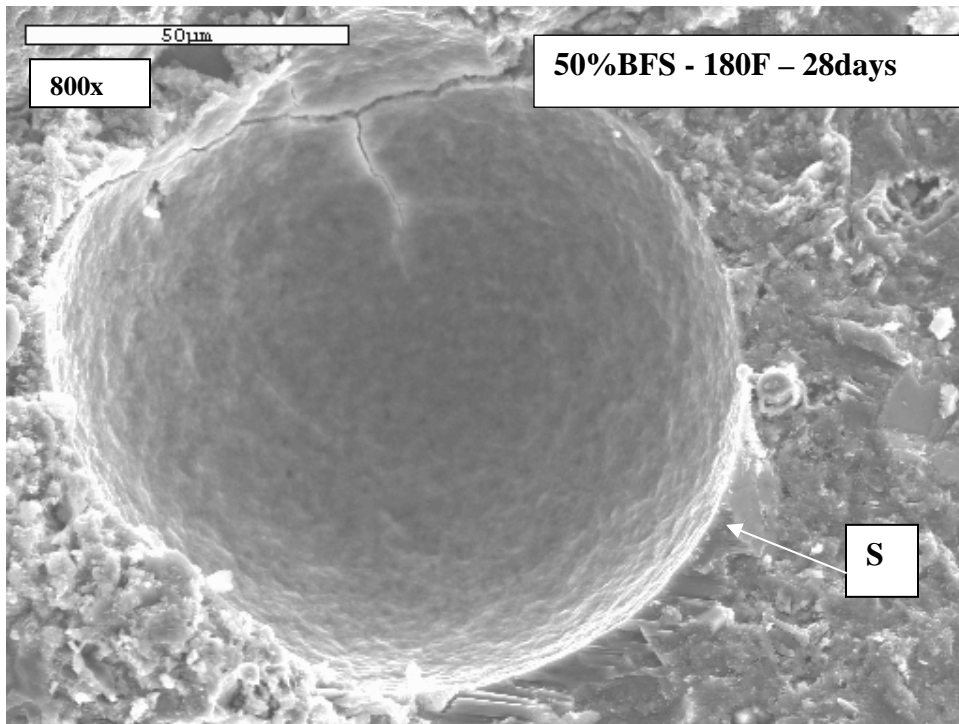


Figure B.21 Slag particle showing reaction on surface

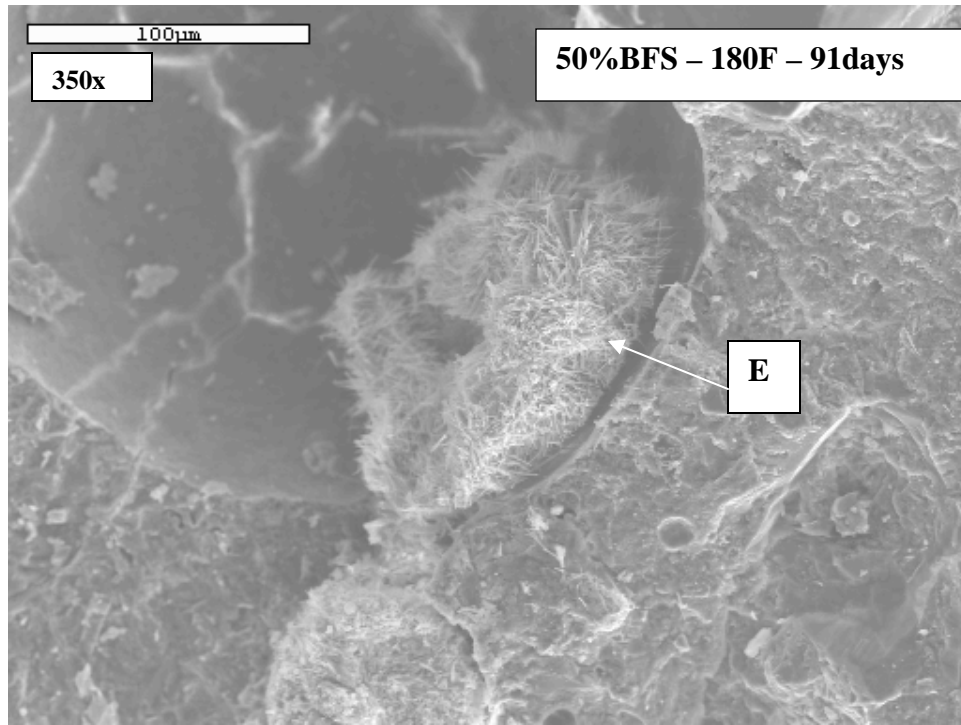


Figure B.22 Ettringite formed around surface of reacting slag particle

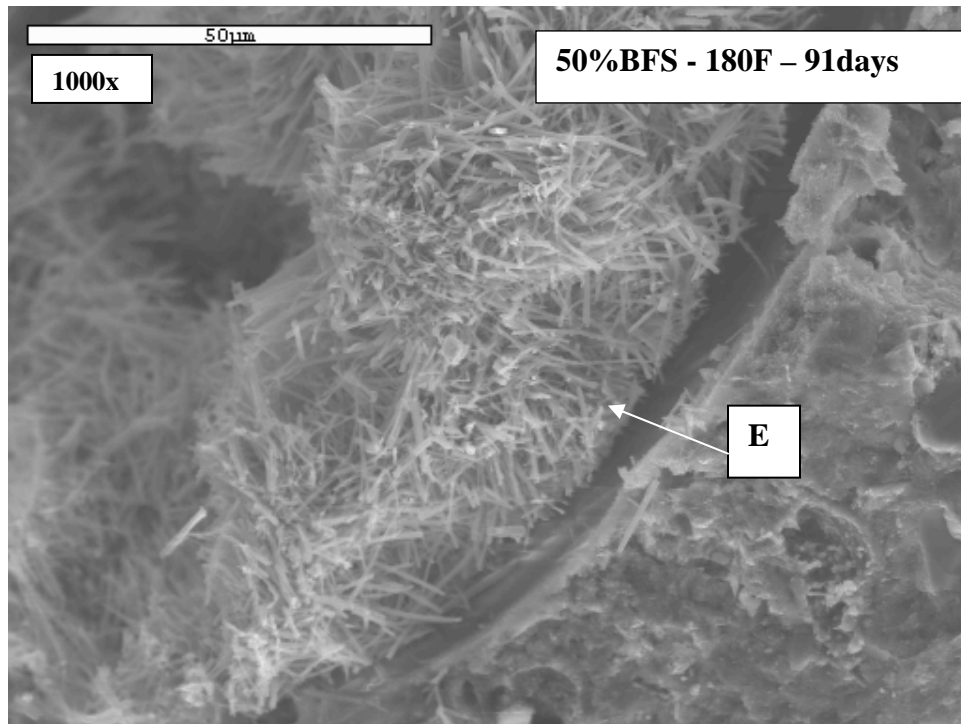


Figure B.23 Close-up view of Figure. B.22

LIST OF REFERENCES

American Concrete Institute, (ACI) Manual of Concrete practice, Part 1: Materials and General Properties of Concrete, Detroit, Michigan, 1999.

ACI 232.2R-96, Use of fly ash in concrete, ACI Manual of Concrete practice, Part 1: Materials and General Properties of Concrete, 34 pp. (Detroit, Michigan, 1999).

ACI 233R-95, Granulated Blast-Furnace Slag as a Cementitious Constituent in Concrete, ACI Manual of Concrete practice, Part 1: Materials and General Properties of Concrete, 18 pp. (Detroit, Michigan, 1999).

Basma, A., Barakat S., and Al-Oraimi, S., “*Prediction of Cement Degree of Hydration Using Artificial Neural Networks*”, ACI Materials Journal Vol. 96, No.2, pp.167-172, 1999.

Campbell, G. and Detwiler, R., “*Development of Mix Designs for Strength and Durability of Steam-Cured Concrete*”, Concrete International 37-39, 1993.

Chini, A.R., and Acquaye, L., “*Effect of Elevated Concrete Temperatures on the Strength and Durability of Concrete*,” Materials and Structures/Materiaux et Constructions. Vol. 38, No. 281 pp. 673-679, August/September 2005.

Detwiler, R., Fapohunda, C., and Natale, J., “*Use of Supplementary Cementing Materials to Increase the Resistance to Chloride Ion Penetration of Concretes Cured at Elevated Temperatures*”, ACI Materials Journal Vol.91, No.1, pp. 63-66, 1994.

Diamond, S., “*Delayed Ettringite Formation – Processes and Problems*”, Cement and Concrete Composite. Vol. 18, pp. 205- 215, 1996.

FitzGibbon, M.E. “*Large pours –2, heat generation and control*”. Concrete, Vol.10, No. 4, pp. 33-5. Dec.1976, London.

Florida Department of Transportation, “*Structures Design Guidelines (LRFD)*,” 2002.

Fraay, A.L.A., Bijen J.M., and de Hann Y.M. “*The reaction of fly ash in Concrete; A critical examination*”. Cement and Concrete Research. Vol 19, No. 2, pp. 235-46, 1989.

Goldstein, J., Newbury, D., Joy, D., Lyman, C., Echlin, P., Lifshin, E., Sawyer L., and Michael, J. Scanning Electron Microscopy and X-ray Microanalysis. A text for Biologists, Material scientists and Geologists. Plenum Press, New York 1992

Goto, S., and Roy, D.M. “*The effect of w/c ratio and curing temperature on the permeability of hardened cement paste*”. Cement and Concrete Research. Vol. 11, No. 7, pp. 575-9, 1981.

Heinz, D., Kalde, M., Ludwig, U., and Ruediger, I., “*Present State of Investigation on Damaging Late Ettringite Formation (DLEF) in Mortars and Concretes*,” ACI SP-177, Bernard Erlin (Editor), American Concrete Institute, Farmington Hills, MI, 1999, pp. 1-14.

Heinz, D., and Ludwig, U., “*Mechanism of Secondary Ettringite Formation in Mortars and Concrete Subjected to Heat Treatment*,” ACI SP-100, John M. Scanlon (Editor), American Concrete Institute, Framington Hills, MI, 1987, pp. 2059-2071.

Hime W.G., and Marusin S. L., “*Delayed Ettringite Formation: Many Questions and Some Answers*,” ACI SP-177, Bernard Erlin (Editor), American Concrete Institute, Farmington Hills, MI, 1999, pp. 199-206.

Hime, W.G., Marusin, S.L., Jugovic, Z.T., Martinek, R.A., Cechner, R.A., and Backus, L.A. “*Chemical and Petrographic Analyses and ASTM Test Procedures for the Study of Delayed Ettringite Formation*.” Cement, Concrete, and Aggregates. CCAGDP. Vol. 22 No. 2. pp. 160-168 December 2000.

Hobbs D.W., “*Expansion and Cracking in Concrete Associated with Delayed Ettringite Formation*,” ACI SP-177, Bernard Erlin (Editor), American Concrete Institute, Farmington Hills, MI, 1999, pp. 159-177.

Johansen V., and Thaulow N., “*Heat Curing and Late Formation of Ettringite*,” ACI SP-177, Bernard Erlin (Editor), American Concrete Institute, Farmington Hills, MI, 1999, pp. 199-206.

Kjellsen K.O., Detwiler R.J., and Gjory O.E. “*Pore Structure of Plain cement pastes hydrated at different Temperatures*”. Cement and Concrete Research. Vol. 20, pp. 927-933, 1990a.

Kjellsen K.O., Detwiler R.J., and Gjory O.E. “*Development of Microstructure in plain hydrated at different Temperatures*”. Cement and Concrete Research. Vol. 21, pp. 179-189, 1990b.

Kosmatka, S., and Panarese, W. “*Design and Control of Concrete Mixtures*,” thirteen edition, Portland cement Association, Skokie, Illinois, 1994.

Lachemi, M. and Aitcin, P., “*Influence of Ambient and Fresh Concrete Temperatures on the Maximum Temperature and Thermal Gradient in a High Performance Concrete Structure*”, ACI Materials Journal (94)(2)(1997) 102-110.

Lam L., Wong, Y.L., and Poon, C.S. “*Degree of hydration and gel/space ratio of high-volume fly ash systems*”, Cement and Concrete Research. Vol. 30, 474 - 756, 2000.

Lawrence C.D., “*Mortar Expansions due to Delayed Ettringite Formation. Effects of Curing Period and Temperature*”. Cement and Concrete Research. Vol. 25, pp. 903-914, 1995.

Maltais, Y., and Marchand, J., “*Influence of Curing Temperature on Cement Hydration and Mechanical Strength Development of Fly ash mortars*”, Cement and Concrete Research. Vol. 27, No. 7, pp. 1009-1020, 1997.

Mehta, P.K., and Monteiro, P.J.M., “*Concrete: Microstructure, Properties, and Materials*”. The McGraw-Hill Companies, Inc., 1993.

Neville, A. M. ‘Properties of Concrete’ 4th Edition, John Wiley & Sons Inc., 1997

Neville, A. M. “*Properties of Concrete*”. 4th Edition, John Wiley & Sons Inc., 2004.

Miller M.F., and Conway, T.,” *Use of Ground Granulated Blast Furnace Slag for Reduction of Expansion Due to Delayed Ettringite Formation,*” Cement, Concrete, and Aggregates, CCAGDP, Vol, 25, No. 2, December 2003, pp. 59-68

Sarkar, L.S., Aimin, X., and Jana, D. “*Scanning Electron Microscopy, X-Ray Microanalysis of Concrete,*” in Handbook of Analytical Techniques in Concrete Science and Technology. Ramachandran, V.S., and Beaudoin, J.J. (Editors), Noyes Publication, US, 2001, pp. 231-273.

Scrivener, K.L., and Lewis, M.C., “*Effect of Heat Curing on Expansion of Mortars and Composition of Calcium Silicate Hydrate Gel ,*” ACI SP-177, Bernard Erlin (Editor), American Concrete Institute, Farmington Hills, MI, 1999, pp. 199-206.

Stark, J and Bollmann, K. “*Delayed Ettringite Formation in Concrete*”. Bauhaus-University Weimar / Germany

Stark, J and Seyfarth, K., “*Ettringite Formation in Hardened Concrete and Resulting Destruction ,*” ACI SP-177, Bernard Erlin (Editor), American Concrete Institute, Farmington Hills, MI, 1999, pp. 125-140.

Tarkhan, S.B. Degree of Hydration for Cement Paste with Fly ash at Elevated Temperatures. Master’s Thesis, University of Florida, 2000.

Taylor, H.F.W., Famy, C., and Scrivener, K.L., “*Delayed Ettringite Formation*”. Cement and Concrete Research. Vol. 31, pp. 683-693, 2001.

Verbeck, G.J., and Helmuth R.A. *Structures and physical properties of cement paste*”. Proc. 5th Int. Symp. On the Chemistry of Cement, Tokyo, Vol. 3, pp. 1-32, 1968.

Zhang, Y.M., Sun W., and Yan, D. H., '*Hydration of high-volume fly ash cement pastes*' Cement and Concrete Composites. Vol. 22, pp. 445 – 452, 2000.

BIOGRAPHICAL SKETCH

Lucy Acquaye has a Bachelor of Science degree in Building Technology from Kwame Nkrumah University of Science and Technology. She taught courses in construction materials and methods the university after her bachelor's degree. In 1998, she was awarded a J.J. Fulbright Scholarship to attend the University of Florida, USA, where she graduated with a Master of Science in Building Construction in August 2000. Since August 2003, she has been a graduate instructor at the Rinker School of Building Construction where she has taught courses in Construction Drawing and Construction Mechanics. Lucy will graduate with a PhD in Building Construction in May 2006.